STUDY OF FXR IN PRIMARY HUMAN HEPATOCYTES AND FXR REGULATED BA HOMEOSTASIS IN PARENTERAL NUTRITION ASSOCIATED LIVER DISEASES

By

Le Zhan

Submitted to the graduate degree program in Pharmacology and the Graduate Faculty of the University of Kansas Medical Center in partial fulfillment of the requirements for the degree of Doctor of Philosophy.

Dissertation Committee Members

_____

Wen-Xing Ding, Ph.D. (Chair)

_____

Grace L. Guo, Ph.D. (Advisor)

_____

Udayan Apte, Ph.D.

_____

Tiangang Li, Ph.D.

_____

Hao Zhu, Ph.D.

Date Defended: 2014-Nov-25

The Dissertation Committee for Le Zhan certifies that this is the

approved version of the following dissertation:

STUDY OF FXR IN PRIMARY HUMAN HEPATOCYTES AND FXR REGULATED BA HOMEOSTASIS IN PARENTERAL NUTRITION ASSOCIATED LIVER DISEASES

_____

Committee Chair, Wen-Xing Ding, Ph.D.

Date approved: 2014-Dec-19

Abstract

Farnesoid X receptor (FXR, *NR1H4*) is a ligand activated transcription factor belonging to the nuclear receptor (NR) superfamily, and is highly expressed in the liver, intestine, and kidney, in both humans and rodents. Bile acids (BAs) are the endogenous ligands of FXR. FXR mainly functions as the BA sensor by regulating genes that are critically involved in BA homeostasis. FXR has also been shown to play important roles in lipid, cholesterol and glucose metabolism, as well as inflammation, tumorigenesis, and liver regeneration. FXR deficiency is implicated in numerous liver diseases and mice with modulation of FXR have been used as animal models to study liver physiology and pathology. Genome-wide studies in mouse livers and intestines suggest FXR's diverse and broadly tissue specific functions. In the first aim, we studied the genome-wide FXR binding and transcriptome profiles upon FXR activation in primary human hepatocytes (PHHs) and HepG2 cells. Chromatin immunoprecipitation followed by massive parallel sequencing (ChIP-seq) was performed in PHHs and HepG2 cells, treated with a synthetic FXR agonist, GW4064 or DMSO control. In parallel, RNA deep sequencing (RNA-seq) and RNA microarray were performed for GW4064 or control treated PHHs and wild type (WT) mouse livers, respectively. ChIP-seq showed similar profiles of genome-wide FXR binding in humans and mice in terms of motif analysis and pathway prediction. However, RNA-seq and microarray showed more different transcriptome profiles between PHHs and mouse livers upon GW4064 treatment. In summary, we have established genome-wide human FXR binding and transcriptome profiles. These results will aid in determining the human FXR functions, as well as

judging to what level the mouse models could be used to study human FXR functions in future studies.

Recent studies in the field of parenteral nutrition (PN) suggest that down-regulation of FXR signaling is critically involved in the pathogenesis of PN associated liver diseases (PNALD), especially PN associated cholestasis (PNAC) in preterm infants. PN is a life-saving therapy for patients who cannot tolerate enteral food intake. However, long-term PN can lead to a spectrum of liver diseases, summarized as PNALD. PNAC is predominately found in preterm infants and neonates, and has high rate of progression into liver failure. Options for clinical management of PNALD are still limited. While it is suggested that multiple risk factors are contributing to the development of PNALD, the pathogenesis of PNALD remains poorly understood. Animal studies obtained from preterm piglets and several mouse models have shed light on the mechanisms underlined. To date, whether FXR and BAs are involved in the development and progression of PNALD is not well studied. In the second aim, we established a valid mouse PN model in our laboratory. Using RNA microarray profiling and serum BA profiling, we identified novel signatures involved in BA homeostasis in adult PN mice. We detected significantly increased gene expression of cytochrome P450, family 7, subfamily a, polypeptide 1 (*Cyp7a1*) and decreased gene expression of cytochrome P450, family 8, subfamily b, polypeptide 1 (*Cyp8b1*) in the livers of PN mice. Several FXR and liver X receptor alpha (LXRα) target genes involved in BA homeostasis were also altered in the livers of PN mice. Consistent with the gene expression alterations, both the levels and the percentages of tauro β-muricholic acid (T-β-MCA) as well as total non-12α-OH BAs in the serum of PN mice increased

significantly compared to saline controls. These results suggest that BA homeostasis could be disrupted in PN patients as well and the deregulation of BA synthesis and metabolism could contribute to the development and progression of PNALD when additional risk factors are present. Additional altered genes and pathways were also detected from the microarray analysis for the PN mice. These results will aid us in future studies of the contributions of FXR and BA signaling, as well as other potential factors to the development and future management of PNALD.

Dedication

In memory of my beloved grandma

A great mom of seven children and a grandma of many

A very decent person with high moral standards

Forever the brightest star in my life

Acknowledgements

To my mentor, Dr. Grace L. Guo, I am sincerely grateful for all the tremendous support and the great opportunities that you have provided me over the last four and half years. You mentorship extends far beyond scientific training. Grace is a very decent person, a great mom of two lovely kids, a very successful laboratory principle investigator, and a very knowledgeable but humble scientist. You are not only the mentor for my graduate training, but also a mentor for life. I still remembered that when I first joined your lab, I was very naïve, both as a person and as a graduate student. And now, after receiving all the thorough, patient and extensive training from your mentorship, I am confident to say that I am much better in both aspects.

To my present committee members, Dr. Wen-Xing Ding (Chair), Dr. Udayan Apte, Dr. Tiangang Li and Dr. Hao Zhu, and my past committee members, Dr. Curtis Klaassen, Dr. Xiao-bo Zhong, Dr. Xiaochao Ma, your critical input and generous support allowed me to get to where I am, especially the continuous support after our lab moved to New Jersey. And thanks to Dr. Hao Zhu again, you helped me tremendously revise my Ph.D. qualification proposal and my final dissertation.

To the current and former members of the Guo laboratory, you guys are the best labmates any one could possibly dream of. Especially to Dr. Bo Kong, your profound knowledge in many fields, fruitful scientific experience and expertise, and also very kind personality helped me in always every single aspect while I worked in the lab. To Dr. Ann Bailey, you helped me build up my knowledge background and confidence when I joined the lab and entered a brand new scientific field. To Mrs. Jess Williams, you are

the best classmate any one could possibly have; you helped me keep on track on almost all the coursework studies in the department. To Dr. Guodong Li and Mrs. Jianliang Shen (Julia), you made all the laborious animal work fun and easy, in KUMC and Rutgers University, respectively.

To our collaborators for the genome sequencing projects: Dr. Hui-Xin Liu, Dr. Yuqi He, Dr. Yu-Jui Yvonne Wan, Dr. Lai Peng, Dr. Dan Li, Dr. Jianwen Fang, Dr. Yaping Fang, Dr. Steve Hart, and once again Dr. Xiao-bo Zhong, all of you helped me so much for my first big project in the laboratory.

To our collaborators for the PN project, Dr. Iván Csanaky, Dr. David Reimer, Mrs. Leslie Bird, Dr. Naureen Memon, Dr. Ill Yang, and Dr. Brian Buckley, your expertise helped me on this project from the very beginning until this day, and thank you for your continuously support in the future as well. Especially to Dr. Iván Csanaky and Dr. David Reimer, you helped me build up my surgical skills and confidence to deal with the complex surgical issues involved in this the project. Nothing could be achieved without your tremendous help!

To the graduate program of the Department of Pharmacology, Toxicology, and Therapeutics, especially the administrative staff Dr. Bruno Hagenbuch, Mr. Cody Tully, I appreciate your assistance, guidance and professionalism, especially your continuous support after our lab moved to New Jersey. The intensive coursework in the first two years in the department also helped me to build up the fundamental knowledge of pharmacology and toxicology, which are and will always be essential to my future scientific training.

To all the people helped us in Rutgers University when we first came here, especially those in Drs. Aleksunes and Richardson's lab, including Dr. Xia Wen, Mrs. Myrna Trumbauer, Miss Kristin Bircsak, Miss Jamie Moscovitz, Dr. Chris Gibson and Dr. Ashley Green. Thanks again for your continuous help and friendship in the future!

To Dr. Jie He, you are a very hard-working and smart scientist, a very nice friend and will always be a scientific mentor in my heart (an "idol" as Ron once said). You helped me go through the tough time in my second year of my graduate study. Your working-hard and more importantly working-smart spirit will always be the motto for me.

To my parents, though we are in different countries for all these years, but your support and love are always with me. Mom, your love and patience guided me to go through the tough years when I first came to the US. Dad, your continuous lectureship over the phone helped me keep up with the hard training.

To my girlfriend, Fei, you have given my life in graduate school lots and lots of fun. To our three lovely cats, Pat, Huajuan, and Tiger (passed away in 2013 spring), you made our lives more colorful and enjoyable, especially when life and science became difficult.

To the funding resources: the graduate training program of the IGPBS and the Department of Pharmacology, Toxicology and Therapeutics in KUMC, NIH funding, CEED funding from Rutgers University.

To all my friends in Kansas and New Jersey, you guys gave me lots of fun and encouragement as well. And to anyone else, who I have inevitably forgotten or could not mention, thank you for your contribution, small or large.

Table of Contents

List of Figures and Tables

List of Abbreviations

ABCB4: ATP-binding cassette, sub-family B (MDR/TAP), member 4

ABCB11: ATP-binding cassette, sub-family B, member 11

ABCC2: ATP-binding cassette, sub-family C (CFTR/MRP), member 2

Abcd2: ATP-binding cassette, sub-family d (ALD), member 2

ABCG5: ATP-binding cassette, sub-family G, member 5

ABCG8: ATP-binding cassette, sub-family G, member 5

ACC: acetyl-CoA carboxylase

ACTBP11: actin, beta pseudogene 11

AF: activation motif

ALA: α-linoleic acid

ALP: alkaline phosphatase

ALT: alanine transaminase

ANIT: α-naphthylisothiocyanate

ANGPTL-3: angiopoietin-like protein 3

AOC3: amine oxidase, copper containing 3

APOA-I: apolipoprotein A-I

APOC-II: apolipoprotein C-II

APOC-III: apolipoprotein C-III

APOE: apolipoprotein E

ASBT: apical sodium dependent bile salt transporter

AST: aspartate aminotransferase

ATP8B1: ATPase, aminophospholipid transporter, class I, type 8B, member 1

BA: bile acid

BAAT: bile acid-CoA: amino acid N-acyltransferase

BACS: BA CoA synthase

BDL: bile duct ligation

BSEP: bile salt export pump

CA: cholic acid

CARM-1: Coactivator associated arginine (R) methyl transferase-1

CCK: cholecystokinin

CCK-OP: cholecystokinin-octapeptide

CETP: cholesteryl ester transfer protein

CD36: cluster of differentiation 36

$^{2}H_{4}$-CDCA: chenodeoxycholic-2,2,4,4-d_{4}acid

CDCA: chenodeoxycholic acid

CDS: coding DNA sequence

ChIP: chromatin immunoprecipitation

ChIP-qPCR: chromatin immunoprecipitation followed by quantitative PCR

ChIP-seq: chromatin immunoprecipitation followed by massive parallel sequencing

ChREBP: carbohydrate-responsive element-binding protein

cJNK1: c-Jun-N-terminal kinase 1

CO: cut off

CREBP: cAMP regulatory element-binding protein

Cyp2b10: cytochrome P450, family 2, subfamily b, polypeptide 10

CYP27A1*:* cytochrome P450, family 27, subfamily A, polypeptide 1

CYP7A1: cytochrome P450, family 7, subfamily A, polypeptide 1; cholesterol 7 alpha-hydroxylase

CYP7B1: cytochrome P450, family 7, subfamily B, polypeptide 1

CYP8B1: cytochrome P450, family 3, subfamily B, polypeptide 1; sterol 12-alpha-hydroxylase

CYP3A4: cytochrome P450, family 3, subfamily a, polypeptide 4

DAVID: Database for Annotation, Visualization and Integrated Discovery

DBD: DNA binding domain

DCA: deoxycholic acid

Dex: Dextrose

DHA: docosahexaenoic acid

DKO: double knockout

DMSO: dimethyl sulfoxide

DRIP-205: vitamin D-interacting protein 205

DR-1: direct repeat separated by one nucleotide

DSS: dextran sulphate sodium

EGF-A: epidermal growth factor-like repeat A

EPA: eicosapentaenoic acid

ER-2: everted repeat separated by two nucleotides

ER-8: everted repeat separated by eight nucleotides

FA: fatty acid

FABP3: fatty acid binding protein 3

FBP1: fructose 1, 6-bis phosphatase

HDL: high-density lipoprotein

FDR: false discovery rate

FGF15/19: fibroblast growth factor 15/19

FGFR4: fibroblast growth factor receptor 4

FOLE: fish oil based lipid emulsion

FOXA1: foxhead box protein A1

FXR: farnesoid X receptor

FXRRE: FXR response element

G6Pase: glucose-6-phosphatase

GCDCA: glycochenodeoxycholic acid

$^{2}H_4$-GCDCA: glycochenodeoxycholic-2,2,4,4-d_4 acid

GCA: glycocholic acid

GCDCA: glycochenodeoxycholic acid

GC/LC: gas or liquid chromatography

GDCA: glycodeoxycholic acid

GGT: γ-glutamyl transferase

GHDCA: glycohyodeoxycholic acid

GLCA: glycolithocholic acid

GLP: glucagon-like peptide

GUDCA: glycoursodeoxycholic acid

GFOD2: glucose-fructose oxidoreductase domain containing 2

GO-BP: Gene Ontology Biological Process

HCC: hepatocarcinogenesis

HDL: high-density lipoprotein

HDCA: hyodeoxycholic acid

HNF-4α: hepatocyte nuclear factor 4 alpha

HS6ST1: heparan sulfate 6-O-sulfotransferase 1

IBABP: ileal bile acid binding protein

IACUC: Institutional Animal Care and Use Committee

ICAM1: intercellular adhesion molecule 1

ICP: intrahepatic cholestasis of pregnancy

IEC: intestinal epithelial cells

IEL: intraepithelial lymphocytes

IL-1: interleukin-1

IL-17: interleukin-17

IL-8: interleukin-8

IP: immunoprecipitation

IR: insulin receptor

IRS1: insulin receptor substrate 1

IR-1: inverted repeat separated by one nucleotide

JAK-STAT: Janus kinase-signal transducer and activator of transcription

KC: Kupffer cell

KEGG: Kyoto Encyclopedia of Genes and Genomes

KO: knockout

LA: linoleic acid

LBD: ligand binding domain

LCA: lithocholic acid

LDL: low-density lipoprotein

LDLR: low-density lipoprotein receptor

LFT: liver functional tests

LPL: lipoprotein lipases

LRH-1: liver receptor homolog 1

L-FABP: liver fatty acid binding protein

MACS: model-based analysis of ChIP-seq

MBD: metabolic bone disorders

α-MCA: α-muricholic acid

β-MCA: β-muricholic acid

γ-MCA: γ-muricholic acid

MCT: median chain triglyceride

MDCA: murideoxycholic acid

MDR2: multidrug resistance protein 2

MDR3: multidrug resistance protein 3

MEME: multiple EM for motif elicitation

MIR122: microRNA 122

MOX: O-methoxylamine hydrochloride

MRP2: multidrug resistance-associated protein 2

MRP3: multidrug resistance-associated protein 3

MSTFA: N-methyl-N-trimethylsilyl trifluoroacetamide

MSUD: maple syrup urine disease

MTP: microsomal triglyceride transfer protein

NAFLD: non-alcoholic fatty liver disease

NASH: nonalcoholic steatohepatitis

NCOR: nuclear corepressor

NFκB: nuclear factor kappa B

NICU: neonatal incentive care unit

NR: nuclear receptor

NR0B2: nuclear receptor subfamily 0, group B, member 2

NR1H4: nuclear receptor subfamily 1, group H, member 4

NTCP: Na/taurocholate cotransporting polypeptide

OA: oleic acid

OATP: organic anion transporting polypeptides

OST-α: organic solute transporter alpha

OST-β: organic solute transporter beta

PA: palmitic acid

PBC: primary biliary cirrhosis

PC: phosphatidylcholine

PCA: principle component analysis

PCR: polymerase chain reaction

PCSK9: proprotein convertase subtilisin/kexin type 9

PEPCK: phosphoenolpyruvate carboxykinase

PFIC: progressive familial intrahepatic cholestasis

PGC-1α (PPARGC1α): peroxisome proliferator-activated receptor gamma, coactivator 1 alpha

PHH: primary human hepatocyte

PHH-DMSO: ChIP-seq for DMSO treated PHHs

PHH-GW: ChIP-seq for GW4064 treated PHHs

PI3K: phosphatidylinositol 3 kinase

PN: parenteral nutrition

PNAC: parenteral nutrition associated cholestasis

PNALD: parenteral nutrition associated liver disease

PNMT: phenylethanolamine N-methyltransferase

PPAR: peroxisome proliferator-activated receptor

PRMT-1: protein arginine (R) methyl transferase-1

PSC: primary sclerosing cholangitis

PUFA: polyunsaturated fatty acids

PXR: pregnane X receptor

qPCR: quantitative polymerase chain reaction

R-PHH-GW: RNA-seq for PHHs

RBC: red blood cell

RCT: reverse cholesterol transport

rIgG: rabbit immunoglobulin G

RNA Pol II: RNA polymerase II

RORα: retinoic acid-related orphan receptor alpha

RORγ: retinoic acid-related orphan receptor gamma

RXRα: retinoic X receptor alpha

SA: stearic acid

SBS: short bowel syndrome

SEM: standard error of the mean

SHP: small heterodimer partner

SIRT1: sirtuin-1

SMRT: silencing mediator of retinoic acid and thyroid hormone receptor

SOLE: soybean oil based lipid emulsion

SR-B1: scavenger receptor B1

SRC-1: steroid receptor coactivator 1

SREBP-1c: sterol regulatory element-binding protein 1c

TCA: taurocholic acid

TDCA: taurodeoxycholic acid

TF: transcription factor

THDCA: tauro hyodeoxycholic acid

TLCA: taurolithocholic acid

TLR4: toll like receptor 4

T-α-MCA: tauro-α-muricholic acid

T-β-MCA: tauro-β-muricholic acid

T-γ-MCA: tauro-γ-muricholic acid

TNFα: tumor necrosis factor alpha

TNFR: tumor necrosis factor alpha receptor

TSBA: total serum bile acid

TSS: transcription start site

TUDCA: tauroursodeoxycholic acid

UDCA: ursodeoxycholic acid

UROC1: urocanate hydratase 1

UTR: untranslated region

VLDL: very low-density lipoprotein

WBKO: whole-body knockout

WT: wild type

Chapter 1: Introduction and Background

1.1 FXR and BA Homeostasis

1.1.1 FXR Gene and Protein

Farnesoid X Receptor (FXR/ *NR1H4*) is a well-characterized type II nuclear receptor (NR) belonging to the NR superfamily. NRs are ligand-activated transcription factors responding to enteral and external metabolites, including steroids, vitamins, dietary lipids, etc. (Mangelsdorf et al. 1995, Chawla et al. 2001). The NRs have been shown to play important roles involved in many aspects of mammalian physiology and/or pathology when they are deregulated. In 1995, FXR was initially cloned in yeast and shown to heterodimerize with retinoid X receptor alpha (RXRα) (Seol, Choi and Moore 1995). Later the same year, the mouse homologue was cloned and subsequently named FXR upon the finding that supra-physiological concentrations of farnesol could activate this NR. Four years afterwards, bile acids (BAs) were confirmed as the endogenous ligands of FXR by several groups simultaneously (Makishima et al. 1999, Wang et al. 1999, Parks et al. 1999).

There were two FXR genes in humans and rodents, *FXRα (NR1H4/Nr1h4)* and *FXRβ (NR1H5/Nr1h5*). FXRβ is expressed in rodents while it is a pseudogene in humans (Otte et al. 2003). Only limited information exists regarding the ligands and functions of FXRβ. Four transcript isoforms are encoded by the single *FXRα/Fxrα* gene in both humans and mice, named FXRα1 to FXRα4, resulting from two different transcription start sites (TSSs) (5' promoter for exon 1 and 3' promoter for exon 3) and subsequent alternative splicing (exon 5) (Huber et al. 2002, Zhang, Kast-Woelbern and

Edwards 2003). The four FXRα proteins differ slightly regarding the amino acid sequences and all four share critical NR features (Huber et al. 2002, Zhang et al. 2003). Studies have only shown slight functional differences among the four FXRα isoforms in terms of expression patterns and transactivation activities (Modica, Gadaleta and Moschetta 2010). The majority of the *in vivo* and *in vitro* experimental technologies that biologists have applied to study the function of FXR, will not differentiate the four isoforms, such as gene knockout, mRNA expression, antibody recognition, etc. In this regard, FXR will be used in this dissertation unless otherwise specified.

FXR is highly expressed in tissues in which BA homeostasis is tightly regulated, including the liver, intestine and kidney. FXR is also expressed moderately in the adrenal gland and minimally in the heart and adipose tissues (Zhang et al. 2003). FXR protein features classic NR structure characteristics (**Figure 1.1**), which includes a N-terminal ligand independent activation motif (AF1), a highly conserved DNA binding domain (DBD) containing two cysteine-coordinated Zn^{2+} finger motifs, a hinge region followed by a moderately conserved C-terminal ligand binding domain (LBD), and a ligand-dependent activation motif (AF2) in the C-terminus (Zhang et al. 2003). It is well acknowledged now that FXR forms heterodimer with RXRα and binds to DNA prior to ligand binding, mediated by the DBD with the two Zn^{2+} finger motifs (Modica et al. 2010). Our genome-wide FXR chromatin binding results also support this theory (Thomas et al. 2010). Previous studies obtained from the association of FXR with individual FXR target genes and recent genome-wide studies confirmed that FXR/RXR heterodimer mainly bind to the IR1 DNA motif (inverted repeat of canonical A/GGG/TCA separated by one nucleotide) (Modica et al. 2010, Thomas et al. 2010, Chong et al. 2010). Other FXR

response elements (FXRRE) include DR-1 (direct repeat separated by one nucleotide) and ER-8 (everted repeat separated by eight nucleotides), etc (Modica et al. 2010). As underlined by the moderately conserved sequence, the LBD of FXR presents a classic NR structure of a 12-α helix bundle, as well as a hydrophobic pocket suitable for accommodating lipophilic molecules such as BAs (Downes et al. 2003). Upon ligand binding, the LBD of FXR undergoes conformational changes, which trigger the release of common NR corepressors and the recruitment of transcriptional coactivators (Downes et al. 2003). Two protein methyl transferase, coactivator associated arginine (R) methyl transferase-1 (CARM-1) and protein arginine (R) methyl transferase-1 (PRMT-1), as well as common NR coactivators, steroid receptor coactivator 1 (SRC-1), peroxisome proliferator-activated receptor gamma coactivator 1-alpha (PGC-1α), and vitamin D-interacting protein 205 (DRIP-205) have been shown to be FXR coactivators (Modica et al. 2010, Savkur et al. 2005, Ananthanarayanan et al. 2004, Rizzo et al. 2005, Pineda Torra, Freedman and Garabedian 2004, Bauer et al. 2002, Zhang et al. 2004). Besides modulations by ligands, FXR itself has been shown to be dynamically regulated by the protein acetylase p300 and its counterpart sirtuin-1 (SIRT1), a NAD+-dependent deacetylase (Kemper et al. 2009). Acetylation at residue lysine 217 in the hinge region of FXR increases its protein stability, but inhibits its ability to heterodimerize with RXRα, resulting in inhibition of DNA binding and subsequent suppression of the target genes.

1.1.2 BAs, the Endogenous Ligand of FXR

BAs are amphipathic molecules synthesized from cholesterol in the liver by two major pathways, the classic and alternative pathways (Russell 2003). The chemical structures of major BAs are shown in **Figure 1.2**. Cytochrome P450, family 7, subfamily A, polypeptide 1 (CYP7A1, also known as cholesterol 7 alpha-hydroxylase), which is located on the endoplasmic reticulum membrane, is the first and the rate-limiting enzyme in the classic pathway (Russell 2003). CYP7A1 and multiple downstream enzymes convert cholesterol into cholic acid (CA) and chenodeoxycholic acid (CDCA). The alternative pathway is initiated by mitochondrial cytochrome P450, family 27, subfamily A, polypeptide 1 (CYP27A1) and followed by cytochrome P450, family 7, subfamily B, polypeptide 1 (CYP7B1) to generate CDCA. Therefore, both CA and CDCA are primary BAs in humans. While CYP7A1 regulates the total amount of BA, cytochrome P450, family 8, subfamily B, polypeptide 1 (CYP8B1, also known as sterol 12-alpha-hydroxylase) determines the ratio of CA: CDCA in the BA pool and CA is less hydrophobic than CDCA. In rodents, most CDCA undergoes hydroxylation at the 6β-position to form α-muricholic acid (α-MCA) (Russell 2003). α-MCA can be further converted to β-muricholic acid (β-MCA) by epimerization of its 7α-OH into 7β-OH (Botham and Boyd 1983). Therefore, CA and α- and β-MCA are the major primary BAs in rodents. Hepatic BA synthesis is also responsible for a major fraction of daily cholesterol turnover in humans.

Primary BAs then undergo multiple biotransformation steps in the liver and during the enterohepatic circulation. Primary BAs are first transformed and activated into CoA-thioesters by the BA CoA synthase (BACS) in the liver. Activated BAs become the substrates for the BA-CoA:amino acid N-acetyltransferase (BAAT) enzymes, which

catalyze the glycine or taurine conjugation of primary BAs (Ridlon, Kang and Hylemon 2006). The conjugation process is highly efficient and the conjugated BAs are referred to as “bile salts”. Compared to primary BAs, the bile salts are more hydrophilic, less cytotoxic and more readily to be secreted into the bile through the canalicular transporting system. Upon postprandial stimulus, BAs are actively secreted from the gallbladder through gallbladder contraction into the small intestine, to allow the absorption of lipophilic nutrients. In the intestine, BAs undergo a second round of multi-step biotransformation mediated by the resident gut bacteria (Ridlon et al. 2006). In the small and large intestines, bacterial bile salt hydrolases can de-conjugate some bile salts into free BAs. In the large intestine, bacterial 7α-dehydroxylase converts CA to deoxycholic acid (DCA), and CDCA to lithocholic acid (LCA), respectively, by removing a hydroxyl group from C-7 (**Figure 1.2**). DCA and LCA are termed secondary BAs and are highly toxic, mainly due to their high level of hydrophobicity compared to CA and CDCA (**Figure 1.2**). DCA is mainly reabsorbed in the large intestine via passive absorption, followed by detoxification in the liver to form taurodeoxycholic acid (TDCA). LCA, on the other hand, is mostly sulfated for fecal excretion, and only a small amount (~1%) will be passively absorbed. In the liver, LCA undergoes either sulfation or hydroxylation to reduce its toxicity. Detoxified LCA will be efficiently secreted into circulation for renal excretion. In human liver microsomes, LCA can be hydroxylated to form hyodeoxycholic acid (HDCA), murideoxycholic acid (MDCA), and CDCA (Li and Chiang 2014).

Among all the natural BA species in humans and rodents, CDCA has been shown to be the most potent FXR activator, mainly due to the optimal interaction

between the 7α-OH group of CDCA and FXR LBD (Modica et al. 2010). The EC_{50} of CDCA and its glycol- and tauro-conjugates was shown to be 50 μM and 10 μM for murine and human FXR, respectively (Makishima 1999). On the contrary, BAs without a 7α-OH group, such as DCA and LCA, are more likely to be partial agonist. In addition, due to the presence of a 12α-hydroxy group, which cannot accommodate with the FXR LBD, CA and DCA actually have relatively low affinity for human FXR (Makishima 1999). It is worth noting that FXR LBD is not completely the same between humans and mice. The mouse FXR LBD has been found to be much more responsive to CA than the human one (Cui et al. 2002). In results, CA becomes more physiological important in mice in terms of FXR activation, since CDCA is converted into α- and β-MCA in mice.

Ursodeoxycholic acid (UDCA), another important natural BA, found predominately in bear, is currently the only FDA approved pharmacological therapy for the management of cholestasis. And it's interesting that UDCA has been shown to be a very weak FXR agonist (Lew et al. 2004).

1.1.3 Enterohepatic Circulation of BAs

As illustrated in **Figure 1.3,** after synthesis and conjugation, primary BAs are actively secreted from hepatocytes into the bile canaliculus through trans-membrane transporter systems. ATP-binding cassette (ABC) family transporters, bile salt export pump (BSEP/ *ABCB11*) and multidrug related protein 2 (MRP2/*ABCC2*) are responsible for active secretion of monoanionic- and dianionic-conjugated BAs, respectively (Modica et al. 2010). BSEP specifically mediates the efflux of BAs while MRP2 also mediates the

transport of other organic substrates, such as bilirubin conjugates, glutathione, drugs, etc. Other major organic constitutes of bile include phospholipids and cholesterol, which form mixed micelles in bile to increase cholesterol solubility as well as to reduce BA cytotoxicity to the bile duct and gallbladder. In addition, normal secretion of phospholipid, mainly phosphatidylcholine (PC), is required for biliary BA secretion. The efflux of PC is mediated by a phospholipid flippase, the multidrug protein 3/2 (MDR3/*ABCB4* in humans, MDR2/*Abcb4* in mice).

Upon postprandial stimulus, duodenum secretes cholecystokinin (CCK), which stimulates gallbladder contraction and the release of BAs into the small intestine. Along the small intestinal tract, BAs mainly function as detergents to facilitate the solubilization, digestion and absorption of lipophilic nutrients. In the distal ileum, conjugated BAs are actively reabsorbed by enterocyte sodium-dependent bile salt transporter (ASBT/*SLC10A1*) (Shneider et al. 1995), while unconjugated BAs are only partially absorbed by passive diffusion. After crossing the apical membrane of enterocytes, BAs are actively shuttled to the basolateral membrane upon binding to the ileal bile acid binding protein (IBABP) (Gong et al. 1994). BAs are then secreted into the portal blood through the heterodimeric organic solute transporter α/β (OST-α/β) (Lee et al. 2006). Once reaching the basolateral (sinusoidal) membrane of hepatocytes, conjugated and free BAs are actively re-absorbed into hepatocytes via Na^+-dependent and -independent mediators, respectively. The Na^+-dependent taurocholate transporter (NTCP) is specific for the uptake of conjugated BAs, while several organic anion-transporting polypeptides (OATPs) have substrate specificities for unconjugated BAs, including OATP1A2, OATP1B1 and OATP1B3 in humans (St-Pierre et al. 2001).

After the enterohepatic circulation, about 90-95% of total BAs are reabsorbed in the intestine with around 0.5 g/day of BAs are secreted into the feces. The loss in the feces will be replenished by the *de novo* BA synthesis in the liver. The BA pool size is defined as the total amount of BAs in the entire enterohepatic circulation. As mentioned earlier, BA compositions in humans and mice are very different. Human BA pool consists of about 40% each of CA and CDCA, and 20% DCA, thus is more hydrophobic. Mouse BA pool consists about 50% CA and 50% α- and β-MCAs, and is more hydrophilic.

BAs are detergent-like molecules, so accumulation of high levels of BAs, especially secondary BAs, can be detrimental. BA cytotoxicity increases linearly with its hydrophobic index, with the order of increasing cytotoxicity being UDCA, CA, CDCA, DCA and LCA (**Figure 1.2**). In this regards, the concentration of intra- and extra- cellular BAs are regulated in multiple levels under normal physiology to ensure BA homeostasis.

1.1.4 FXR as the BA Sensor

As a transcription factor, FXR mainly functions to induce and to a much lesser extent, suppress the transcription of its direct target genes. The combined effects from direct and indirect transcriptional regulation by FXR play a major role in maintaining BA homeostasis. By inducing the expression of its target genes, small heterodimer partner, (SHP/*NR0B2*) in the liver, and fibroblast growth factor 15/19 (FGF15 in mice, FGF19 in humans) in the intestine, FXR activation indirectly suppresses the expression of CYP7A1 and CYP8B1 in the liver (Kong et al. 2012b). Both SHP and FGF15/19 are

unique in their corresponding superfamilies. Specifically, SHP, an atypical nuclear receptor, lacks the classical NR DNA-binding domain and mainly functions as a transcriptional repressor by heterodimeric interaction with various transcriptional regulators, including many NRs (Garruti et al. 2012). SHP has been shown to suppress the gene expression of CYP7A1 and CYP8B1 by interfering with the transactivation activity of liver receptor homolog-1 (LRH-1) *in vitro* (Goodwin et al. 2000). FGF15/19, unlike most FGFs, lacks a heparin-binding site and FGF15/19 acts like hormones and binds to the cell surface fibroblast growth factor receptor 4 (FGFR4) to initiate the downstream signaling events (Inagaki et al. 2005). Using novel genetic modified mouse models, the most recent *in vivo* studies suggest that the intestinal FXR-FGF15 pathway plays a major role in suppressing the gene expression of *Cyp7a1*, whereas the hepatic FXR-SHP pathways is less important for *Cyp7a1* suppression in mice (Kong et al. 2012a). In addition, both pathways are suggested to be critical in suppressing *Cyp8b1* expression (Kong et al. 2012a).

Following BA synthesis in the liver, FXR regulates BA homeostasis through direct targeting. First, FXR regulates BA amidation by positively regulating the gene expression of BAAT and BACS (Pircher et al. 2003). Second, FXR activation directly induces the expression of BA transporters BSEP (Ananthanarayanan et al. 2001) and MRP2 (Kast et al. 2002) to facilitate BA export from the hepatocytes. FXR also directly regulates the PC transporter MDR2 (Liu et al. 2003) and the cholesterol transporters ATP-binding cassette, sub-family G, member 5 (ABCG5) and ATP-binding cassette sub-family G, member 8 (ABCG8) to maintain coordinated biliary secretion of BAs, cholesterol and phospholipids (Li et al. 2011). NTCP and OST-α/β are also expressed in

the liver, and mediate BA transport across the basolateral membrane. FXR activation down-regulates the liver BA uptake transporter NTCP via induction of SHP (Denson et al. 2001), as well as by direct up-regulation of OST-α/β to facilitate BA efflux to the systemic circulation (Lee et al. 2006). The combined effects of FXR on NTCP and OST-α/β in the liver help to decrease the intracellular levels of BAs in hepatocytes. In the intestine, FXR activation could indirectly suppress the expression of the uptake transporter, ASBT, as well as directly induce the sinusoid efflux transporters, OST-α/β, to protect the enterocytes from intracellular BAs build-up. The inhibition of ASBT by FXR was first shown by induction of SHP after FXR activation in human intestinal cell lines (Neimark et al. 2004). Later on, intestinal FGF15/19 was shown to mediate the inhibition of ASBT in different human and mouse cell lines as well (Sinha et al. 2008). Finally, inside the enterocytes, FXR activation induces IBABP through direct promoter binding (Grober et al. 1999).

Similar to the liver and intestine, FXR also regulates the active transport of BAs in the kidney and bile duct. In both sites, ASBT mediates the uptake of conjugated BAs, in the canalicular membrane of cholangiocytes and the apical membrane of proximal renal tubular cells (Craddock et al. 1998). While multidrug related protein 3 (MRP3/*ABCC3*) and OST-α/β are involved in BAs efflux back to bile from cholangiocytes in the biliary tract, OST-α/β is responsible for renal secretion of BAs back to systemic circulation in the kidney (Ballatori et al. 2005). The proper functions of ASBT and OST-α/β could ensure the sensing of normal BA levels in the circulation as well as the avoidance of renal secretion of BAs in the urine, respectively.

1.1.5 Cholestasis and FXR

The coordinated function of the molecular machinaries involved in the enterohepatic circulation of BAs maintain the proper levels of intra- and extra- cellular BAs to avoid BA cytotoxicity. And disruption of the normal BA homeostasis could lead to cholestasis. Cholestasis is defined as the retention of BAs in the hepato-biliary tract (Trauner, Meier and Boyer 1998). There are many causes of cholestasis. Depending on whether the cause is inside or outside the liver, cholestasis is classified mainly as intra- or extra- hepatic. The cause of Extrahepatic cholestasis occurs outside the liver and can be caused by bile duct tumors, stones in the common bile duct, pancreatitis, pressure on the bile ducts due to a nearby mass or tumor, primary sclerosing cholangitis (PSC), etc.. In these cases, the normal bile flow from the gallbladder into the intestine is disrupted. Intrahepatic cholestasis occurs inside the liver and can be caused by genetic mutations, alcoholic liver disease, bacterial abscess in the liver, total parenteral nutrition, lymphoma, pregnancy, primary biliary cirrhosis (PBC), viral hepatitis, etc.. And in these cases, the normal bile flow from the liver into the gallbladder is disrupted. Intrahepatic cholestasis will be the primary focus in this dissertation.

Mutations in several genes, which encode the various transporters involved in BA circulation as mentioned above, have been linked to a class of genetic diseases, progressive familial intrahepatic cholestasis (PFIC). Currently, there are three known types of PFIC: PFIC-1, PFIC-2, and PFIC-3. PFIC-2 is linked to mutations in the major human BA transporter BSEP, which is also linked to intrahepatic cholestasis of pregnancy (ICP) (Song et al. 2014). PFIC-1 and PFIC-3 are linked to the genes encoding phospholipids transporters, ATPase, aminophospholipid transporter, class I,

type 8B, member 1 (*ATP8B1*) and MDR3 (*ABCB4*, MDR2/*Abcb4* in mice), respectively (Groen et al. 2011). ATP8B1, also called FIC-1, is a P-type ATPase. In complex with the accessory protein transmembrane protein 30A (TMEM30A), FIC-1 flips PC from the outer to the inner leaflet of plasma membrane, whereas MDR2/3 flops PC in the reverse direction (Groen et al. 2011). Deficiency in MDR2/3 leads to the absence of PC in bile. PCs function as BA chaperones, preventing BA toxicity to the biliary epithelium. The free or "unchaperoned" BAs in the bile of patients with MDR3 deficiency cause cholangitis. Therefore, unlike PFIC-1 or PFIC-2, PFIC-3 is associated with markedly elevated serum levels of γ-glutamyl transferase (GGT), a marker of biliary injury (Li and Chiang 2014). Finally, the inheritance pattern of all these three forms of PFIC is autosomal recessive. These genetic disorders underline the importance of these transporters involved in the enterohepatic circulation of BAs.

Clinically, biochemistry and histology examinations are commonly used to diagnose cholestasis and identity the etiology. Serum biomarkers of cholestasis include elevated levels of total serum bile acids (TSBA), bilirubin, alkaline phosphatase (ALP), and GGT (Li and Crawford 2004). Evaluation of these biomarkers alone could not provide a definitive diagnosis of the cause of cholestasis. Therefore, histological examination of the liver is often required for a more accurate diagnosis. Histological markers for cholestasis include bilirubin pigment accumulation that gives hepatocytes a reddish brown color, hepatocellular degeneration, bile duct proliferation, the presence of inflammatory cells typically in periportal regions, and at later stages, peribiliary fibrosis (Li and Crawford 2004).

While many genetic and non-genetic causes could lead to cholestatic liver diseases, UDCA is currently the only pharmaceutic drug approved by the FDA for the treatment of cholestasis regardless of the etiology. Although PBC patients treated with UDCA showed an improvement in liver biochemistry, jaundice, and ascites, UDCA did not decrease mortality or requirement of liver transplantation (Gong et al. 2008). And overtime, if the underlying cause of cholestasis is not resolved, the disease will progess to fibrosis, and eventually cirrhosis.

In this regard, various animal models of cholestasis have been developed to study the molecular and cellular pathologenesis of cholestasis, in order to discover novel treatment for the disease (Rodriguez-Garay 2003). For intrahepatic cholestasis, the most commonly used animal models are genetic deficency-induced, estrogen-induced, endotoxin-induced and drug-induced cholestasis (Rodriguez-Garay 2003). Several genetic engineered mouse models have been developed to mimic the human PFICs. Cholestatic liver abnormalities have been recapituated well in mice with deficient ATP8B1, BSEP and MDR2 protein, respectively (Shah et al. 2010, Groen et al. 2011, Zhang et al. 2012b). Interestingly, the severity of cholestatic disorders in mutant mice also depends on the genetic background, i.e., the mouse strains. For both *Atp8b1* and *Abcb11* mutants, C57BL/6J mice have shown greater liver injury than other stains (Zhang et al. 2012b, Shah et al. 2010). For extrahepatic cholestasis, common bile duct ligation is mostly used. In the later part of this disseration, a special type of intrahepatic cholestasis, named parenteral nutrition associated cholestasis (PNAC), will be discussed in detail.

The improtance of FXR involved in BA homeostasis and cholestasis has been further confirmed by studies using various genetic modified mouse models. Unlike mice with deficient ATP8B1 or MDR2, FXR whole body knockout mice (FXR-WBKO) didn't show severe cholestatic phenotypes in early age under normal feeding condition (Sinal et al. 2000). Nevertheless, FXR-WBKO mice have elevated levels of serum BAs and triglycerides, featuring hepatic steatosis, which eventually lead to spantaneous hepatocellular carcinogenesis (Kim et al. 2007). And upon challenge with diet containing 1% CA, FXR-WBKO mice developed severe hepatotoxicity even with only 5 days of treatment (Sinal et al. 2000). Using gain-of-function strategies, recent studies have shown that intestinal FXR activation protected mice from both cholestasis and spontaneous hepatocellular carcinogenesis (Modica et al. 2012, Degirolamo et al. 2014). Modica et al showed that constitutive intestinal FXR activation protected mice against obstructive extrahepatic cholestasis following bile-duct ligation or administration of α-naphthylisothiocyanate (ANIT), as well as intrahepatic cholestasis from MDR2 defiency (Modica et al. 2012). As expected, liver damage was further exacerbated in FXR and MDR2 double knockout (DKO) mice. Furthermore, they also showed that FGF19 administration protected the mice from obstructive extrahepatic cholestasis through the reduction of total BA pool size without further induction of adaptive hepatic responses (Modica et al. 2012). Using similar strategy, by crossing FXR-WBKO mice with intestinal specific transgenic iVP16FXR mice, the same group showed that constitutive intestinal FXR activation was able to rescue FXR-WBKO mice from BA overload, and to prevent hepatocarcinogenesis (HCC) formation by maintaining BA homeostasis via restoration

of intestinal FXR-FGF15 signaling, limiting hepatic inflammation and proliferation while maintaining the intestinal epithelium integrity (Degirolamo et al. 2014).

Figure 1.1 Schematic Protein Structure of FXR

From left to right: N-terminal activation motif (AF1), DNA binding domain (DBD), hinge region (Hinge), C-terminal ligand binding domain (LBD), and C-terminal activation motif (AF2). * For FXRα1 and FXRα3, there are four additional amino acids, MYTG, between the DBD and the hinge region, which are not present in FXRα2 and FXRα4.

Figure 1.2 Chemical Structures of Major BAs

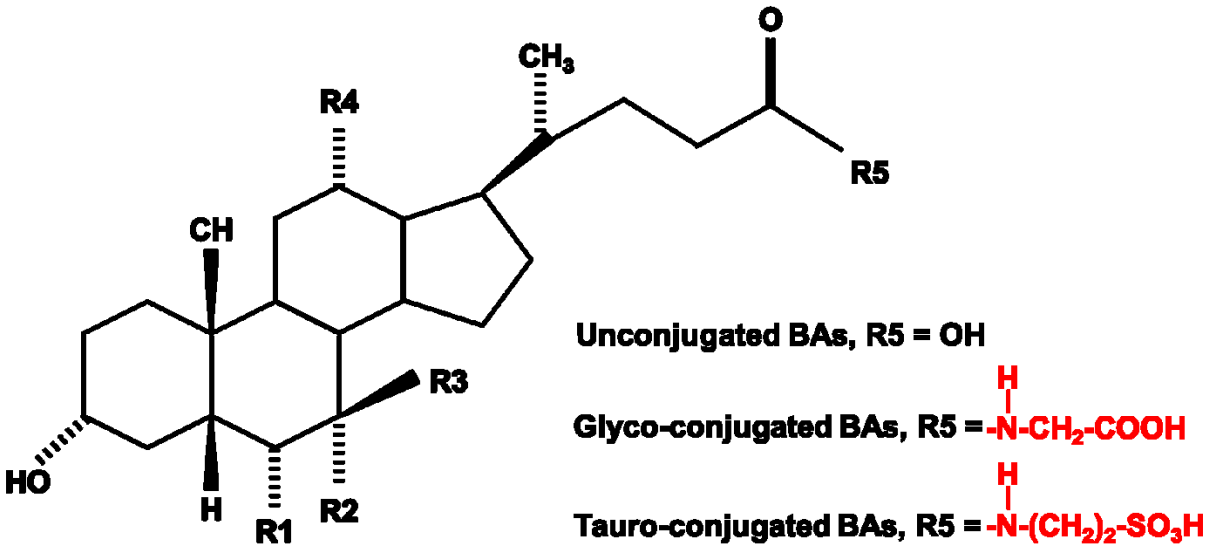

	R1	R2	R3	R4
UDCA	H	OH	H	H
CA	H	OH	OH	OH
CDCA	H	OH	OH	H
DCA	H	H	H	OH
LCA	H	H	H	H
α-MCA	β-OH	OH	H	H
β-MCA	β-OH	H	OH	H

Figure 1.3 Enterohepatic Circulation of BAs

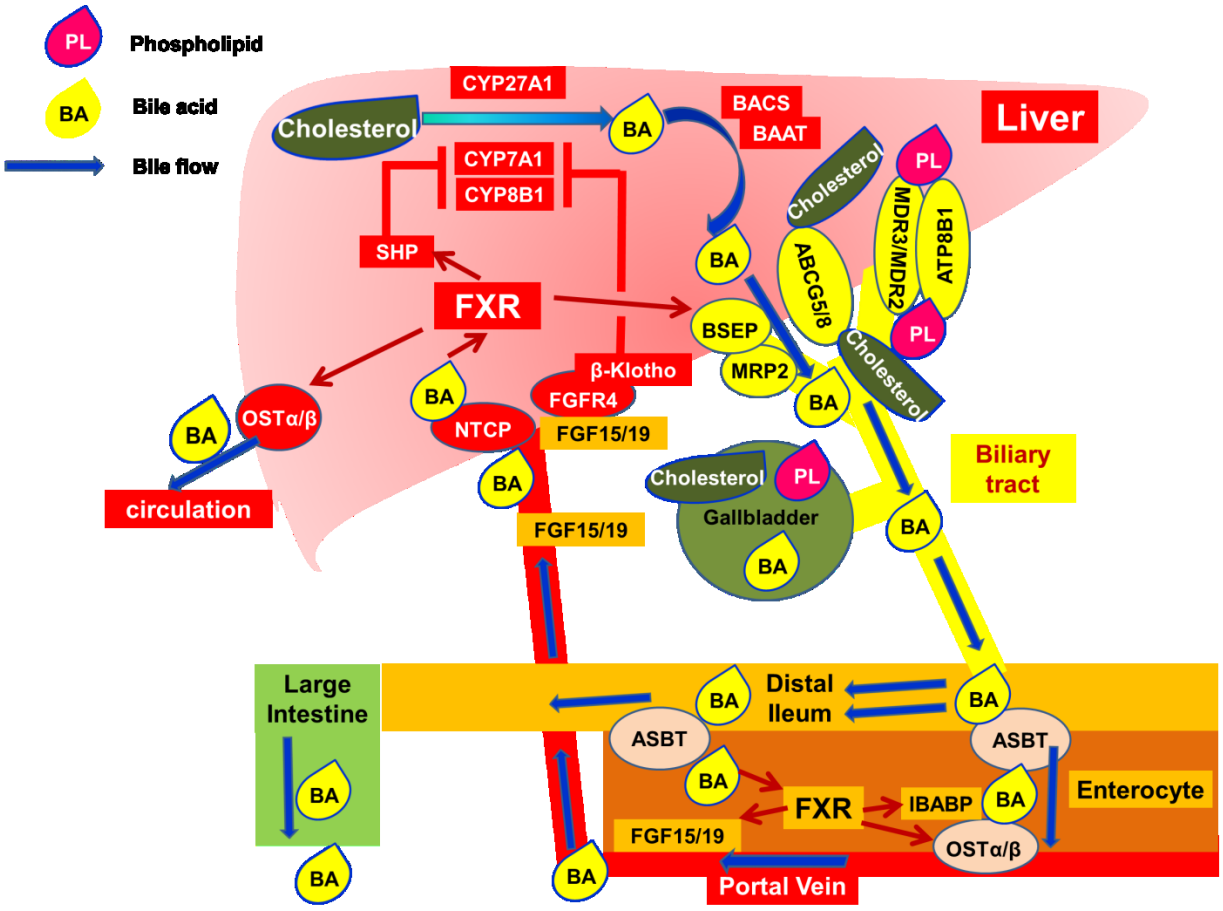

See detailed description in the text.

1.2 FXR beyond the BA Sensor

1.2.1 FXR Regulation of Triglyceride/Cholesterol Metabolism

As mentioned above, FXR-WBKO mouse exhibited a potential proatherogenic serum lipoprotein profile (Lambert et al. 2003). In detail, under normal feeding, FXR-WBKO mice had markedly elevated serum levels of cholesterol, cholesterol esters, triglycerides, and phospholipids (Sinal et al. 2000). Besides, serum levels of very low-density lipoprotein (VLDL), LDL, and high-density lipoprotein (HDL) were increased in FXR-WBKO mice. In the liver, hepatic triglyceride levels were also increased significantly in FXR-WBKO mice, while hepatic cholesterol levels were similar to control mice (Sinal et al. 2000).

Triglyceride accumulation in our body is mainly derived from two sources, dietary absorption in the intestinal tract and *de novo* synthesis in the liver. In the intestinal lumen, dietary triglycerides are emulsified by BAs and then hydrolyzed by lipase, generating a mixture of free fatty acids (FAs) and monoglycerides, which then enter into the enterocytes where they are re-esterified to form triacylglycerol. The triacylglycerol is the major component of chylomiron. After entering the systemic circulation, chylomicrons exchange components with HDL to receive apolipoprotein C-II (APOC-II) and apolipoprotein E (APOE). APOC-II is the cofactor for lipoprotein lipase (LPL) activity. Once the triglycerides are distributed, the chylomicron returns APOC-II to HDL and keeps APOE. While chylomiron is mainly responsible for absorption of exogenous lipid nutrients, VLDL functions as the internal mechanism of lipid circulation by transporting endogenous triglycerides, phospholipids, cholesterol, and cholesteryl esters. Once in

the blood stream, VLDL also picks up APOC-II and APOE from HDL. Then VLDL will encounter LPL in the capillary beds in the body, which removes triglycerides from VLDL for storage or energy production. VLDL then meets HDL again, transferring APOC-II back and keeping APOE, whereas HDL transfers cholesteryl esters to VLDL in exchange for phospholipids and triglycerides, mediated by the cholesterylester transfer protein (CETP). Excessive triglyerides are primarily cleared by FA metabolism through β-oxidation.

FXR activation regulates BA synthesis in the liver, suggesting that FXR activation could indirectly regulate lipid emulsion and subsequent triglyceride absorption in the gut, leading to increased levels of triglycerides in the body. For *de novo* synthesis of triglycerides, studies have shown that FXR suppresses sterol regulatory element-binding protein-1c (SREBP-1c) and microsomal triglyceride transfer protein (MTP), again through its important target, SHP (Watanabe et al. 2004, Hirokane et al. 2004). SREBP-1c is a master transcription factor involved in *de novo* FA synthesis in the liver, and regulates the expression of many critical genes in lipogenesis (Brown and Goldstein 2009). MTP is a microsomal transport protein facilitating VLDL efflux from the liver (Wetterau, Lin and Jamil 1997). In terms of triglyceride clearance, it has been shown that FXR activation could induce APOC-II and syndecan-1 (Kast et al. 2001, Anisfeld et al. 2003), whereas suppress APOC-III, angiopoietin-like protein 3 (ANGPTL3) and carbohydrate-responsive element-binding protein (ChREBP) (Claudel et al. 2003, Watanabe et al. 2004). Syndecan-1 is a transmembrane herpain sulfate proteoglycan involved in the clearance of lipoprotein remnants (Anisfeld et al. 2003). Unlike APOC-II, APOC-III inhibits LPL and hepatic lipase, therefore inhibiting hepatic uptake of

triglyceride-rich particles (Claudel et al. 2003). ANGPLT3, a member of the angiopoietin-like family of secreted factors, also inhibits LPL and thus increases plasma triglyceride levels. Finally, ChREBP is a glucose-activated transcription factor, which induces the expression of hepatic glycolytic and lipogenic genes. In summary, the combined effects of FXR activation on these target genes involved in triglyceride homeostasis suggest a beneficial role of FXR activation for lowering the plasma triglyceride levels.

The role of FXR modulation in cholesterol homeostasis has been studied extensively as well. In FXR-WBKO mice, serum cholesterol levels increased significantly, whereas hepatic cholesterol levels were not (Sinal et al. 2000). A follow-up study showed more detailed plasma cholesterol profiles in these mice. 1st, FXR-WBKO mice had increased plasma HDL levels and markedly decreased plasma HDL cholesterol ester clearance. 2nd, FXR-WBKO mice had increased plasma non-HDL cholesterol and APOB-containing lipoprotein synthesis. 3rd, intestinal cholesterol absorption was elevated in FXR-WBKO mice. 4th, biliary cholesterol elimination was also increased in FXR-WBKO mice (Lambert et al. 2003). It was first shown in this study that FXR-WBKO mice exhibited reduced expression of hepatic genes involved in reverse cholesterol transport (RCT), especially scavenger receptor B1 (SR-B1). In the liver, SR-B1 mainly functions in facilitating the uptake of cholesteryl esters from circulating HDLs. This process drives the transport of cholesterol from peripheral tissue towards the liver for fecal excretion and is defined as the RCT. RCT is a protective mechanism against the development of atherosclerosis. Several studies have confirmed that FXR activation would induce the gene expression of mouse *Sr-b1* (Zhang et al.

2006a, Zhang et al. 2010, Chao et al. 2010). A most recent study confirmed that FXR directly regulates *Sr-b1* gene expression via intron binding (Li et al. 2012b). In terms of cholesterol secretion, BA activation of FXR was shown to induce the levels of ABCG5 and ABCG8 in mouse livers, through a common FXRRE located in the intergenic promoter shared by *Abcg5* and *Abcg8* (Li et al. 2011). Using HepG2 cells, it was shown that FXR activation could repress the gene expression of the proprotein convertase subtilisin/kexin type 9 (PCSK9). PCSK9 is a recently discovered LDL receptor (LDLR) inhibitor, which binds to the epidermal growth factor-like repeat A (EGF-A) domain of the LDLR, resulting in LDLR degradation and decreased clearance of LDL cholesterol. Therefore, PCSK9 inhibition has been proposed to be a powerful weapon to lower LDL cholesterol levels (Steinberg and Witztum 2009).

On the contrary, using DKO strategies, studies have shown that FXR deficiency actually reduced the development of atherosclerosis in LDLR-KO mice and/or APOE-KO mice (Zhang et al. 2006b, Guo et al. 2006). In line with this, guggulsterone [4,17(20)-pregnadiene-3,16-dione], a nature product extracted from the resin of guggul tree, was shown to decrease LDL cholesterol in humans (Urizar et al. 2002). Guggulsterone was shown to be a highly effective antagonist of FXR (Urizar et al. 2002). The same year, another study showed that FXR activation could suppress APOA-I production in mice (Claudel et al. 2002). APOA-I is the major protein component of HDL in plasma. Overall, FXR activation in the liver induces SR-BI to enhance HDL uptake, whereas suppresses APOA-I to lower HDL production. In genetic deficient animal atherosclosis models, additional KO of FXR could help alleviate the desease progression during intial disease development. But in long-term high fat fed mice, FXR

deficiency caused hypertriglyceridemia may override the beneficial effects and further amplify the desease progression due to high fat feeding itself. While the research about FXR and cholesterol homeostasis from different animal models is still under debate (Li and Chiang 2014), more patients guided translational studies may provide better understanding of the function of FXR in humans.

1.2.2 FXR Regulation of Glucose Metabolism

The role of FXR in controling glucose homeostasis has also been studied extensively (Modica et al. 2010, Li and Chiang 2014).In diabetic mouse models, activation of FXR represses the expression of the genes encoding three rate-limiting enzymes involved in gluconeogenesis, phosphoenolpyruvate carboxykinase (PEPCK), glucose-6-phosphatase (G6Pase) and fructose 1, 6-bis phosphatase (FBP1) (Cariou et al. 2006, Ma et al. 2006). Consistently, FXR-WBKO mice had elevated levels of circulating and muscle free FAs (Ma et al. 2006), whereas FXR activation decreased free FA levels and increased insulin sensitivity in mice (Zhang et al. 2006a). Another important FXR target, FGF15/19, has been shown to repress hepatic glucose production and promote glycogen synthesis, without induction of lipogenesis (Kir et al. 2011). FGF15 defient mice failed to properly maintain blood concentrations of glucose and normal postprandial synthesis of liver glycogen. It was shown that FGF15/19 downregulated the expression of genes involved in gluconeogenesis through dephosphorylation and inactivation of the transcription factor cAMP regulatory element-binding protein (CREBP) (Kir et al. 2011). This in turn decreased the expression of *Pgc-*

1α and other genes involved in hepatic glucose metabolism. Translational studies further showed that patients with non-alcoholic fatty liver disease (NAFLD) and/or insulin resistance had decreased levels of fasting FGF19 or impaired response to FGF19 signaling (Schreuder et al. 2010, Wojcik et al. 2012). In line with these studies, FXR activation in mice was associated with decreased free FA levels and increased insulin sensitivity (Zhang et al. 2006a). These studies linked FXR indirectly with glucose homeostasis, mainly through FXR-SHP, FXR-FGF15/FGF19, FXR-BAs pathways.

In addition, most recent studies also implicate a direct regulation between FXR and glucose homeostasis. It was shown that glucose flux in hepatocytes could regulate FXR through direct post-translational modification (Berrabah et al. 2014). In this study, FXR was shown to interact with and be O-GlcNAcylated by O-GlcNAc transferase in its N-terminal AF1 domain. Increased FXR O-GlcNAcylation enhanced both FXR gene expression and protein stability. Elevated glucose levels thus increased FXR O-GlcNAcylation, its protein stability and transactivational activity. In fast-refed mice, FXR was undergone O-GlcNAcylation in fed conditions, which was associated with increased expression of direct FXR target genes and decreased liver BA content (Berrabah et al. 2014). In other studies, FXR was found to be expressed in both human and murine pancreatic β cells and may be involved in glucose-dependent insulin secretion (Popescu et al. 2010, Renga et al. 2010, Dufer et al. 2012), while the underlying mechanism is still under investigation.

1.2.3 FXR in Tumorigenesis and Liver Regeneration

As mentioned above, FXR is critically involved in BA, lipid and glucose metabolism, so it is not surprising that animals with FXR modulation are used to study tumorigenesis. However, only until seven years after the initial report of FXR-WBKO mice, it was first reported that FXR deficiency would lead to spantaneous HCC formation (Kim et al. 2007). In detail, at 12 months of age, both male and female FXR-WBKO mice showed a high prevalence of degenerative hepatic lesions, altered cell foci and liver tumors, including hepatocellular adenoma, carcinoma and hepatocholangiocellular carcinoma. At 3 months of age, FXR-WBKO mice had increased mRNA levels of the proinflammatory cytokine interleukin-1beta (IL-1β) and elevated protein levels of β-catenin and its target c-myc. Cell proliferation was also increased in these mice. Once again, FXR-dependent and independent pathways were speculated to play a role in the HCC formation. As mentioned earlier, combining FXR-WBKO and transgenic expression of FXR specifically in the intestine, Degirolamo et al showed that intestinal FXR re-activation was enough to prevent the spontaneous HCC formation in the FXR-WBKO background (Degirolamo et al. 2014). In detail, intestinal selective FXR re-activation normalized the enterohepatic circulation of BAs by up-regulation of the FXR-FGF15 signaling cascade and subsequent reduction of hepatic BA synthesis in FXR-WBKO mice. In addition, cellular proliferation and hepatic inflammation were also attenuated in these mice, indicated by reduced levels of cyclinD1 and signal transducer and activator of transcription 3 (STAT3) activation, respectively. These findings suggest, once again, the beneficial role of selective activation of intestinal FXR versus hepatic FXR against liver damage.

Similar to HCC formation, normal liver re-growth is also critically linked with intact FXR function. Huang et al first showed that FXR-dependent BA signaling is critical for liver regeneration after 2/3 partial hepatectomy (PHX) (Huang et al. 2006). PHX has been commonly used as a model to study liver regeneration since it was first introducted in rodents in 1931 (Higgins and Anderson 1931). The entire process of PHX and liver regeneration consists of several well-orchestrated phases, starting with rapid induction of proliferative factors activating the quiescent hepatocytes and priming their subsequent proliferation, followed by re-establishment of normal liver size, and finally the re-established quiescence. Later on, using albumin promoter drived hepatocyte-specific FXR KO (FXR-hepKO) mice, Borude et al showed that deficiency of hepatic FXR did not completely inhibit but delayed liver regeneration after PHX (Borude et al. 2012). The overall lanscape of liver regrowth in FXR-hepKO mice was unaffected, whereas a delay in peak hepatocyte proliferation from day 2 to day 3 after PHX was observed. Moreover, decreased levels of cyclin D1 and its association with cyclin-dependent kinase 4 (CDK4) were detected in FXR-hepKO mice after PHX compared to control mice, correlating with decreased phosphorylation of the retinoblastoma (Rb) protein and eventually, delayed cell proliferation in the livers. In the mean time, another paper further showed that induction of forkhead box protein m1b (FOXM1B) was dramatically reduced in FXR-hepKO mice, but not affected in enterocytpe specific FXR KO (FXR-entKO) mice after liver injury (Zhang et al. 2012a). Together these data indicate the requirement of a cell autonomous mechanism for hepatic FXR to activate FOXM1B and potentially other factors that are critically involved in regulating cell cycle in the liver. Detailed profiles of liver regeneration/repair after PHX in FXR-entKO mice

were presented in the later study (Zhang et al. 2012a). As expected, defective liver regeneration were observed in FXR-entKO mice in either PHX model or CCl_4-induced liver injury model (Zhang et al. 2012a). In addition, induction of intestinal FGF15 was blocked in FXR-entKO mice. Finally, ectopic expression of FGF15 rescued the defective liver regeneration in both FXR-entKO and FXR-WBKO mice. It was proposed that the protective roles of FGF15 in these liver injury models was resulted from not only its important role in maintaining BA homeostasis, but also its mitogenic activities. Indeed, mice with FGF15 deficiency (FGF15-KO) showed marked liver injury and mortality after PHX (Uriarte et al. 2013). Protein abundance of CYP7A1 increased dramatically during early phase of liver regeneration after PHX (6 to 24 hours (hrs)) in FGF15-KO mice, resulting in persistent elevation of intrahepatic BA levels. Treating the FGF15-KO mice with adenovirally delivered FGF15 or BA sequestrant cholestyramine dramatically reduced hepatic BA levels and significantly prevented the lethal outcome from PHX (Uriarte et al. 2013). In addition, adenoviral-FGF15 treatment also reduced mortality after extensive PHX in WT littermate control mice. While CA feeding in WT mice induced liver injury, proliferation of hepatocytes and cholangiocytes was significanlty reduced in CA-fed FGF15-KO mice. Kong et al further showed that FGF15-KO mice had much weaker activation of those important signaling pathways involved in liver regeneration after PHX, including STAT3, nuclear factor-kappa B (NF-kB), and mitogen-activated protein kinase (MAPK) signaling pathways (Kong et al. 2014). In WT mice, PHX induced the expression of many immediated-early responses genes and growth factors at early time points (10min and 30min) after PHX. However, the induction of these genes in the liver was reduced or delayed in the FGF15-KO mice. In summary,

both hepatic and intestinal FXR are critical for liver regeneration/repair. It is also important to note that FGF19 is generally considered as a tumor promoter and FGF19 has been shown to regulate and promote the proliferation of liver cells (Desnoyers et al. 2008).

1.2.4 Genome-wide Study of FXR in Mice

Other than the critical roles of FXR involved in BA, lipid and glucose homeostasis, it is suggested that FXR activation may also play a role in anti-inflammation by antagonizing the NF-kB signaling in the liver (Wang et al. 2008). To this point, the roles of FXR plays in many cellular processes have been studied in depth. And in order to comprehensively understand the functions of FXR in a genome-wide scale, chromatin immunoprecipitation coupled with massive parallel DNA sequencing (ChIP-seq) was first performed for FXR, in mouse livers and intestines in our laboratory (Thomas et al. 2010). This study first showed the globally tissue specific FXR binding, with only 11% of total binding sites shared between mouse livers and intestines. FXR binding sites were widely distributed in upstream (defined as 0-10 kilobase (kb) upstream of transcription start site (TSS) of the associated RefSeq gene), intragenic, downstream (0-10 kb downstream of 3' end of the gene), and intergenic of the genes retrieved. Novel binding sites were identified within known FXR target genes. Novel and tissue specific FXR binding motifs were also discovered, indicating possible involvement of tissue specific chromatin modifications and transcription factors in modulating FXR function. Finally, pathway analysis obtained from the Database for Annotation, Visualization and

Integrated Discovery (DAVID), indicates a much wider roles of FXR in cellular metabolism than previously appreciated (Thomas et al. 2010). The same year, using similar technique, another genome-wide study also showed the existence of a asymmetric IR1 motif for FXR binding, and the involvement of LRH-1 in co-regulating several FXR target genes (Chong et al. 2010). Two years later, genome-wide study for LRH-1 in the liver were reported by the same group (Chong et al. 2012). This study extended the co-regulation of FXR and LRH-1 in lipid metabolism in a global scale. Furthermore, genome wide co-regulation of FXR and hepatocyte nuclear factor 4 alpha (HNF4α) were reported (Thomas et al. 2013). In this study, FXR was found to have direct protein-protein interaction and cooperative binding with HNF4α. And genes co-bound by the two NRs were highly enriched in the pathways of complement and coagulation cascades, and drug metabolism. These studies add another level of complexity involved in FXR function, pathway specific coordination/modulation of FXR transactivation. Finally, studies of genome-wide binding sites of hepatic FXR in both healthy and dietary obese mice suggest that FXR-binding sites are likely functionally inactive in obesity (Lee et al. 2012). Among the binding sites detected, a large proportion were found to be unique in healthy or obese mice. Most surprisingly, direct gene repression by FXR activation was suggested to be common, when increased occupanies of FXR and RXRα to the selected FXR target genes were correlated with decreased expression levels of those genes. And the authors suggest that FXR could mediate direct gene repression by binding to the DNA as a FXR/RXRα heterodimer or as a FXR monomer or homodimer (Lee et al. 2012). In summary, genome-wide studies of NRs not only revealed the global picture of their global gene regulation network, but

also could lead to the discoveries of novel and complex underlying mechanisms of how they function.

1.3 Parenteral Nutrition Associated Liver Diseases

1.3.1 Parenteral Nutrition and the Associated Liver Diseases

Most recently, FXR was shown to play an important role in a special type of liver disease, parenteral nutrition associated liver disease (PNALD), especially PN associated cholestasis (PNAC) in neonates (El Kasmi et al. 2013). Parenteral nutrition (PN), also known as intravenous feeding, which was first introduced by Dudrick et al in 1967 (Dudrick et al. 1968), is a method to obtain nutrition into the body through the veins. PN is mainly used for patients who cannot or should not obtain their nutrition through eating, and therefore is essential for them to maintain nutritional status and/or growth. To replace the enteral route of feeding, PN normally contains a combination of nutrients, including carbohydrates (dextrose) for energy, proteins (amino acids), lipids (fat), electrolytes, and trace elements. In 2002, a statement from the National Institute of Diabetes and Digestive and Kidney Diseases (NIDDK) summarized that 20,000 patients in the United States were supported by PN due to intestinal failure (www2.niddk.nih.gov/NR/rdonlyres/9CCC34A3-3CFE-4D89-93DF-1ADEE3AA3E32/0/DDICC_June_25_2002_Minutes.pdf). Without PN therapy, patients with intestinal failure mostly died from malnutrition (Dorney et al. 1985). However, long-term PN feeding will lead to a spectrum of hepatobiliary diseases, including cholestasis, steatosis, fibrosis, and end stage liver complication, cirrhosis, summarized as PNALD (Kumpf

2006). Among these, there are 3 major types of PN associated hepatobiliary disorders: steatosis, cholestasis, and gallbladder sludge/stones, while overlap can exist (Kumpf 2006). As mentioned in the 1st and 2nd parts of this chapter, FXR is critically involved in all these three clinical conditions. Therefore, these three abnormalities will be the primary focus in this 3rd part.

Like other liver diseases, liver functional tests (LFTs) are normally used to assess the liver health/damage in PNALD patients. LFTs are a range of blood tests that provide information about liver health. Common serum biomarkers tested include activities of liver enzymes, such as alanine transaminase (ALT), aspartate transaminase (AST), ALP and GGT, as well as levels of albumin, bilirubin (direct and indirect), prothrombin time (PT), and activated partial thromboplastin time (aPTT), etc. Elevated levels of these serum markers are associated with potential damage to the hepatobiliary tract. Among these, albumin is specifically made in the liver. ALT and AST are mainly made by the parenchymal cells. Very smaller amounts of ALT are also present in the heart, kidneys, muscles, and pancreas, whereas AST is also found in red blood cells (RBCs), cardiac and skeletal muscles. Therefore, ALT and AST are not specific to the liver. The ratio of AST to ALT is sometimes useful in differentiating the causes of liver injury. If both elevated amounts of ALT and AST are found in in the blood, liver damage is most likely present. ALP is an enzyme mainly found in the cells lining the biliary ducts, also in bone and placental tissues. Measurement of bilirubin includes both unconjugated (indirect) and conjugated (direct) bilirubin. Unconjugated bilirubin is generated by the normal breakdown of heme, which is a part of hemoglobin in the RBC. Unconjugated bilirubin in the blood is taken up into hepatocytes, and is highly insoluble in water.

Therefore, it is made water-soluble by UDP-glucuronyl-transferase (UGT) in the liver and subsequently secreted into bile, which is mediated by the ATP-dependent transporter MRP2. Accumulation of bilirubin or the conjugates in the body causes jaundice. High levels of free, unbound bilirubin are especially toxic to newborns as it can pass through the partially developed blood brain barrier (BBB), causing bilirubin encephalopathy, which can result in permanent neurological damages in the newborns. GGT is a critical enzyme that is present in the cell membranes in many tissues. PT and aPTT are parameters of the blood coagulation cascades associated with normal liver function since coagulation factors are predominantly produced in the liver. These tests and liver biopsies followed by histological exams are the major clinical assessments to analyze the development and progression of PNALD, as well as many other liver diseases.

PN associated steatosis, or hepatic fat accumulation, is found predominantly in adults and is generally benign (Kumpf 2006). Mild to moderate elevations of serum transaminase levels are commonly seen, with less pronounced elevations of serum ALP and bilirubin concentrations. Elevations of these serum biomarkers generally occur within 2 weeks after patients start to receive PN therapy and may return to normal even when PN therapy is continued (Kumpf 2006). Most adult patients are asymptomatic. Overfeeding may be the cause of steatosis and is therefore likely not as common now because the estimated calorie requirements for PN have decreased accordingly compared to the practices in more than 15 years ago (Kumpf 2006). Though steatosis is generally considered as a non-progressive lesion, long-term PN may lead to the progression to fibrosis or even cirrhosis (Craig et al. 1980, Cavicchi et al. 2000). The

prevalence of liver diseases in adults was evaluated in a group of 90 patients enrolled from 1985 to 1996, receiving home PN due to permanent intestinal failure in France (Cavicchi et al. 2000). Among them, 57 patients had liver biopsies followed by histological evaluations. The Kaplan-Meier method was used to determine the occurrence of chronic cholestasis and other PNALDs (bilirubin level ≥ 60 μmol/L [3.5 mg/dL], portal hypertension, liver encephalopathy, ascites, gastrointestinal bleeding, and histologically identified fibrosis or cirrhosis). Analyzed results showed that 65% patients (58) developed chronic cholestasis (median duration of PN was 6 months with the range from 3 to 132 months), and 41.5% (37) developed complicated PNALDs (median duration of PN was 17 months with the range from 2 to 155 months) (Cavicchi et al. 2000). Among these, extensive fibrosis was found in 17 patients (median duration of PN was 26 months with the range from 2 to 148 months) and cirrhosis was found in 5 patients (median duration of PN was 37 months with range from 26 to 77 months). The prevalence of PNALDs was 26% ± 9% after 2 years and 50% ± 13% after 6 years of home PN therapy, respectively. Among all patients with PNALD, 6 died from liver diseases. Multivariate analysis showed that chronic cholestasis was significantly associated with a PN-independent risk for liver disease (for example, alcohol use or viral hepatitis), a bowel remnant shorter than 50 cm in length, and infusion of lipid content equal to or more than 1 g/kg of body weight per day (g/kg/day). Complicated home PNALD was significantly associated with chronic cholestasis and infusion of lipid content equal to or more than 1 g/kg/day. Despite that the number of total patients enrolled in this study is relatively small plus 15 of them had pre-existing risks for liver diseases, the study did show a strong implication that liver complications were common

in patients receiving long-term PN therapy. In addition, pre-existing risk factors for liver diseases increased the risk for PNALD, leading to increased risk for progression to severe liver disorders.

PN associated cholestasis (PNAC) is a special type of cholestasis occurs predominantly in children but may also occur in adult patients after receiving long-term PN as mentioned above (Peyret et al. 2011). PNAC is defined as cholestasis in the setting of PN therapy once all other causes of cholestatic liver diseases have been excluded (Kumpf 2006). Elevated concentration of serum conjugated bilirubin is typically considered as the primary indicator of cholestasis in clinics, defined as the concentration > 2 mg/dL. Elevated concentrations of serum ALP and GGT are often present in cholestasis as well, whereas serum ALT and AST may or may not be elevated. ALP and GGT are sensitive markers for hepatobiliary diseases, but not as specific as conjugated bilirubin. The prevalence of PNALD in neonates was well documented in one particular large historic cohort study published in 2007 (Christensen et al. 2007). From 2002 to 2006, a total of 1366 neonatal patients received PN therapy for ≥ 14 days in the neonatal intensive care unit (NICU) in the Intermountain Healthcare system. The incidence of PNALD increased along with prolonged PN duration. In detail, the incidence of PNALD in neonates receiving PN were 14% for 14-28 days, 43% for 29-56 days, 72% for 57-100 days, and 85% for >100 days of PN therapy. Highest risk factors for developing PNALD in these patients include low birth weight (<750 g), gastroschisis and jejunal atresia. Among patients who developed PNALD, death rate after 28 days of PN therapy was much higher in those who had the highest serum levels of conjugated bilirubin and liver transaminase ($p<0.0001$) (Christensen et al. 2007).

Combining liver biopsies and LFTs, a subsequent study reported additional risk factors for neonatal populations receiving long-term PN (Peyret et al. 2011). Between January 1998 and December 2007, 42 infants received PN for more than 2 years in an approved home parenteral center in France (Peyret et al. 2011). The median age of PN onset was 1.5 ± 0.5 (SEM, standard error of the mean) years, and the median duration of PN was 7.9 ± 0.8 (SEM) years. None of these patients died from hepatic complications or from direct complications of PN. Among them, 24 patients (57%) developed biochemical abnormalities in a median length of 2.9 ± 0.4 (SEM) years after commencement of PN therapy. Risk factors for biochemical abnormalities identified were younger age when PN therapy initiated, longer duration of PN, higher rate of catheter-related infections, and higher volume and calorie content of PN. It is also important to note that the reported median frequency of catheter-related infections was 1.1 ± 0.2 (SEM) infections per patient per year of PN, which corresponded to a high incidence of 7.5 ± 1.2 (SEM) infections for each patient during the entire PN duration. 43% of patients with median age of 3.2 ± 0.9 years had undergone liver biopsies. Histological analysis revealed high incidence of liver fibrosis in these children (94%), which was significantly associated with a shorter bowel remnant and a longer duration of PN therapy. While the only risk factor identified for cholestasis was the percentage of total energy intake from lipid contribution, no risk factor was identified for steatosis (Peyret et al. 2011). Unpublished data from follow-up histological studies mentioned in the paper also revealed critical indications: steatosis was stable or decreased during the 10-year period for most patients; cholestasis primarily depended on individual patient with large variety; and most strikingly, fibrosis was stable or increased but never showed any sign of decrease

(Peyret et al. 2011). In line with this finding, another study aiming to define predictive factors for the progression of PN associated liver fibrosis (PNALF) for children with short bowel syndrome (SBS) concluded that, biochemically confirmed cholestasis (direct bilirubin ≥ 2 mg/dL) could not reflect the presence or degree of biopsy-confirmed PNALF (Fitzgibbons et al. 2010). In summary, all these studies suggested that after discharge from PN therapy, follow-up with refined diagnosis and hepato-protective management should be performed routinely for the identified high-risk populations (Fitzgibbons et al. 2010).

Finally, prolonged gallbladder stasis after long-term PN therapy may progress into gallbladder sludge or gallstones, with subsequent development of cholecystitis (Kumpf 2006). Cholecystectomy, due to cholecystitis, is generally considered as detrimental and not recommended for patients receiving long-term PN due to intestinal failure (Sitzmann et al. 1990). Formation of gallbladder sludge/stones can occur in both adult and pediatric patients and is generally considered to be associated more with the lack of enteral stimulation than PN itself (Kumpf 2006). As mentioned before, entero-hormone CCK is responsible for mediating gallbladder contraction and BA secretion upon postprandial stimulus. Therefore, the lack of oral stimulus during PN therapy will lead to decreased release of CCK and impaired bile flow and gallbladder contractility. It has been reported that CCK secretion decreased significantly in severe SBS patients receiving long-term PN, even after the stimulation from a liquid diet (Ling et al. 2001). It was first reported in a well-designed, randomized, double-blind controlled study, that intravenous administrations of cholecystokinin-octapeptide (CCK-OP) prevented the formation of biliary sludge in adult patients receiving long-term PN (Sitzmann et al.

1990). In this study, patients who had received PN therapy for more than 21 consecutive days were recruited. For each patient, ultrasound was performed weekly followed by a final volume and empty assessment of the gallbladder in response to the assigned treatment. The study was concluded even after randomization of 15 of the total patients, as statistical significance was achieved (Sitzmann et al. 1990). Ultrasound showed that none of the patients in CCK-OP group developed sludge whereas 5 of the 8 patients in the placebo group had sludge (*p-value* ≤ 0.02). In addition, volume and emptying studies showed significant contraction of the gallbladder in patients receiving intravenous CCK-OP but not saline control (Sitzmann et al. 1990). However, the same type of treatment didn't reach significant improvement in a later trial widh neonatal patients (Tsai et al. 2005). PN associated gallstones were detected in 10% of children in the study, while most were asymptomatic. CCK-OP prophylaxis was shown ineffective in preventing gallstone formation in children receiving long-term PN (Tsai et al. 2005). In addition, UDCA was shown also ineffective for dissolving gallstones in these patients, once detected (Tsai et al. 2005).

1.3.2 Etiology and Management of PNALD

Intestinal Failure and Lack of Enteral Stimulation

It is well accepted now that the most effective treatment for PNALD is enteral stimulation, even in a very small amount (Ziegler and Leader 2006). It is suggested that the underlying mechanisms may involve the induction of endogenous gut mucosal growth factors, increased splanchnic blood flow, stimulation of enterohepatic circulation

and subsequent BA homeostasis, and several others (Ziegler and Leader 2006, Kumpf 2006). Nevertheless, for patients with permanent intestinal failure, clinical management is still challenging. The cause of intestinal failure related to PNALD can be divided into two major categories: 1st, actual or effective decrease of the gut mucosal surface area, such as massive small bowel reduction caused SBS; 2nd, diseases of gut mucosal, such as inflammatory bowel disease (IBD) (Ziegler and Leader 2006). As discussed, shorter length of bowel remnant due to intestinal failure is associated with higher risk of developing PNALD, in both adult and pediatric patients. Unfortunately, patients with SBR are dependent on long-term PN and options are very limited when liver failure happens, after which combined liver and bowel transplantations are often required.

Prematurity and Low Birth Weight

As mentioned, PNAC is predominantly found in neonates. In one PN study involved in 62 premature newborns with birth weight less than 2,000 g, cholestasis was identified in 50% of the newborns with very low birth weight < 1000 g, but only 7% if birth weight was > 1500 g (Beale et al. 1979). On one hand, prematurity and/or low birth weight may be independent or associated risk factors for PNALD, since many neonates demanding PN therapy are those with prematurity and low birth weight. Though it is well accepted now that longer duration of PN will lead to higher incidence of PNALD, no correlation was found between the duration of PN therapy with the onset of cholestasis in this study (James, Hendry and MacMahon 1979). On the other hand, the immature neonatal liver may be the *bona fide* reason for the increased incidence of PNAC since

jaundice and temporary elevation of serum indirect bilirubin levels are commonly found even in more than half of the full-term babies. In preterm infants, the enterohepatic circulation is not well-established as reflected by diminished levels of both hepatic uptake and synthesis of BAs (Kumpf 2006). In this regard, BA cytotoxicity may not be the direct cause of the so called PNAC, indicated by jaundice and elevated serum levels of direct bilirubin. It is possible that the hepatic system for bilirubin metabolism and/or transport is not fully functional in these preterm infants. It is also suggested that the premature liver is more susceptible to BA cytotoxicity due to the reduced rate of sulfation of primary and secondary BAs (Kumpf 2006). In this regard, maintaining and/or improving normal liver development could be a putative and more direct therapeutic strategy for PNALD management.

Infections

There are two major causes of infections in patients receiving long-term PN: 1st, sepsis due to bacterial and/or fungal infection related to the central venous catheter system; 2nd, bacterial overgrowth in the small intestine (Kumpf 2006). Bacterial and fungal infections are highly associated with PNAC (Kumpf 2006). Jaundice and elevated serum concentration of total bilirubin can occur within several days after the initial insult from infection (Kumpf 2006). Endotoxins, such as bacterial lipopolysaccharide (LPS), could activate liver Kupffer cells to stimulate the release of pro-inflammatory cytokines in the liver, leading to systemic liver inflammation and exacerbating PNALD. Good clinical practice is needed to minimize catheter related infections. It is also important for

the patients to maintain proper handling and aseptic techniques, as well as minimize manipulations of the catheters in home PN settings.

Small intestine bacterial overgrowth (SIBO) occurs when large amounts of resident bacteria in the lower small intestine and/or colon colonize the upper small intestine. Reduced enterohepatic circulation caused by SBS, and intestinal stasis caused by motility abnormalities such as chronic intestinal pseudo-obstruction, predispose PN patients to SIBO (Kumpf 2006). It is suggested that the bacteria originated from the lower bowel and colon may produce and retain hepato-toxins in the small intestine, such as LCA, which is predominantly found in the large intestine and readily excreted into feces under normal conditions. Intestinal stasis and/or dysplasia could also lead to bacterial translocation and subsequent release of endotoxins into the portal vein, causing hepatic inflammation.

Cycling of PN

Cyclic PN infusion is common in the current clinical practice due to two major reasons. First, it's more convenient for the patients, especially long-term, to receive the infusion in the evening during their sleep, as well as to maintain their regular physical activity during the daytime. Second, it has been shown that continuous PN infusion was associated with hyperinsulinemia and fat deposition in the liver, leading to steatosis and increased risks for the development of other liver complications (Kumpf 2006). In summary, cyclic PN is beneficial, especially for patients receiving long-term PN therapy.

Basic PN Components and Improvements

Since PN was first introduced into clinic, many side effects, which are associated with the lack or excess of certain nutrients in the PN formulations, have been reported. And over the course of more than 50 years of clinical practice, many PN related abnormalities due to nutrient deficiency/overload have been resolved. Early dextrose-based PN formulations, which contain little or no fat, were implicated in the development of PN associated steatosis (Kumpf 2006). Dextrose-based PN formulation may lead to the development of essential FA deficiency (EFAD), which not only will impair normal neurodevelopment but may also lead to impaired lipoprotein production and triglyceride secretion (Kumpf 2006). Thus, excessive carbohydrates in the dextrose-based PN may induce lipogenesis and subsequent fat deposition in the liver. The combined effect could result in hepatic steatosis. In line with this, later studies suggested that excess calorie intake, either individual or combined, regardless of source (dextrose, fat, amino acid, etc.), could contribute to the development of PN associated steatosis (Kumpf 2006). It is suggested that overfeeding, regardless of the type of nutrient in PN, could stimulate insulin release followed by induction of lipogenesis and suppression of FA oxidation (Kumpf 2006).

Amino acid components in early PN were derived from protein hydrolysates. Later clinical studies found significant aluminum contamination in this type of protein source (Klein et al. 1984). Animal studies also linked high levels of aluminum contamination to the development of cholestasis (Kumpf 2006). In this regard, protein hydrolysates were subsequently replaced by crystalline amino acid, which though doesn't contain cysteine and taurine in the standard formulation. In adults or older

infants, cysteine and taurine can be synthesized from methionine but not in the premature infants. As mentioned before, taurine is critically involved in BA conjugation and solubilization. In early clinic practice, taurine deficiency was indeed found in premature infants, as well as both pediatric and adult patients after long-term PN therapy (Geggel et al. 1985). In these patients, taurine deficiency may contribute directly to the development of PNAC. In one study mentioned earlier, which was designed to assess the potential beneficial effect of CCK-OP in PNALD patients (Tsai et al. 2005), the potential beneficial effect of taurine supplementation in PN was also evaluated. Using multivariate analysis, taurine supplementation was shown to reduce the incidence of PNAC, with markedly and significantly decreased serum levels of conjugated bilirubin in preterm infants (*p-value* < 0.07) and in infants with necrotizing enterocolitis (*p-value* < 0.01), respectively (Spencer et al. 2005). Thanks to these studies, specialized neonatal amino acid formulation has become a standard and essential component of the current neonatal PN regimen. Tremendous efforts have also been made in recent years in order to refine the lipid components in PN solution, which will be discussed in detail in the next section.

Patients receiving long-term PN may also develop choline deficiency as choline is not considered essential and therefore not contained in the crystalline amino acid solution, which does contain methionine. While choline can be synthesized endogenously from methionine, it was suggested that this conversion might be less efficient when methionine was given intravenously than normally absorbed in the gut and pass through the portal vein (Chawla et al. 1985).

Intravenous Fat Emulsion

In the United States, there are currently only two FDA-approved lipid emulsions for PN therapy, Intralipid, a soybean oil based lipid emulsion (SOLE), and Liposyn II, a mixture of half soybean oil and half safflower oil based lipid emulsion. Intralipid mainly contains linoleic acid (LA, 53%), oleic acid (OA, 24%), as well as less amount of palmitic acid (PA), α-linoleic acid (ALA) and stearic acid (SA), but lacks of long-chain polyunsaturated FA (LC-PUFA) eicosapentaenoic acid (EPA) and docosahexaenoic acid (DHA). LA is a polyunsaturated omega-6 FA (ω-6 FA), and the precursor for the biosynthesis of arachidonic acid (AA). The metabolism of AA predominantly results in the formation of the pro-inflammatory eicosanoids, including 2-series prostaglandins, 2-series thromboxanes and 4-series leukotrienes (Calder 2007). These eicosanoids mediate multiple pro-inflammatory pathways, including the release of pro-inflammatory cytokines such as interleukin-6 (IL-6), initiation of leukocyte chemotaxis, vasodilation, and the stimulation of pain pathways (Calder 2007). It is also important to note that LA and its derivative γ-linolenic acid (GLA) are also precursors for the production of epoxyeicosatrienoic acids (EETs) and 1-serial prostaglandins, respectively. EETs, produced by cytochrome P450 epoxygenase, are considered as anti-inflammatory mediators due to their ability to decrease the activity of cyclooxygenase and platelet aggregation (Spector et al. 2004). Nevertheless, the potential beneficial roles of EETs and GLA in PNALD have not been documented.

Other components contained by SOLE, which are also critically linked to PNALD, are the high levels of phytosterols, including plant sterols and stanols. Plant sterols are structurally similar to cholesterol, but differ from cholesterol by the presence of an extra

ethyl group (sitosterol and stigmasterol) or methyl group (campesterol) at C-24 of the sterol side chain (Othman, Myrie and Jones 2013). Plant stanols are saturated sterols, which are less abundant in nature compared to plant sterols. Extremely elevated levels of plant sterols in the plasma and tissue, will lead to the development of sitosterolemia (STSL, also known as phytosterolemia). STSL is a rare autosomal recessive genetic disease caused by homozygous or compound heterozygous mutations in the genes encoding either one of the two ABC family transporters, ABCG5/8, resulting in xanthoma and premature atherosclerotic disease (Othman et al. 2013). Functional ABCG5/8 in the liver and mainly in the intestinal, will rapidly remove the absorbed plant sterols out from the hepatocytes and enterocytes for fecal excretion, respectively (Othman et al. 2013). *In vitro* studies using hepG2 cells and cultured mouse hepatocytes isolated from WT or FXR-WBKO mice showed that, stigmasterol and its derivative stigmasterol acetate, were FXR antagonists (Carter et al. 2007). Beta-sitosterol (β-sitosterol), the most abundant plant phytosterol, however, didn't show any inhibitory effect to the transactivation activity of FXR in this *in vitro* study (Carter et al. 2007). in 1993, Clayton el al first reported that plasma levels of phytosterol were positively associated with the severity of PNAC in children receiving PN therapy (Clayton et al. 1993). In this study, plasma concentrations of sterols were measured by gas chromatography-mass spectrometry (GC-MS) in 29 children receiving PN with age range from 2 months to 9 years as well as in 29 age-matched controls. Among the 29 children receiving PN, 5 developed severe PNAC (bilirubin > 100 μmol/L; AST > 200 IU/L). The elevated plasma concentrations of phytosterols and sitostanol in these 5 children (around 1500 μmol/L) were as high as those found in STSL patients (total

phytosterols, 1300-1800 μmol/L). Besides, all these 5 children had intermittent thrombocytopenia. In 2 of the 5 patients, a subsequent reduction of lipid intake to less than 50 mL/kg/wk was associated with decreased plasma phytosterol concentrations and improved outcome from LFTs and platelet counts. Finally, the serum levels of phytosterol in the children with mild cholestasis and the age matched controls were approximately 300 and 40 μmol/L, respectively. It was then proposed that phytosterolemia might contribute to the pathogenesis of PNALD. However, it is still debatable that the increased serum levels of phytosterols seen in this study could result from the severe cholestatic liver complications, which possibly were partially caused by and could lead to the impaired hepatic transporting system, since adult patients receiving higher amount of SOLE in their PN normally don't develop cholestasis in short-term. Another recent study also reported significant higher levels of phytosterols in 16 SBS patients receiving PN therapy (SBS-PN) compared to 8 SBS patients (SBS-only) and 21 healthy controls without PN (Ellegard, Sunesson and Bosaeus 2005). Serum levels of phytosterols plus cholesterol, and markers for BA and cholesterol synthesis, were quantified by gas or liquid chromatography (GC/LC). In addition, patients in both SBS-PN and SBS-only groups showed lower serum levels of cholesterol, higher levels of lathosterol (824, 808, and 228 μmol/100mmol cholesterol for SBS-PN, SBS-only, and controls, respectively) and significantly higher levels of 7α-hydroxy-4-cholesten-3-one (C4) (207, 191, and 18 nmol/L in SBS-PN, SBS-only and controls, respectively. *p-value* <0.05, between controls and SBS). Therefore, SBS alone could be a contributing factor of higher levels of cholesterol and BA synthesis compared to controls.

As mentioned, SOLE also contains small amount of ALA, another essential ω-3 FA. ALA is the precursor for the production of long change PUFAs (LC-PUFAs), EPA and DHA, which are critical for normal human physiology, especially neurodevelopment in infants during the critical period. Though EPA can be synthesized from ALA in humans, the relative efficiency is very low. EPA can also give rise to DHA, catalyzed by similar enzymes involved in the formation of EETs from AA, but the efficiency is even lower. In contrary to AA, EPA and DHA are precursors for the production of 3-series prostaglandins, 3-series thromboxanes and 5-series leukotrienes (Calder 2007). These mediators are generally considered less pro-inflammatory and some anti-inflammatory. EPA and DHA are also precursors for the synthesis of the recently discovered resolvins, which are involved in resolution of cellular inflammation by inhibiting the production and transportation of inflammatory cells and mediators to the inflammation sites (Serhan et al. 2002).

In contrary to SOLE, a new generation of fish oil based lipid emulsion (FOLE), Omegaven (Fresenius Kabi, Bad Homburg, Germany), contains relatively large amounts of EPA and DHA, median amount of OA as well as small amounts of AA, ALA, LA, PA and SA (El Kasmi et al. 2013). In addition, there is no phytosterols in FOLE. The beneficial roles of FOLE in alleviating PNALD have been shown recently in many clinical studies with different underlying mechanisms proposed.

One prospective, randomized, and double-blind study, which was reported 2 years ago by researchers from Taiwan, particularly evaluated the overall effects of ω-3 FAs on immune and inflammatory modulations in patients receiving PN therapy (Han et al. 2012). Thirty-eight patients were randomized into 2 groups with PN regimen

containing equal volume and calorie contributions from glucose, nitrogen, and lipid from 2 different lipid emulsions for 7 days. One group (n=12) received a 50:50 mixture of SOLE and another vegetable oil, which is rich in MCT (SOLE/MCT, also commonly known as MCT/LCT (long chain triglycerides), indicating the mixture of MCT in the other vegetable oil and LCT in SOLE). The other group (n=18) received a combination of SOLE and FOLE (SOLE/FOLE). Test results of blood inflammatory cytokines showed significant differences in the two groups in regards to serum concentrations of interleukin-1 (IL-1), interleukin-8 (IL-8), and interferon-γ (IFN-γ) on postoperative day 4 (*p-value* < 0.05), as well as IL-1, IL-8, IFN-γ, IL-6, and tumor necrosis factor alpha (TNF-α) on postoperative day 7 (*p-value* < 0.05). A trend toward reduced serum levels of inflammatory cytokines was identified in the SOLE/FOLE group compared to the SOLE/MCT group. Insignificant results also linked the usage of FOLE to reduced incidence of postoperative liver dysfunction and infections (Han et al. 2012). Another single-center, randomized, placebo-controlled trial compared the effects of different intravenous fat emulsions in patients receiving PN therapy due to systemic inflammatory response syndrome (SIRS) and sepsis in a university hospital (Sungurtekin et al. 2011). The patients were assigned to receive SOLE/MCT mixture or FOLE based PN infusion for over 7 days. In the group of patients with sepsis, those receiving SOLE/MCT had significantly higher levels of hepatic steatosis, measured by ultrasound on days 7 and 10, whereas in the group of SIRS patients, no significant differences in inflammatory markers were observed. Nevertheless, the significant differences found in the sepsis group demonstrated both hepato-protective and anti-inflammatory effects of FOLE

(Sungurtekin et al. 2011). These studies suggest that FOLE may be associated with decreased liver injury, mainly due to the anti-inflammatory effects of the ω-3 FAs.

FOLE has also been shown to reverse PNALD in patients previously received SOLE based PN. In 2011, Le et al reported the significant reverse of PNAC in 79 pediatric patients switched from SOLE to FOLE, as indicated by reduction of median serum levels of total and direct bilirubin from 7.9 and 5.4 mg/dL into 0.5 and 0.2 mg/dL, respectively (*p-value* < 0.0001). In addition, serum levels of triglyceride, total cholesterol, LDL, and VLDL significantly decreased by 51.7%, 17.4%, 23.7%, and 47.9%, respectively, after the replacement of SOLE by FOLE. Though FOLE only contains low levels of the essential ω-3 FAs (ALA) and ω-6 FAs (LA), none of the patients in this study developed EFAD. Hence, FOLE was proposed by the authors to be the preferred lipid emulsion for patients receiving PN who developed PNAC and/or dyslipidemia. In line with these findings, a number of other studies also showed that parenteral fish oil as monotherapy could prevent EFAD in PN-dependent patients (Gura et al. 2008, de Meijer et al. 2009, Le et al. 2011, de Meijer et al. 2010).

Most recently, replacement of SOLE with combinations of lipid emulsions were also reported. A recent randomized, double-blind, controlled study evaluated the potential beneficial effects of using SMOFlipid (Fresenius Kabi, Bad Homburg, Germany) versus Intralipid in 53 preterm infants (gestational age < 34 weeks) receiving PN for at least 7 days (Rayyan et al. 2012). SMOFlipid is a mixture of 30% soybean oil, 30% MCTs, 25% olive oil, and 15% fish oil. Serum levels of total and direct bilirubin decreased significantly in the SMOFlipid group than the Intralipid control group. In addition, in the plasma and RBCs, levels of EPA and DHA were significantly higher, and

the ratio of ω-6/ω-3 FAs was significantly lower in the SMOFlipid group (*p-value* < 0.05 vs control). These alterations of lipid profiles were considered beneficial for the preterm infants. Another study tested the combination of 1:1 ratio of Omegaven and ClinOleic (Baxter, Maurepas, France), an olive/soybean oil based lipid emulsion, in five premature infants (gestational age ≤ 35 weeks) with SBS and cholestasis (Lilja et al. 2011). ClinOleic has higher ω-9 monounsaturated FAs (ω-9 FAs) and lower ω-6 FAs than Intralipid. After receiving FOLE/ClinOliec based PN therapy for the time periods ranging between 7 and 17 months, direct bilirubin levels normalized in all the patients receiving based PN. In addition, none of these patients developed irreversible intestinal failure-associated liver disease (IFALD), though all the patients were preterm, had gone through multiple major surgical operations, and had experienced more than one episode of sepsis. Finally, the mixture of FOLE/ClinOliec didn't cause any adverse effect in these preterm infants, and all of them grew and developed well with normal liver function with 2 extremely premature infants (gestational age 23–26 weeks) had signs of delayed development (Lilja et al. 2011). The safety and efficacy outcomes of the mixture of FOLE/ClinOliec versus ClinOliec-only was also compared in another large retrospective study in PN patients in Poland (Pawlik, Lauterbach and Hurkala 2011). 152 preterm infants (gestational age < 32 weeks) with very low birth weight (< 1500 g) received the same FOLE/ClinOliec mixture in their PN, whereas185 matched preterm infants with very low birth weight received ClinOleic-only based PN. All these patients started their corresponding PN therapy on the 1st day of lives. The newborns in the FOLE/ClinOliec group had significantly lower incidence of cholestasis (0.66%) versus those in the ClinOleic-only group (4.86%) (*p-value* < 0.025). Besides regular histological

and biochemical tests, plasma and erythrocytes DHA concentrations were also determined in these newborns with a high-performance LC-MS method (Pawlik et al. 2011). It was also showed that the risk for the preterm infants to develop retinopathy, which required laser therapy, was markedly lower in patients in the FOLE/ClinOlei group, though it was not statistically significant.

In the US, FOLE (Omegaven) is currently approved by the FDA only under compassionate use for the treatment of PNALD and is dosed as a 10% lipid emulsion at 1 g/kg/day. In contrast, Intralipid is administered as a 20% lipid emulsion at up to 3 g/kg/day. Despite the mounting evidence for the beneficial impact of FOLE on improvement and reversal of PNALD, it has also been suggested that the impact may simply result from the reduced administration of lipid content (Cowan, Nandivada and Puder 2013), rather than the distinct properties of FOLE as discussed above. To resolve this debate, Nehra et al asked the question that whether a reduction of SOLE in PN solution from 2-3 g/kg/d into 1 g/kg/d is associated with a reduced incidence of PNAC. The hypothesis was tested by a retrospective study of the medical records of 61 neonatal patients (Cowan et al. 2013). These patients, based on the amount of SOLE intake mentioned above, were divided into 2 groups (n=29, 1 g/kg/d group; n=32, 2-3 g/kg/d group). Baseline characteristics, including overall enteral intake, the duration of PN, the number of surgical procedures and catheter related infections were all similar between the 2 groups. Analyzed results showed that there was no difference in terms of the incidence of PNAC (51.7% for 1 g/kg/d group, 43.8% for 2-3 g/kg/d group, *p-value* = 0.61), nor the time towards the development of PNAC (32.6 ± 24.1 days for 1 g/kg/d group, 27.7 ± 10.6 days for 2-3 g/kg/d group, *p-value* = 0.48) between the 2 groups. In

addition, among all the patients developed PNAC, 44.8% made successful transition from PN feeding into full enteral feeding, whereas 55.2% had to switch into the FOLE-PN, after which serum levels of direct bilirubin normalized in all patients.

1.3.3 Study of PNALD in Animal Models

To understand the underlying mechanisms of the pathogenesis of PNALD, and to seek novel management and treatment strategies, studies of PNALD in various animal models have been reported, including mice, rats, rabbits, guinea pigs, pigs, and dogs (Puiman and Stoll 2008). Compared to the large amount of clinic reports related to PNALD, literatures about PNALD in animal models are, however, still limited. Majority of literatures are based on mice, rats and pigs, especially newborn piglets, and these will be discussed in detail in this chapter.

As mentioned, PN with no or very little amount of lipid content could induce hepatic steatosis. An early study well-recapitulated this clinic issue in a rat PN model (Hall et al. 1984). Adult rats were assigned to receive lipid-free dextrose-PN (Dex-PN, other major nutrients were included) or PN with lipids (PN). Hepatic triglyceride levels increased around threefold in Dex-PN rats and twofold in PN rats (*p-value* < 0.02). Endogenous FA synthesis in the liver also elevated, as reflected by the fourfold and twofold increase of the activity of hepatic acetyl-coenzyme A carboxylase (ACC) in Dex-PN and PN rats, respectively, when compared to controls. And the elevated levels of hepatic triglyceride correlated positively with the increased activity of hepatic ACC (R^2 = 0.82). However, activities of hepatic microsomal enzymes involved in lipid synthesis

were similar in the two groups. In addition, both PN regimens inhibited hepatic triglyceride secretion, which negatively correlated with total hepatic lipid contents (R^2 = -0.89). Hepatic uptake of a radiolabeled triglyceride emulsion and hepatic lipase activity were both increased in the Dex-PN rats, whereas both decreased in PN rats (Hall et al. 1984). On the contrary, the levels of adipose and cardiac lipase were lower in Dex-PN rats and higher in PN rats, respectively. Dex-PN also significantly suppressed triglyceride FA oxidation, which was less suppressed in the PN rats. Finally, suppression of free FA oxidation was only seen in Dex-PN rats (Hall et al. 1984). These results suggested that enhanced hepatic FA synthesis and reduced triglyceride secretion were likely the underlying causes of hepatic steatosis in Dex-PN rats (Hall et al. 1984). In another study published the same year, Wood et al showed that isocaloric substitution of PN glucose with lipid by 60% would not exacerbate the hypercalciuria condition observed in Dex-PN rats. It was mainly because of these early studies that PN with lipid administration became standard practice (Kumpf 2006). Though rat is a good rodent model to study PNALD in adult settings, it is still difficult to use infant rats to mimic human neonatal conditions. In 1989, newborn rabbit PN models were reported by two different groups (Gleghorn et al. 1989, Hata et al. 1989). Gleghorn et al showed that PN rabbits had higher percentage of LCA, unconjugated bilirubin and total calcium in their gallbladder bile content (Gleghorn et al. 1989). In addition, elevated serum markers of liver injury as well as histologically mild steatosis and edema were observed in the livers of these PN rabbits. Hata et al showed that excessive amount of non-protein calories in PN rabbits was correlated with increased occurrence of histology-proven cholestasis (Hata et al. 1989). Subsequently, study of PNALD in non-human primates

was also reported (Friday and Lipkin 1990). Due to the relative high maintenance requirement, it's not a popular model for PN study.

Study of PNALD in Pigs/Piglets

More than two decades ago, it was already suggested that infant and pediatric piglets were excellent animal models for the study of PNALD, due to their relatively large body sizes readily accessible for surgical manipulations, and more importantly, their high levels of similarities to human neonates, in terms of development and nutritional requirements (Borum 1993). In 1985, Goldstein et al first reported a study, using piglets to evaluate the effect of PN during the phase of rapid intestinal growth and development in three 6-week-old weaned piglets (Goldstein et al. 1985). PN fed piglets had the same total body weight gain but reduced growth of the stomach, small bowel and pancreas compared to chow fed controls (Goldstein et al. 1985). Gallbladder sludge was replicated in PN piglets in a later study (Truskett et al. 1987). Five female piglets receiving lipid-free PN (Dex-PN) developed "sludge" in their gallbladder, had decreased basal bile flow and bile salt secretion, and responded weakly to bile salt stimulation, when compared with age-matched controls. LFTs and liver histology, however, didn't show any obvious abnormalities (Truskett et al. 1987). In 1996, Duerksen el al first demonstrated that the newborn piglet was a valid model to study neonatal PNAC (Duerksen et al. 1996). Eight newborn piglets, receiving PN therapy for 3 weeks, had significantly lower rates of both BA-dependent and BA-independent bile flow compared to 9 milk-fed newborn controls (Duerksen et al. 1996). BA secretions in PN piglets were

less than 50% of the control values, whereas total cholesterol and phospholipid secretions were less than 5% of the control values. Intravenous administration of taurocholic acid (TCA) failed to stimulate bile flow in the PN piglets compared to orally fed animals. PNAC was validated by the elevated levels of both liver and serum bilirubin in these newborn piglets (Duerksen et al. 1996).

In 1997, Van Aerde et al first evaluated the effects of different lipid emulsion in PN, on the lipid compositions and function of the intestinal brush border membrane (BBM) and the enterocyte microsomal membrane (EMM) (van Aerde et al. 1997). Major membrane phospholipid contents in the jejunal and ileal BBM and EMM, including phosphatidylcholine (PC) and phosphatidylethanolamine (PE), were evaluated. Different compositions of the four major FAs (LA, OA, PA, and SA) were detected in both PC and PE in the BBM and EMM of the jejunums and ileums in 21-day-old milk-fed piglets, when compared to those in newborn animals. Different compositions of membrane FAs were also detected among the three groups of animals, fed by milk orally, lipid-free PN (Dex-PN), or PN with SOLE, respectively. In addition, FOLE was also tested in this study. Compared to PN with SOLE, PN with FOLE or SOLE/FOLE altered the FA contents in BBM and EMM. It was therefore proposed that the lipid composition of PN regimen could potentially modify the membrane lipid content and the related functions in other organs as well. In 1998, Dudley et al showed that parenterally fed 3-day-old piglets had significant lower rate of absolute total mucosal protein synthesis (the amount of protein synthesized per gram of mucosa) than enterally fed animals (Dudley et al. 1998). However, the absolute synthesis rate of the important gut enzyme lactase phlorizin hydrolase (LPH) was shown unaffected by the route of nutrient administration

in this study (Dudley et al. 1998). These studies suggest that PN feeding could alter basic cellular functions in the lipid and protein levels.

In 2002, Sangild et al reported an interesting study comparing the effect of PN feeding and enteral feeding in both preterm (gestation age, 107d, delivered by caesarean section (C-section) and term (gestation age, 115d) piglets (Sangild et al. 2002). These piglets were fed with either intravenous PN or enteral sow's milk for 6 days after birth. Upon delivery, preterm piglets had lower blood pH, reduced oxygen saturation and neutrophil granulocyte function, impaired intestinal uptake of immunoglobulin G from colostrum, and altered relative weights of visceral organs (small intestine, liver, spleen, pancreas, and adrenals) compared to term piglets. Both preterm and term piglets had increased pancreatic weight (30-75%) and amylase activity (0.5- to 13-fold) after the 6 days of feeding period, but much more in milk-fed than in PN-fed piglets (*p-value* < 0.05). Compared to oral feeding, 6 days of PN feeding was associated with significant intestinal weight lost for both age groups (60% of the values in milk-fed piglets, *p-value* < 0.001). For PN term piglets, intestinal weight was even lower than at birth (-20%, *p-value* < 0.05). And only did PN term piglets have increased intestinal maltase activity and decreased absorption of glucose and proline compared to other groups. Compared to milk-fed piglets, lactase activity was seen increased in preterm piglets (up 50%, *p-value* < 0.05). For both age groups, the relative mRNA levels of LPH and sodium-coupled glucose transporter 1 (SGLT-1) were increased in PN-fed animals. These valuable results obtained in preterm piglets suggest that PN feeding may induce GI atrophy and modify postnatal maturation of many GI functions in preterm infants as well (Sangild et al. 2002). The same group subsequently showed that PN also affected

gut barrier function in the neonatal piglets (Kansagra et al. 2003). Jugular venous and bladder catheters were planted in the colostrum-deprived newborn piglets under general anesthesia. After 6 days of feeding with either oral formula or intravenous PN, all piglets were gavaged with a mixed solution of lactulose, mannitol, and polyethylene glycol 4000 (PEG 4000). Urine samples were collected over the next 24 hrs. After that, small bowel samples were harvested for functional analysis. Peripheral organ tissues, especially intestinal contents were used for bacterial culture and identification. PN-fed piglets had significantly higher urinary recovery (%dose) of lactulose (2.93 vs. 0.18) and PEG 4000 (12.78 vs. 0.96) (*p-value* < 0.05 for both), whereas recovery of mannitol (53 vs. 68) was similar. Incidence of bacterial translocation was similar in the two feeding groups. Jejunal myeloperoxidase activity increased significantly in PN-fed piglets compared to controls (*p-value* < 0.001), and was, however, weakly correlated with the urinary recover of lactulose (R^2 = 0.32) and PEG 4000 (R^2 = 0.38). Among the tight junction proteins analyzed, PN only increased the protein levels of claudin-1. In summary, it was suggested that PN induced dysfunction of the gut barrier was associated with increased intestinal permeability, rather than bacterial translocation (Kansagra et al. 2003).

In 2006, Wang et al reported detailed morphological and molecular analysis of PN induced liver injury in neonatal piglets (Wang et al. 2006). Seven newborn piglets were included in each group (PN or enteral nutrition (EN). Liver histology showed prominent steatosis (grade >2) in 6 of the 7 PN piglets, whereas only 2 EN piglets had minimal steatosis (grade ≤ 1). Gel electrophoresis showed strong signals of DNA fragmentation in cultured primary piglet hepatocytes from PN but not EN piglets. Test results showed significantly lower levels of ATP and higher activation of caspase-3

activity (9.9 fold) in the livers of PN piglets. Western blot showed markedly increased cleavage of apoptotic markers, including poly (ADP-ribose) polymerase (PARP), caspase-7, -8, and -9 in the livers of PN piglets. Protein levels of Bax, Fas and cytosolic cytochrome c were also up-regulated whereas Bcl-2 and proliferating cell nuclear antigen (PCNA) were slightly down-regulated in the livers of PN piglets. However, levels of markers of the endoplasmic reticulum-mediated apoptosis, including caspase-12 and binding immunoglobulin protein (BiP, also known as 78 kDa glucose-regulated protein, or GRP78), were similar between the two feeding groups. These results indicated that short-term PN in neonatal piglets could induce hepatic steatosis and oxidative stress, triggering mitochondrial and Fas pathways mediated apoptosis in the liver. In 2010, Stoll et al further showed that prolonged PN feeding in neonatal piglets could induce hepatic inflammation, steatosis, and even insulin resistance (Stoll et al. 2010). In this study, newborn piglets were fed with either enteral formula (EFor) or intravenous PN for 17 days. After PN feeding for 7 or 13 days, fasting i.v. glucose tolerance tests (IVGTT) were performed and evidence of insulin resistance were shown in PN piglets. PN animals also had higher levels of fasting plasma glucose and insulin than EFor piglets. On day 17, 1hrbefore tissue harvesting, low-dose hyperinsulinemic-euglycemic clamps (CLAMP) were performed and results showed that PN piglets had markedly decreased insulin sensitivity, compared to EFor piglets. Western blot showed that PN piglets had significantly reduced protein abundance of insulin receptor (IR), insulin receptor substrate 1 (IRS1), and phosphatidylinositol 3 kinase (PI3K) in the livers and skeletal muscles. Relative mRNA levels of many hepatic pro-inflammatory genes, phosphorylation of c-Jun-N-terminal kinase 1 (cJNK1), and plasma protein levels of IL-6

and TNF-α were all higher in PN piglets compared to controls. These detailed analysis linked chronic PN feeding to the development of insulin resistance, hepatic steatosis and inflammation in newborn piglets (Stoll et al. 2010). In a later study, Jain et al showed that PN-fed newborn piglets had dramatically decreased plasma levels of HDL, FGF19, glucagon-like peptide (GLP)-1 and GLP-2, and increased plasma triglyceride levels (Jain et al. 2012). One group of PN piglets also received CDCA infusion through additional duodenal catheter (PN+CDCA). CDCA treatment significantly improved conjugated bilirubin levels compared with the PN-only piglets. Normalized levels of total serum BAs and liver triglyceride were seen in the PN+CDCA piglets. ELISA showed that CDCA treatment significantly induced plasma levels of FGF19, GLP-1 and GLP-2. This study suggested that enteral CDCA treatment not only could resolve PNALD, but also could improve intestinal atrophy by induce GLP-2 (Jain et al. 2012). This study in part revealed the underlying mechanism by which minimal enteral intake could improve PNALD in patients.

In 2014, the same group reported another important study and showed that not only new generation lipid emulsions, FOLE and SMOFlipid, could reverse but also prevent PNALD in chronic PN-fed preterm pigs (Vlaardingerbroek et al. 2014). Compared to SOLE based PN (SOLE-PN), preterm piglets fed with FOLE based PN (FOLE-PN) or SMOFlipid based PN (SMOF-PN) for 14 days had significantly decreased serum levels of total bilirubin, conjugated bilirubin and GGT, though still higher than EN-fed piglets. Liver BA pool was increased in both SOLE-PN and FOLE-PN, but not SMOF-PN piglets. Plasma TSBA levels were highest in SOLE-PN, median high in FOLE-PN, and low in SMOF-PN piglets (similar to EN piglets). Liver triglyceride levels

were only increased in the SOLE-PN group, and with statistical significance. Among the hepatic genes tested, mRNA levels of *ABCB11*, *CYP7A1*, *FXR* and *MRP3* were down-regulated in all PN groups, whereas mRNA levels of *OST-α* was up-regulated only in SOLE-PN group. CYP7A1 protein levels increased only in the FOLE-PN group, yet plasma C4 concentration decreased significantly in all PN groups compared with EN group. Most importantly, PN with FOLE or SMOFlipid were able to maintain similar plasma level of FGF19, but not with SOLE when compared with EN group. Though *in vitro* data in this study still supported the idea that plant phytosterols may cause liver injury due to the suppression of FXR signaling, *in vivo* data contradicted the theory, mainly supported by the protective effect from SMOF-PN, which also contains considerable amounts of phytosterol.

As mentioned, PN rat model has also been used extensively to study the underlying mechanism of PNALD. In fact, studies conducted in rats and pigs (piglets) showed extensively overlapping findings in many aspects. In this regard, only studies obtained in pigs/piglets are discussed in detail here.

Study of PNALD in Mice

Unlike piglets and rats, surgical operations and subsequent PN infusion in newborn mice are still technically challenging. However, the well-established genetic engineering techniques in mice have provided indispensable opportunities for biologist to study the underlying mechanistic and genetic mechanisms for all sorts of human diseases, including PNALD.

Early PN studies conducted in adult mice mostly focused on the interplay between PNALD and the associated intestinal dysfunctions. Kiristioglu et al first showed that 7 days of PN infusion in mice was associated with significantly increased incidence of bacterial translocation to the mesenteric lymph node in the gut (40% in PN mice vs. 12.5% in controls) (Kiristioglu and Teitelbaum 1998). PN infusion significantly decreased the subpopulations of CD4+, CD8-; CD4+, CD8+; and CD8+, CD44+ gut intraepithelial lymphocytes (IEL) (*p-value* < 0.05), which were stained for CD4, CD8, and CD44 and counted by flow cytometry. Relative mRNA levels of IFN-γ increased 53% (*p-value* < 0.05), whereas levels of TGF-β1 decreased 75% (*p-value* = 0.1) in the isolated gut IELs of PN mice when compared with controls. In cultured intestinal epithelial cells (IEC), it was shown that increase of IFN-γ and decrease of TGF-β1 was associated with loss of intestinal tight junction (Madara and Stafford 1989). It was then suggested that these alterations in the IELs might affect the tight junctions between the IECs, and thus subsequently damage the integrity of the gut epithelial layer, leading to bacterial translocation (Kiristioglu and Teitelbaum 1998). In a later study reported in 2002, it was shown that the subpopulation of thymus-derived CD8αβ+ IELs declined by 92% (*p-value* < 0.01), whereas proliferation of IELs also declined significantly (Kiristioglu et al. 2002). In 2003, PN studies in IFN-γ KO mice showed that measured intestinal permeability in the KO mice was significantly lower than in PN-fed WT mice, though still higher than saline-infused control mice, suggesting that additional factors (cytokines) may also contribute to PN-associated gut epithelial barrier dysfunction (Yang, Finaly and Teitelbaum 2003). In 2007, this group further showed that PN infusion significantly diminished the expression of IEC-derived IL-7 (Yang et al. 2007), which

together with the IL-7 receptor (IL-7R), have been found in both thymic and intestinal epithelial cells (Watanabe et al. 1995, Watanabe et al. 2003, Yamazaki et al. 2003). IL-7 has been shown to play an essential role for the homeostatic proliferation and survival of naive peripheral T cells (Tan et al. 2001). Indeed, administration of exogenous IL-7 to PN mice significantly attenuated PN-associated IEL alterations, whereas blocking IL-7 receptor (IL-7R) with an exogenous anti-IL-7R antibody in normal chow-fed mice led to similar alterations in the IELs seen in PN mice. In 2008, subsequent studies obtained from transgenic mice showed that intestinal specific overexpression of IL-7 significantly attenuated many phenotypic and functional alterations of the IELs seen in PN mice (Yang, Gumucio and Teitelbaum 2008). The same year, Sun et al reported that PN infusion induced significant decline of the expression of IEL-derived cytokine interleukin-10 (IL-10) (Sun et al. 2008), which has been found to be a central modulator of the gut mucosal immune system in mice (Berg et al. 2002). Sun et al also showed that PN administration decreased the expression of several tight junction molecules, including zonula occludens-1, E-cadherin, and occluding when compared to controls (Sun et al. 2008). Convincingly, as demonstrated, administration of exogenous IL-10 partially attenuated the intestinal alterations observed in vehicle treated PN mice (Sun et al. 2008). In 2010, Feng et al reported the potential beneficial role of the PI3K/phospho-Akt (PI3K/Akt) signaling pathway in reversing intestinal atrophy observed in PN mice (Feng, McDunn and Teitelbaum 2010). A head-to-tail peptide dimer of the Akt-binding domain of the T-cell lymphoma-1 protein (TCL-1) was administered to activate the PI3K/Akt pathway in PN mice. PN mice treated with the effective peptide (PN+TCL-1) had increased protein abundance of p-Akt (Ser473) in the jejunal epithelial cells compared

to control peptide treated (PN+Ctrl). Phosphorylation of downstream effectors, including β-catenin and glycogen synthase kinase-3β (GSK-3β), were also decreased in PN+Ctrl mice but not in PN+TCL-1 mice. TCL-1 treatment also prevented the decline of gut epithelial cell proliferation and partially decreased the levels of apoptosis observed in PN+Ctrl mice. Similar activity reduction was also detected for the mammalian target of rapamycin (mTOR) pathway in PN+Ctrl mice, and subsequently corrected by TCL-1 treatment (Feng et al. 2010). These results suggest a potential strategy to maintain gut integrity in PN patients by regaining proliferation as well as retaining apoptosis of IECs through activation of the PI3K/Akt signaling pathway. In 2013, Feng et al reported another study showed that the loss of gut epithelial barrier function presented in PN mice was almost fully prevented in TNF-α receptor 1 (TNFR1) and TNFR2 DKO mice (TNFR1R2-DKO) and partially prevented in TNFR1-KO mice but not in TNFR2-KO mice when received intravenous PN feeding (Feng and Teitelbaum 2013). In addition, PN TNFR1R2-DKO mice had similar expression levels of intestinal gap junctional proteins to those found in saline-infused controls. Blockade of TNF-α signaling also prevented intestinal epithelial dysfunction and loss of junctional proteins in PN mice. Though these studies in various mouse models have linked PN therapy with intestinal dysfunction, none has provided valid data to directly correlate intestinal dysfunction to the development of PN associated liver injury, which is seen strongly in patients with intestinal failure as mentioned in the sections of clinical studies.

To fill this missing gap, one groundbreaking study published in 2012 in *Hepatology* by El Kasmi et al showed that liver toll-like receptor 4 (TLR4) signaling was critically involved in the pathogenesis of PNALD in adult mice with preexisting intestinal

injury induced by dextran sulphate sodium (DSS) pretreatment (El Kasmi et al. 2012). DSS, a chemical agent, was shown to induce intestinal damage followed by increased intestinal permeability. DSS pretreatment is a common research strategy to induce intestinal inflammation in animals to mimic human clinical conditions such as NEC and SBS, while the underlying mechanism is not completely known yet (Laroui et al. 2012). In the study, 6-8 weeks old adult mice were pretreated with 2.5% DSS in water or saline control for 4 days (El Kasmi et al. 2012). Pretreated mice were then put on continuous infusion with SOLE-PN or saline control for 7 (PN7d/DSS, PN7d/Saline) or 28 (PN28d/DSS, PN28d/Saline) days. In contrary to many early published studies using mice and those using rats and piglets, SOLE-PN infusion alone in this study only caused mild increase of serum levels of ALT, AST, and bilirubin in the PN7d/Saline and PN28d/Saline mice. There was indeed a trend towards development of liver injury in these mice as shown by the significantly increased levels of portal vein LPS and TSBAs (more than 2 fold for both). These findings are more consistent with the clinical observations in adult patients, for which short-term PN will not likely cause severe liver injury when compared to neonates. However, SOLE-PN induced dramatic liver injury in DSS pretreated mice, demonstrated by significantly elevated serum markers, including ALT, AST, bilirubin, GGT, and TSBA, as well as increased gene expression of *Il6, Tnf-α,* and *Il-1β* in purified primary mouse Kupffer cells (KCs) but not in whole liver homogenates. PN28d/DSS mice were associated with much more severe liver injury, including increased expression of *Il6, Tnf-α,* and *Il-1β* from even whole liver homogenates, as well as prominent KC hypertrophy and hyperplasia, associated with neutrophils recruitment, hepatic inflammatory infiltrates, hepatocyte apoptosis, and

parenchymal peliosis (El Kasmi et al. 2012). Next, the PN7d/DSS model was tested in the TLR4 mutant mice (PN7d/DSS-TLR4-KO), which had impaired LPS-TLR4 signaling (El Kasmi et al. 2012). Most strikingly, liver injury and cholestasis were both significantly attenuated in PN7d/DSS-TLR4-KO mice. ALT and AST levels decreased significantly (*p-value* < 0.05), whereas serum bilirubin and TSBA levels also decreased dramatically in PN7d/DSS-TLR4-KO mice. This study suggests that the combination of diminished enteral stimulus due to PN infusion, plus additional intestinal dysfunction/dysmotility (DSS pretreatment, NEC, SBS, etc.), together could promote intestinal bacterial overgrowth, which will lead to exacerbated intestinal inflammation and compromised gut barrier function. These eventually increased gut absorption and subsequent liver exposure to TLR agonists, such as bacterial endotoxins, and further exacerbated liver injury caused by PNALD.

As mentioned in previous sections of this chapter, studies obtained from both patients and newborn piglets have shown that new generations of lipid emulsion have been proven to be extremely beneficial and effective to both prevent and reverse PNALD. El Kasmi et al again used the PN/DSS mouse model to study the underlying mechanisms. Indeed, FOLE-PN mice had significantly attenuated liver injury compared to SOLE-PN mice (El Kasmi et al. 2013). By adding selected stigmasterols to the FOLE-PN (FOLE-PN-Stig/DSS), they were able to replicate the liver injury in DSS pretreated mice infused with FOLE-PN-Stig. In addition, hepatic mRNA expression of *Abcb11, Abcb2, Fxr* and liver X receptor (*Lxr*) decreased significantly in SOLE-PN/DSS but not FOLE-PN/DSS mice, whereas expression of *Abcg5* and *Abcg8* increased significantly in FOLE-PN/DSS but not SOLE-PN/DSS mice when compared with saline-infused

controls (El Kasmi et al. 2013). The relative low levels of ABCG5/8 transporters in SOLE-PN mice will aid in accumulation of plant sterols in the liver, whereas decreased protein abundance of BSEP and MRP2 will further promote the development of cholestatic liver diseases, especially in newborn populations in which the premature livers are even more vulnerable to PNALD. Indeed, mice with TLR4 deficiency or mice treated with antibiotics had significantly lower incidence of cholestasis and liver injury, as well as restored expression of *Abcb11, Abcc2*, *Lxr* and *Fxr* (El Kasmi et al. 2013). It was also proposed that stigmasterols might activate macrophages and synergize with intestinal endotoxins to promote the development and progression of PNALD in patients who had intestinal failure (El Kasmi et al. 2013).

1.4 Significance of the Studies of FXR and BA signaling Involved in Human Liver Functions

1.4.1 Genome-wide Studies of FXR in PHHs

As discussed throughout this chapter, there are limitations in biological research conducted in animal models in terms of studying human diseases, mainly due to species differences and technical challenges. Though extensive studies of the functions of FXR have been reported by using *in vitro* cell culture and *in vivo* animal models, how FXR function exactly in humans, are not yet fully investigated. To partially fill this gap, we performed genome-wide binding and RNA profiling analyses in PHHs and HepG2 cells, to compare and contrast FXR function in human hepatocytes versus in mouse livers on a global scale.

1.4.2 Studies of FXR Regulated BA Homeostasis in PNALD

As mentioned, both FXR gene expression and FXR regulated pathways were down-regulated in the livers of PN-fed piglets and PN/DSS mice. The down-regulation of liver FXR signaling and the lack of enterohepatic circulation caused by PN could potentially disrupt the normal BA homeostasis in patients receiving PN as well. To data, the potential contributions of BA cytotoxicity involved in the development and progression of PNALD is not yet studied. To address these questions, and to further study the mechanisms underlying the pathogenesis of PNALD, we developed a mouse PN model and characterized valuable signatures for the PN mice. These results will also be critical in aiding our future studies.

Chapter 2: Materials and Methods

2.1 Genome-wide Studies in PHHs and HepG2 cells

Cells and Treatment

Primary human hepatocytes (PHHs) used in this study were obtained through the Liver Tissue Cell Distribution System from the University of Pittsburgh (Kostrubsky et al. 1999, Li et al. 2012a). Only diagnostic and demographic information were obtained and provided by the supplier, no identifier was obtained. Comprehensive information of the PHH donors received in this study was listed in **Table 3.1**. PHHs were cultured in 37 °C, 5% CO_2 upon arrival. Three hs later, medium were refreshed with serum-free HMM Hepatocyte Maintenance Medium supplemented with dexamethasone, insulin, and GA-1000 (Lonza, Switzerland). Next morning, cells were treated with 5 μM GW4064 (Thomas et al. 2010), a synthetic FXR agonist, or control vehicle, DMSO. Cells were collected for chromatin and RNA isolation at 1 or 24 hrs after the treatment, respectively. HepG2 cells were obtained from ATCC (Manassas, VA). To obtain chromatin and RNA samples, same treatments and procedures as for PHHs were performed for HepG2 cells when the cells reached 95% confluence. RNA was isolated using TRI Reagent (Invitrogen, CA), according to the manufacture's instructions. FXR activation was confirmed by the induction of known human FXR target genes using Reverse Transcriptase (RT) quantitative PCR (RT-qPCR). Primer sequences are listed in **Table 2.1**.

Chromatin Immunoprecipitation

Onehrafter GW4064 treatment, cells were fixed in 1% formaldehyde for 10 minutes (mins), followed by quenching with glycine and rinsing with cold PBS. Afterwards, cells were collected and lysed. Nuclei were released and sonicated into 200-700 base-pair (bp) DNA fragments. Aliquot chromatin was incubated overnight with 5 μg anti-FXR antibody (1:1 mixture of sc-1204x and sc-13063x, ChIP grade) (Santa Cruz Biotechnology, CA), or control rabbit immunoglobulin G (rIgG, sc-2027) (Santa Cruz Biotechnology, CA). Chromatin-antibody complex were pulled down with prewashed Dyna beads (Invitrogen, CA), washed and eluted. DNA fragments associated with FXR or control antibodies were eluted and purified. Input genomic DNA was obtained through similar elution and purification procedures. Quality of ChIP assay was confirmed by qPCR with primers amplifying known FXRREs of human FXR target genes (promoter regions of BSEP (bile salt export pump) and OST-β (organic solute transporter beta) as well as the negative control (promoter region of IL-8 (interleukin-8). Primer sequences are listed in **Table 2.1**. PHH samples from four donors, with good FXR activation and pull-down efficiency, were selected to pool together for the generation of sequencing libraries (**Table 3.1**). For HepG2 cells, only chromatin samples obtained from GW4064 treated cells were used for sequencing library preparation. Primer sequences used for qPCR followed by ChIP experiments (ChIP-qPCR) are listed in **Table 2.1**.

Sequencing Library Preparation for ChIP-seq and RNA-seq

Equal amounts of chromatin from the selected four PHH donors were pooled together, followed by ChIP assay to generate DNA for ChIP-seq library preparation. Equal amounts of RNA from the selected PHHs were pooled together as well for RNA-seq library preparation. DNA and RNA sequencing libraries were prepared using the Illumina TrueSeqTM DNA and RNA Sample Prep Kit (Illumina, CA), respectively. The quality of all library samples was confirmed by Agilent Bioanalyzer (Agilent Technologics, CA) before the sequencing reactions. For ChIP-seq, purified library DNA ranging from 400 to 500 bp was fractionated on an agarose gel, followed by extraction and purification before sequencing. All libraries were sequenced 100 bp paired-end on Illumina HiSeq2000 sequencing system.

ChIP-seq Data Analysis

Genome Analyzer Pipeline Software (Illumina, CA) were used for both primary image data files processing and base calling. All sequenced paired-end reads were aligned to Homo sapiens version 19 (hg19) reference genome using bowtie (version 0.12.7) (Langmead et al. 2009). Only uniquely mapped reads were included. Regions with read enrichment were detected using Model-based Analysis of ChIP-Seq (MACS v 1.4.1) method (Zhang et al. 2008). By comparing with the rIgG background, non-specific peaks with false discovery rate (FDR) greater than 0.1 were eliminated. Identified peaks were further split by Mali Salmon's Peak Splitter (http://www.ebi.ac.uk/bertone/software.html) and filtered by p-value of Poisson

distribution lower than 10-5. Peaks were annotated using R packages (http://www.r-project.org) based on the ENSEMBL version 65 human genes.

Motif Analysis for ChIP-seq

For each ChIP-seq dataset, the sequences for the summit regions (201 bp), spanning 100 bp up and downstream from the summit of each peak, were retrieved. The top 500 sequences with the highest peak score were selected for motif analysis based on MEME (Multiple Em for Motif Elicitation) (Bailey et al. 2009).

ChIP-seq Validation

To validate the ChIP-seq results, we first identified the IR-1 site for each peak, which was located inside the peak summit regions (201 bps) used for motif analysis. Then the genome sequences spanning the IR-1 sites were retrieved to design qPCR primers. ChIPed DNA from individual donors and pooled samples were used for qPCR validation. The primer sequences are listed in **Table 2.1**.

Microarray for GW4064 and Vehicle Control Treated C57BL/6J Mice

C57BL/6J (hereafter referred to as wild type (WT) mice (n=3) were treated with either GW4064 (100 mg per kg body weight) or vehicle three times as previously described (Kong et al. 2012b) (first dose at 8 am, second dose at 6 pm, third dose at 8 am the second day). Mice were fasted overnight starting from the second dose and liver tissues were collected at 2 hrs after the third dose. All mice used for microarray study were

maintained in pathogen-free animal facilities in the Laboratory of Animal Research, under a standard 12-h light/dark cycle (6:00AM/6:00PM) with free access to standard chow and autoclaved tap water. Animal protocols and procedures were approved by the Institutional Animal Care and Use Committee (IACUC) at the University of Kansas Medical Center. Total RNA from livers was prepared with TRIzol Reagent (Invitrogen, CA), and the whole transcription expression levels were determined using Mouse Gene 1.0 ST Array system manufactured by Affymetrix, Inc.. Microarray data were analyzed using the Affymetrix Power Tools (http://www.affymetrix.com).

RNA-seq Data Analysis

For RNA-seq in PHHs, RNA was pooled from selected PHH donors. After sequencing, the obtained reads were aligned to the Homo Sapiens reference genome (hg19) using TopHat (version 2.0.0) (Trapnell et al. 2012).The resulted alignments were then assembled into transcripts using Cufflinks (version 2.0.2). Cuffdiff, a component of the Cufflinks package, was used to estimate FPKM (fragments per kilobase of exon model per million mapped fragments) and identify differentially expressed transcripts. Finally the Baggerley's test was used to perform the differential expression analysis.

Pathway Analysis for ChIP-seq and RNA-seq

Functional genes from ChIP-seq and RNA-seq were selected and analyzed using the Functional Annotation Tool in DAVID (http://www.david.niaid.nih.gov). For a pathway or

process to be defined, the threshold count was set at 2 with a minimum EASE (Expression Analysis Systematic Explorer) score, a modified Fisher Exact Test, of 0.1. Categories from DAVID with false discovery rates (FDRs) less than or equal to 0.1 were considered as statistically significant.

Data Files Access for ChIP-seq and RNA-seq

All sequencing data files discussed in this publication have been deposited in NCBI's Gene Expression Omnibus (Edgar, Domrachev and Lash 2002) and are accessible through GEO Series accession number GSE57312 (http://www.ncbi.nlm.nih.gov/geo/query/acc.cgi?acc=GSE57312)

Statistical Statement

For RT-qRCR experiments for PHHs, due to the difficulty of repeating sample collection from individual PHH donors, PHHs from different donors served as experimental replicates to validate FXR activation for the pooled PHH samples.

Table 2.1 Primers Used for Quantitative PCR for Human Genes

Primer Name	Forward Primer Sequence (5' - 3')	Reverse Primer Sequence (5' - 3')	Amplicon
RT Human *18S*	GAGCGAAAGCATTTGCCAAG	GGCATCGTTTATGGTCGGAA	101
RT Human *BSEP*	AGTTGCTCATCGCTTGTCTACG	GCTTGATTTCCCTGGCTTTG	153
RT Human *OST-β*	GCAGCTGTGGTGGTCATTAT	TAGGCTGTTGTGATCCTTGG	490
RT Human *FXR*	CGCCTGACTGAATTACGGACA	TCACTGCACGTCCCAGATTTC	114
ChIP Human *BSEP*	TTCACAACCTTTTCCAACCTCGGTT	TGTCACTGAACTGTGCTTGGGCTG	131
ChIP Human *OST-β*	AATGAAAGCACTGGGCTACTGGTG	TCCAGGGTGACTGACCTCTTGAAT	99
ChIP Human *IL-8*	ACTCAGGTTTGCCCTGAGGGGA	TGCCTTATGGAGTGCTCCGGTG	136
ChIP Human *ACTBP11*	GCTTGGTGGCTGAAGAGTGA	ACCCCATGTAATCACGAGGC	106
ChIP Human *AOC1*	GATTCTGTAGCGCCGAGTCA	ATCCTGTACCCTCTACCCCG	293
ChIP Human *FABP3*	GGGCAGCCACCTTTATCCAA	TCTTCCCACCAAGCCTTAGC	296
ChIP Human *HS6ST1*	CTCTGATGGCCCTCCTGTTG	AGCCATGGCCACTCATAACC	250
ChIP Human *GFOD2*	TTTGGCAGGTTCTGGGACTC	GAGAATCTGTCCACTGCCCC	120
ChIP Human *PNMT*	ATCCGCATCCAGGGTTTGTT	AAGTCTCCTTGGGAGAGGCA	295
ChIP Human *UROC1*	CTGGGGAGGACATTGCTCTG	AGATGCAGATCCCCACATCG	188

2.2 Studies of PNALD in Animal Models

Animals and Surgery

All animal protocols and procedures were approved by the Institutional Animal Care and Use Committee (IACUC) of the Rutgers University. Unless otherwise specified, all mice used for the PNALD study were maintained in the pathogen-free animal facilities in the Comparative Medicine Resources at the Nelson Animal Facility at Rutgers University, under a standard 12-h light/dark cycle (6:00AM/6:00PM) with temperature-, humidity- controlled conditions. Mice were fed at *ad libitum* with standard mouse chow and autoclaved tap water. C57BL/6J (WT) mice used in this study were obtained from the Jackson Laboratory (Bar Harbor, ME)

For the surgery of jugular vein catheterization, mice were anesthetized with 80mg/kg ketamine and 10 mg/kg xylazine via intraperitoneal injection, followed by placement of a central venous catheter (polyurethane tubing, 1F in O.D.,) (SAI Infusion Technologies, IL) into the right jugular vein. After inserting the catheter into the right atrium of the mouse, the patency was verified by carefully withdrawing minimal amount of blood from the jugular vein. Once the correct insertion was confirmed, the saline solution in the catheter was replaced by heparin/glycerol catheter lock solution (SAI Infusion Technologies, IL) followed by securing the proximal end of the catheter with a stainless steel plug (SAI Infusion Technologies, IL), to maintain the catheter patency during the post-operative recovery period. The proximal end of the catheter was then tunneled subcutaneously and exited between the shoulder blades. The outside part of catheter was secured with a wound clip on the back of the mouse to prevent potential damage from the surgical mouse. On the next day, the fully recovered surgical mouse

was placed in a plastic harness (SAI Infusion Technologies, IL) and the catheter was flushed with saline. Catheter patency was confirmed with blood withdraw again before connecting the catheter to an infusion pump (Harvard Apparatus, MA) through the extension line (SAI Infusion Technologies, IL). Mice were then kept on intravenous infusion of normal saline (NS, 0.9%) at an initial rate of 6mL/d and had free access to mouse chow (Rodent Diet 5001; LabDiet) and water. The next day, PN mice started to receive intravenous PN infusion prepared by CAPS, Inc. (Englewood, NJ), and still had free access to water but not mouse chow. One day after, the infusion rates for both saline and PN mice were increased to 8mL/d, and kept as 8mL/d throughout the study period with the PN solution providing a caloric intake of 10.62 kcal/24 hrs (detailed list of nutrients in PN solution was presented in **Table 2.2**). It has been reported and well-accepted in the research field, that graded infusion period is necessary for the mice to adapt to the continuous infusion of fluid and nutrients (Omata et al. 2013). All saline control and PN mice were housed individually in metabolic cages to prevent PN mice from coprophagia.

At the end of the study period, blood was collected from the retro-orbital plexus and kept in heparin coated anti-coagulant tubes. Blood samples were then centrifuged at 8,000g for 10min to collect plasma. Tissues were quickly collected and snap frozen in liquid nitrogen for future analysis.

Serum Biochemical Analysis

Commercially available testing kits were used to measure serum levels of biomarkers, including alanine transaminase (ALT), aspartate transaminase (AST), and

alkaline phosphatase (ALP) (Pointe Scientific, MI), and total serum bile acids (TSBA) (Diazyme Laboratories, CA). Procedures were scaled up or down based on the manufacturer's instructions.

RNA Isolation, RT-qPCR and Microarray Analysis

For RNA isolation, frozen mouse tissues were homogenized for 30 seconds (secs) in TRI reagent (Invitrogen, CA) with a polytron homogenizer, then undergone the isolation procedures according to the manufacturer's instructions. Live gene expression was analyzed by RT-qPCR. After rigorous analysis of gene expression in saline and PN mice, RNA samples (n=3) obtained from saline and PN mouse livers were pooled, respectively, for microarray analysis (Microarray-PN/Saline). Whole liver transcription expression levels were then determined using Mouse Gene 2.0 ST Array system manufactured by Affymetrix, Inc. Microarray data were analyzed using the Affymetrix Power Tools (http://www.affymetrix.com). Data retrieved from the microarray analysis were further validated by RT-qPCR analysis. All the primer sequences for mouse genes are listed in **Table 2.3**.

Histological Analysis

Mouse liver and intestinal tissues were removed at sacrifice, fixed in 10% neutral phosphate buffered formalin. Fixed livers were processed by the University of Connecticut Veterinary Medical Diagnostic Laboratory (Storrs, CT), where tissues were embedded in paraffin, sectioned into slides, and stained with hematoxylin and eosin (H&E) according to standard staining protocols.

Organic Extraction and Ultra Performance Liquid Chromatography/Mass Spectrometry (UPLC/MS) Profiling of Serum BAs

For simple protein precipitation, 900uL of pre-chilled acetonitrile (ACN) was added to 90uL of plasma samples with 20uL of internal standards, followed by vortex and centrifugation at 11,000 x g for 10min at 4^{o}C. The supernatant was then transferred to a fresh tube, completely dried under a vacuum evaporator, and reconstituted in 50:50 methanol/water (v:v). Further purification is done by centrifugation with a 10 kDa molecular size exclusion membrane. The final BA extracts were introduced to the Thermo Finnigan Ultra Performance Liquid Chromatography (UPLC) system (Thermo Fisher Scientific, MA) coupled with a Thermo Finnigan LTQ XL Ion Trap Mass Spectrometer (Thermo Fisher Scientific, MA). An Electrospray (ESI)/ITMS was operated in multiple MS/MS and SRM (Selective Reaction Monitoring) modes for simultaneous determination of 23 bile acid including: CA, CDCA, DCA, LCA, UDCA,TCA, T-CDCA, TDCA, taurolithocholic acid (TLCA), tauroursodeoxycholic acid (TUDCA), glycocholic acid (GCA), glycochenodeoxycholic acid (GCDCA), glycodeoxycholic acid (GDCA), glycolithocholic acid (GLCA), and glycoursodeoxycholic acid (GUDCA), β-MCA, α-MCA, ω-muricholic acid (ω-MCA), tauro-β-muricholic acid (T-β-MCA), tauro-α-muricholic acid (T-α-MCA), tauro-ω-muricholic acid (T-ω-MCA), HDCA, taurohyodeoxycholic acid (THDCA), and glycohyodeoxycholic acid (GHDCA).

For BA standards, CA, CDCA, DCA, LCA, UDCA, glycocholic acid hydrate, taurocholic acid sodium salt hydrate, sodium glycochenodeoxycholate, sodium taurochenodeoxycholate, sodium glycodeoxycholate, sodium taurodeoxycholate hydrate, sodium taurolithocholate, and sodium tauroursodeoxycholate, were purchased

from Sigma-Aldrich (St. Louis, MO); sodium glycolithocholate, GUDCA, sodium tauroursodeoxycholate, β-MCA, α-MCA, ω-MCA, tauro-β-muricholate, tauro-α-muricholate, tauro-ω-muricholate, HDCA, THDCA, and GHDCA were purchased from Steraloids, Inc. (Newport, RI). For internal standards, chenodeoxycholic-2,2,4,4-$d_4$acid ($^2H_4$-CDCA) and glycochenodeoxycholic-2,2,4,4-d_4 acid ($^2H_4$-GCDCA) were purchased from C/D/N Isotopes, Inc. (Pointe-Claire, Quebec, Canada).

Statistical Analysis

Student's *t*-test was used to compare the data obtained from the saline and PN groups. *P-value* < 0.05 was considered statistically significant.

Table 2.2 Components of Parenteral Nutrition per 100 mL

Component	Amount	Unit
Concentrated amino acid *	4	g
Dextrose	25.5	g
Lipid #	3	g
Sodium phosphate	1.34	mM
Potassium chloride	1.6	mEq
Sodium chloride	3.2	mEq
Potassium acetate	12	mEq
Magnesium sulphate	0.8	mEq
Calcium gluconate	1.32	mEq
Multitrace®-5 concentrate §	0.1	ml
Heparin	500	U
Multi-vitamin ¥	2	ml
Protein content (amino acid)	4	g
Nitrogen content	0.632	g
Non-protein calorie	116.7	kcal
Carbohydrate calorie	86.7	kcal
Lipid calorie	30.0	kcal
Protein calorie	16	kcal
Total calorie	132.7	kcal

***** Clinisol 15%, obtained from Baxter International Inc., Deerfield, IL.

Intralipid 20%, obtained from Baxter International Inc., Deerfield, IL.

§ Multitrace®-5 concentrate, contains zinc, copper, manganese, chromium, and selenium, obtained from American Regent, Inc. Shirley, NY.

¥ Infuvite Adult, obtained from Baxter International Inc., Deerfield, IL.

Table 2.3 List of qPCR Primers Used for Mouse PN Studies

Gene	Forward Primer Sequence (5' - 3')	Reverse Primer Sequence (5' - 3')
β-actin	GCGTGACATCAAAGAGAAGC	CTCGTTGCCAATAGTGATGAC
Fxr	TCCGGACATTCAACCATCAC	TCACTGCACATCCCAGATCTC
Bsep	CTGCCAAGGATGCTAATGCA	CGATGGCTACCCTTTGCTTCT
Ost-α	GTCTCAAGTGATGAACTGCCA	TTGAGTGCTGAGTCCAGGTC
Ost-β	GTATTTTCGTGCAGAAGATGCG	TTTCTGTTTGCCAGGATGCTC
Mrp3	AGAGCTGGGCTCCAAGTTCT	TGGTGTCTCAGGTAAAACAGGTAGCA
Ntcp	GGCCACAGACACTGCGCT	AGTGAGCCTTGATCTTGCTGAACT
Fgf15	GCCATCAAGGACGTCAGCA	CTTCCTCCGAGTAGCGAATCAG
Shp	CGATCCTCTTCAACCCAGATG	AGGGCTCCAAGACTTCACACA
Cyp7a1	AACAACCTGCCAGTACTAGATAGC	GTGTAGAGTGAAGTCCTCCTTAGC
Cyp7b1	CAGCTATGTTCTGGGCAATG	TCGGATGATGCTGGAGTATG
Cyp8b1	AGTACACATGGACCCCGACATC	GGGTGCCATCCGGGTTGAG
Cyp27a1	GCCTCACCTATGGGATCTTCA	TCAAAGCCTGACGCAGATG
Cyp2b10	GACTTTGGGATGGGAAAGAG	CCAAACACAATGGAGCAGAT
Cyp17a1	TGGCTTTCCTGGTGCACAATC	GGAGGTGAGTCCGGTCATTGAA
Abcg5	TGGATCCAACACCTCTATGCTAAA	GGCAGGTTTTCTCGATGAACTG
Abcg8	CCGTCGTCAGATTTCCAATGA	GGCTTCCGACCCATGAATG
Fas	GCTGCGGAAACTTCAGGAAAT	AGAGACGTGTCACTCCTGGACTT
Srebp1c	GGAGCCATGGATTGCACATT	GCTTCCAGAGAGGAGGCCAG
Nurr77	AGCTTGGGTGTTGATGTTCC	AATGCGATTCTGCAGCTCTT
Lxrα	GGGAGGAGTGTGTGCTGTCAG	GAGCGCCTGTTACACTGTTGC
Lpl	AGGACCCCTGAAGACAC	GGCACCCAACTCTCATA
Abcd2	CACAGCGTGCACCTCTAC	AGGACATCTTTCCAGTCCA
Lepr-b	GCATGCAGAATCAGTGATATTTGG	CAAGCTGTATCGACACTGATTTCTTC
Marco	GCACTGCTGCTGATTCAAGTTC	AGTTGCTCCTGGCTGGTATG
Nocturnin	ACCAGCCAGACATACTGTGC	CTTGGGGAAAAACGTGCCT
Acc	TGACAGACTGATCGCAGAGAAAG	TGGAGAGCCCCACACACA
Scd1	CCGGAGACCCCTTAGATCGA	TAGCCTGTAAAAGATTTCTGCAAACC
Cd36	GATGACGTGGCAAAGAACAG	TCCTCGGGGTCCTGAGTTAT
Sult1e1	GTGGAAAAATGCAAGGAGGA	GGGTGGCAGGTGAGTTTTTA
Pgc-1α	CGGAAATCATATCCAACCAG	TGAGGACCGCTAGCAAGTTTG

Chapter 3: Genome-wide Binding and Transcriptome Analysis of Human FXR in PHHs and HepG2 Cells

(Portions of this section are adapted from Zhan et al. (2014), PLoS ONE 9(9): e105930. doi:10.1371/journal.pone.0105930 (Zhan et al. 2014))

3.1 Introduction

Farnesoid X receptor (FXR, *NR1H4*) is a ligand activated transcription factor belonging to the nuclear receptor (NR) superfamily (Forman et al. 1995), and is highly expressed in the liver, intestine, and kidney, both in humans and rodents (Zhang et al. 2003). Bile acids (BAs) are the endogenous ligands of FXR (Makishima et al. 1999). FXR mainly functions as the BA sensor by regulating genes that are critically involved in BA homeostasis, including BA biosynthesis, conjugation, and enterohepatic circulation (Sinal et al. 2000). In addition, it has been shown that FXR is also involved in lipid and glucose homeostasis, inflammation, and tumorigenesis (Sinal et al. 2000, Ma et al. 2006, Wang et al. 2008, Kim et al. 2007). FXR normally forms a heterodimer with retinoid X receptor alpha (RXRα) and binds to DNA elements as FXR response elements (FXRREs) (Forman et al. 1995). The most common DNA motif bound by FXR is an inverted repeat separated by one nucleotide (IR1). Upon ligand activation, the heterodimer normally activates the expression of its target genes.

Chromatin immunoprecipitation - deep sequencing (ChIP-seq) analysis has been widely used to study the functions of various NRs, including androgen receptor (AR), estrogen receptor alpha (ERα), glucocorticoid receptor (GR) etc. (Jia et al. 2008, Gao et al. 2008, John et al. 2008). This approach has aided in discovering novel pathways

regulated by these NRs. We and others have reported the genome-wide binding analysis of FXR in mice (Thomas et al. 2010, Chong et al. 2010, Lee et al. 2012). These studies suggest broad functions of mouse FXR as well as novel molecular mechanisms, by which FXR regulates its target genes. First of all, FXR could bind to multiple sites within a known FXR target gene. For example, FXR binds to both the promoter and 3' gene regulatory regions of the *Nr0b2* gene, which encodes small heterodimer partner (SHP) (Thomas et al. 2010), and this pattern of binding likely enhances chromatin interaction and subsequent gene expression (Li et al. 2010). Secondly, many new target genes of FXR are identified in the liver and/or intestine, including the *Sqstm1* gene, which encodes the protein p62, an important component of autophagy (Williams et al. 2012). Thirdly, FXR cooperates with other transcription factors, most likely orphan nuclear receptors, to modulate transcription of genes involved in specific biological processes. For exp., FXR and LRH-1 (liver receptor homolog-1) co-regulate genes involved in lipid homeostasis (Chong et al. 2012, Thomas et al. 2013). Fourthly, FXR elicits tissue-specific binding patterns, indicating differential regulation of chromatin structures as well as FXR functions among different organs/cells. Lastly, FXR binding could suppress gene expression, which could be altered during disease state, such as obesity (Lee et al. 2012). Taken together, these studies suggest that FXR may regulate diverse physiological and pathological processes in mice, underlying that tissue- or even pathway-specific modulations of FXR may provide better treatment strategies to various lipid- and BA-associated diseases. Indeed, recent literatures have highlighted FXR as a potential therapeutic target for different metabolic diseases, such as parenteral nutrition associated cholestasis (El Kasmi et al. 2013), vertical sleeve

gastrectomy (Ryan et al. 2014), and more commonly nonalcoholic steatohepatitis (NASH) (Deng et al. 2013, McMahan et al. 2013), while only limited treatment options are currently available for these diseases.

To date, the binding of human FXR in primary human hepatocytes (PHHs) or hepatoma cell lines has been characterized to limited genes, including *ABCB4* (ATP-binding cassette, sub-family B, member 4)*, ABCB11, FGF19* (fibroblast growth factor 19)*, ICAM1* (intercellular adhesion molecule 1), *and NR0B2* (Ananthanarayanan et al. 2001, Sinal et al. 2000, Holt et al. 2003, Huang et al. 2003, Qin et al. 2005). However, the genome-wide FXR binding profile in humans is not yet available. More importantly, little information is known about species similarities and differences in terms of FXR binding between humans and mice, which are needed urgently to determine to what degree the murine models can be used to study the role of FXR in various physiological and/or pathological conditions.

In this study, using ChIP-seq and RNA-seq techniques, we determined the genome-wide binding and transcriptome profiles of human FXR in PHHs, as well as genome-wide binding profiles in HepG2 cells. We compared and contrasted the binding patterns and gene regulation profiles of FXR between human and mouse livers, as well as between PHHs and HepG2 cells.

3.2 Results

FXR Activation in PHHs

To identify genome-wide FXR binding sites in primary human hepatocytes, we first validated FXR activation in the PHHs obtained in this study. Upon 24 hrs of GW4064 treatment, mRNA levels of classic FXR target genes (BSEP, OST-β) were induced in PHHs from individual donors (**Figure 3.1 A**). Pooled chromatin samples, which were collected after 1hrGW4064 treatment, showed significant enrichment of FXR binding to known FXR targets (promoter regions of *BSEP* and *OST-β*), but not the negative control (promoter region of *IL-8*) (**Figure 3.1 B**). ChIPed-DNA, generated from pooled chromatin from selected donors (**Table 3.1**), as well as pooled RNA was then used to generate DNA and RNA sequencing libraries. Indeed, many known human FXRREs were detected with relatively high peak values in this study, in both DMSO and GW4064 treated PHHs (**Table 3.2**). Again, multiple FXR binding sites were found in the *NR0B2* and *OST-β* gene in our datasets (**Table 3.2**), which resembled the binding patterns of FXR to these genes in mice (Thomas et al. 2010).

In ChIP-seq, the peak summit of each peak (binding site) was a single bp position within the peak with the highest coverage given by the MACS analysis. Due to the relatively large size of fragmented library DNA obtained in this study (average 350 bp for ChIP-seq), and the subtle differences in the local chromatin environment in different samples, we saw slightly different peak width and peak summit values for the same binding sites in the two datasets. For example, for the binding site located in the intron of *FGF19* gene, the peak width was 1000 and 851 bps in the ChIP-seq datasets from DMSO treated PHHs (PHH-DMSO) and GW4064 treated PHHs (PHH-GW), respectively. And the peak summits in the two datasets were 3665 and 3695 bps

downstream from the TSS of *FGF19*, respectively. Nevertheless, these peaks were indicating the same binding site.

Comparison of Global FXR Binding between PHHs and Mouse Livers

When cut off score (CO score) for ChIP-seq data analysis was set as 20, a total of 2759 and 5235 FXR binding sites were identified from PHH-DMSO and PHH-GW, respectively. Human and mouse FXR binding profiles in livers were compared between these human data with our previous genome-wide mouse FXR binding data, which were obtained from WT mice treated with GW4064 (referred to as mLiver-GW, which was not normalized to the rIgG control though) (Thomas et al. 2010). The following results were obtained by comparing the global binding pattern in these datasets: 1st, genomic distributions of FXR binding sites were similar in PHHs compared to those in mice (**Figure 3.2)**. Briefly, around 43% peaks were located in intergenic, 21% in upstream 0-10 kb, 22% in introns, 10% in downstream 0-10 kb, 2% in 5' untranslated region (UTR), 1% in 3' UTR, and 1% in coding DNA sequence (CDS) regions of their associated RefSeq genes in both PHH-DMSO and PHH-GW. This site-distribution pattern was similar to that in mice. Though in mouse livers, around 30% peaks were located in introns and 15% in upstream 0-10 kb region (Thomas et al. 2010). 2nd, the distribution patterns of total FXR binding sites relative to transcription start sites (TSSs) of the associated RefSeq genes, and FXR's intron binding patterns were both similar to those in mice as well. The highest frequency of total binding events was located within 0-10 kb up and downstream of TSSs (**Figure 3.3 A**). Most intron binding events were located in

the 1st intron and the number of total binding events in individual intron decreased as the intron number increased (**Figure 3.3 B**). These patterns were almost identical to those in mice (Thomas et al. 2010).

Motif Analysis of FXR Binding Sites in PHHs

The most commonly reported FXR binding motif is an IR1 in both mice and humans. This motif has been reported in many human FXR target genes, such as *ABCB11, FGF19, NR0B2,* and *OST-β* (Holt et al. 2003, Ananthanarayanan et al. 2001, Goodwin et al. 2000). When we select the top 500 peaks from PHH-GW and PHH-DMSO, the most common motif found in PHH-GW was an IR-1 with a putative nuclear half site, whereas in PHH-DMSO it was the IR1 motif (**Figure 3.4**). And interestingly, when we select the top 501-1000 peaks to run motif analysis, we only obtained the IR-1 motif from both datasets (data not shown). The presence of IR-1 with nuclear half site was also similar to our previous motif analysis in mouse livers (Thomas et al. 2010).

Validation of ChIP-seq and Novel FXR Targets in PHHs

After motif analysis, we were able to precisely locate the IR-1 site associated with each peak summit for most peaks in our datasets. The subtle position difference (mostly around 50bp) from the IR-1 site to the peak summit for each FXR target was most likely caused by a combination of relatively large DNA fragments used for our sequencing analysis and the technical limitation of the sequencing processing and data analysis.

Since most classic FXR targets were presented correctly in the datasets (**Table 3.2**), we then focused on validating novel FXR targets.

ChIP-qPCR was performed on chromatin samples from pooled PHH samples, as well as individual PHH donors. For many FXR targets, we were unable to detect valid Ct value from rIgG control from qPCR experiments for individual PHH donors, mainly due to limited quantity of chromatin samples. Nevertheless, we were able to confirm enhanced FXR pull-down from GW4064 treated PHHs comparing to DMSO control, for the promoter regions of *BSEP* and most selected novel targets, but not the negative controls. And for those FXR targets, of which FXR pull-down was not further enhanced upon GW4064 treatment, we were able to calculate their FXR pull-down efficiency after normalizing to rIgG control from pooled PHH samples **(Figure 3.5 A, B).** Without valid Ct values from the rIgG control pull-down, we couldn't differentiate these FXR targets from the negative controls. For exp., the binding score for PNMT (phenylethanolamine N-methyltransferase) in PHH-DMSO and PHH-GW were 55 and 68, respectively, which were close. Indeed, ChIP-qPCR showed similar FXR pull-down efficiency from pooled PHH samples (**Figure 3.5 B,** around 3 fold for both control and treatment). The promoter region of *OST-β* showed the same trend as well (**Figure 3.1 B**).

In this regard, to better illustrate FXR binding in both DMSO and GW4064 treated PHHs, only ChIP-qPCR data for pooled PHHs were presented. We were able to validate FXR pull-down for most selected novel targets with relatively high binding scores (9 out of 11 peaks were validated, with binding scores equal to or above 50 in either PHH-DMSO or PHH-GW (**Figure 3.5**). This trend was consistent with our previous findings in mouse livers (Thomas et al. 2010).

Microarray, RNA-seq and their Correlation with ChIP-seq Datasets

Using microarray, we obtained a gene expression profile from WT mouse livers treated with GW4064 (M-mLiver-GW) normalized to vehicle control. When set cut off fold induction (CO fold) as 1.5 and *p*-value <0.05 (unpaired *t*-test), we obtained 102 different genes with altered expression levels, up or down more than or equal to 1.5 fold. From RNA-seq for GW4064-treated PHHs (R-PHH-GW), which was normalized to DMSO control, we obtained 143 genes with $\log_2$ fold enrichment ≥2 (fold change ≥4, both up- and down- regulated) and *p*-value <0.05. The percentage of genes found in microarray and RNA-seq, which was also bound by FXR from ChIP-seq, was plotted in **Figure 3.6** based on the fold induction from microarray and RNA-seq. Among all the genes found in M-mLiver-GW, over 50% were bound in mLiver-GW for both up- and down- regulated. However in R-PHH-GW, around 50% up-regulated genes were bound in PHH-GW, whereas only a few down-regulated genes were actually bound in PHH-GW. Interestingly, *FGF19* and cytochrome P450, family 7, subfamily A, polypeptide 1 (*CYP7A1*) were the top up- and down-regulated FXR targets in R-PHH-GW, respectively.

Pathway Analysis for ChIP-seq and RNA-seq for PHHs

A major difference between the mLiver-GW dataset and the PHH-GW dataset was that, more than 5,000 genes and 10,000 peaks were found in mLiver-GW compared to 5,231 peaks identified in PHH-GW. The lack of IgG control for the mLiver-GW may well explain this major difference as non-specific peaks may present in the

mouse FXR binding study. Another difference was that the majority of the peaks in mLiver-GW were associated with RefSeq genes, which encode proteins with known functions, whereas in PHH-GW only around 50% peaks were. In order to compare and contrast the functional detail of FXR binding in humans and mice, two major analyses from DAVID were performed, the Kyoto Encyclopedia of Genes and Genomes (KEGG) and the Gene Ontology Biological Process (GO-BP) analysis. Similar to our previous study, functional genes associated with peaks located in the upstream 0-10 kb promoter regions were selected to run DAVID analyses. Overall, more categories were enriched in PHH-GW than PHH-DMSO. And most categories enriched in PHH-DMSO were also presented in PHH-GW. In this regard, only categories and their corresponding FXR targets from PHH-GW were presented and compared with mLiver-GW. All significantly enriched KEGG categories (with FDR <0.1) (**Table 3.3 A**), and the corresponding genes (**Table 3.5 A**) obtained were listed, whereas most non-redundant categories (with gene count >5) from GO-BP were presented (**Table 3.3, 3.5 B**). From DAVID analyses, we could see overall similar pathways enriched from mLiver-GW and PHH-GW, though the number of genes retrieved from PHH-GW was smaller. Nevertheless, the percentage of genes found in each category was similar between the two datasets. For R-PHH-GW, 291 functional genes with $\log_2$ fold ≥1 (fold change ≥2, up- and down- regulated), and *p*-value ≤0.05 were retrieved for KEGG and GO-BP analyses. Note that the cut off fold change used for pathway analysis is smaller than the cut off used for the ChIP-seq/RNA-seq correlation analysis. For pathway analysis, the cumulative effect from many altered genes in a single pathway could be of functional importance as well, though the level of fold change for individual gene was relatively low. All categories from

KEGG and non-redundant categories from GO-BP, and the corresponding genes were presented (**Table 3.4 A, B**). In agreement with previous correlation study presented in **Figure 3.6**, both similar and different categories were enriched from R-PHH-GW. Interestingly, many genes involved in chemokine signaling pathway (KEGG) and chemotaxis (GO-BP) were enriched in R-PHH-GW (**Table 3.4),** and most of these were not directly bound by FXR.

Genome-wide FXR Binding Profiles in HepG2 Cells

As expected, common FXR targets were also identified in the ChIP-seq analysis for GW4064 treated HepG2 cells (HepG2-GW) (**Table 3.1**). Similar results in terms of FXR activation (**Figure 3.1 A, B**), genomic and functional distributions of FXR binding sites (**Figure 3.2**, **Figure 3.3 A, B**), and FXR binding motif (**Figure 3.4**) were obtained from the HepG2-GW as well. Similar to PHH-DMSO, the most common binding motif identified for HepG2-GW was also an IR1, without a nuclear half site.

3.3 Discussion

In this study, combining the widely used ChIP-seq and RNA-seq techniques, we have characterized the genome-wide FXR binding and transcriptome profiles upon ligand activation in selected PHHs and HepG2 cells. From the three datasets, we were able to detect almost all previously identified important human FXR targets, which have diverse physiological functions. Comparing the global FXR binding patterns, we showed

that the patterns in PHHs and HepG2 cells were very similar to those identified in mouse livers in terms of genomic distribution, intron binding pattern, and the association with TSSs of RefSeq genes. These phenomena were in agreement with the conserved function of FXR in transcriptional regulation.

Most convincingly, the motifs found in this study were almost identical to those found in mice. Interestingly, the putative nuclear receptor half site was enriched significantly only from the top 500 peaks in PHH-GW, neither in the top 501 to 1000 peaks nor the top 500 peaks from PHH-DMSO (**Figure 3.4**). In the chromatin level, the co-binding of FXR and other transcription factors to certain targets may potentially correspond to higher levels of pull-down from ChIP assay, leading to higher enrichment scores for these genes. Previous genome-wide binding analysis of LRH-1 in mice has shown that LRH-1 could bind to the nuclear half site next to IR1, and co-regulate transcription of FXR target genes involved in lipid metabolic processes in mice (Chong et al. 2012). The top 500 peaks identified in this study are associated with genes not only involved in lipid metabolism, but in diverse cellular processes. This could indicate a common mechanism of how FXR regulate gene transcription in different cellular processes, while with different cofactors involved. This type of co-regulation has been well studied for ERα (Lupien et al. 2008). Moreover, the presence of a nuclear receptor half site adjacent to the IR-1 in both PHH-GW and mLiver-GW indicates the similarities of FXR functions from mice to humans in a greater extent by indicating the existence of similar type of cofactors for FXR in different species. This mechanistic similarity implicates that tissue- and even pathway- specific FXR modulation in mice can be translated into therapeutic benefits in humans.

Using multiple pathway analysis tools (KEGG and GO-BP from DAVID), the current study predicts that human FXR could participate in the regulation of diverse physiological processes (**Table 3.3, 3.4, 3.5**). Furthermore, similar pathways were enriched from PHH-GW compared to mLive-GW. More genes were obtained from mLiver-GW than PHH-GW. As a result, more pathways were enriched in mLiver-GW (Thomas et al. 2010). Future studies are needed in order to determine to what degree the lack of IgG control contributes to the increased output from mLiver-GW. Overall, the comparison studies presented in this study will be valuable information for researchers in correlating and translating previous and future mouse FXR studies to human FXR functions.

RNA-seq analysis for DMSO and GW4064 treated PHHs also further confirmed the reliability of GW4064 treatment and FXR activation in this study. Interestingly, *FGF19* and *CYP7A1* were the top up-regulated and down-regulated target genes in PHHs, respectively, whereas in mice *Fgf15* is only found to be expressed and induced in the intestine (Kong et al. 2012b).

When correlating the results from ChIP-seq with RNA-seq for PHHs, and microarray for mouse livers, different trends were observed for genes down-regulated following GW4064 treatment (**Figure 3.5**). In addition, only a small portion of target genes showed similar change in R-PHH-GW and M-mLiver-GW. This difference may be due to several reasons. First, there are different baseline regulatory network in different species, such as the different expression patterns of FGF19 in humans versus Fgf15 in mice. Besides, the genetic background of the PHH donors could be heterogeneous since we didn't receive certain donor information upon tissue collection, such as races,

patient condition, etc. And the inbred C57BL6/J mice were relatively homogenous. Second, for many FXR target genes, the expression levels may be already high in control mice due to activation of FXR by the largely stable bile acid pool, while the levels of residual bile acids in PHHs could be very low. In this regard, GW4064 treatment wouldn't further induce the expression of these genes in mice. In line with this, for many FXR target genes in mice, we detected similar FXR binding from ChIP assay when comparing GW4064 treated versus vehicle control treated mouse livers (data not shown). But we did see dramatic increase of FXR binding from GW4064 versus DMSO treated PHHs (see data in **Table 3.2**, **Figure 3.1** and **Figure 3.5**). Indeed, both the magnitude of relative fold change levels and the number of altered genes were much larger in R-PHH-GW than M-mLiver-GW. Third, gene expression in the mouse livers could be affected by whole body physiology, such as circadian rhythms, hormones, fast/feeding cycles, physical activity and energy level, etc. Fourth, for microarray study, we cannot completely rule out the contributions from other cell types in mouse livers, such as endothelial cells and liver Kupffer cells, while in the enriched PHHs, the number of other liver cell types was minimal. Finally, technical differences between RNA-seq and microarray could be another minor factor as well. Among all these factors, the first two that affecting the baseline expression levels of many FXR target genes, could be the major causes of the differences we saw between the *in vivo* and *in vitro* studies. While certain technical limitations existed, the correlation/comparison study still provides valuable information for human FXR function. For R-PHH-GW, mRNA level down-regulation was observed for only a few FXR target genes found in ChIP-seq. But for M-mLiver-GW, the percentage of up- and down- regulated genes also presented in ChIP-

seq was similar. Lee et al have shown that direct gene suppression by FXR is common in mice (Lee et al. 2012). The correlation study presented here implicates that FXR may play less important roles in direct gene suppression in humans.

When comparing HepG2 cells to PHHs, FXR bound to genes in overall similar pathways, even though the total number of peaks found in HepG2-GW was only half of that found in PHH-GW (data not shown). Previous studies in HepRG cells, another human hepatoma cells, showed overall more similar mRNA expression profiles than HepG2 cells, when compared to PHHs and human liver specimens, especially for drug metabolism genes (Hart et al. 2010). It is possible that for these genes, not only the signal regulation network was different in HepG2 cells, but the associated chromatin structures also changed. The altered FXR binding and gene expression of BSEP in HepG2 cells was an example to show the complexity of gene regulation. Nevertheless, to a greater extent, our data indicate that HepG2 cells represent PHHs well in terms of FXR binding. However, to study the role of FXR in drug metabolism, HepRG cells may be a better model.

The FXR gene sequence is highly conserved across species, and the protein sequence is very similar between humans and mice (Maglich et al. 2003, Gardes et al. 2013). This similarity indicates the overall conserved and important functions of FXR in different species, further confirmed by our genome wide binding studies. On the other hand, the differences between species, from genome landscape, cellular components, all the way to physiology and pathology could contribute to the differences identified in this study, especially for gene expression.

In summary, we have obtained valuable information of genome-wide binding and transcriptome analyses of human FXR in PHHs. Detailed analysis of the ChIP-seq data indicates that the global binding patterns of FXR in HepG2 cells and PHHs are similar to those in mouse livers. In addition, similar biological pathways were enriched from genes bound by FXR in PHHs compared to those enriched in mouse livers. We also identified and validated novel FXR target genes, with and without alteration of mRNA levels. Species differences were found for specific pathways and within gene families involved in similar pathways. In a major extent, mouse model is a suitable model for studying human FXR functions.

Figure 3.1 Validation of FXR Activation

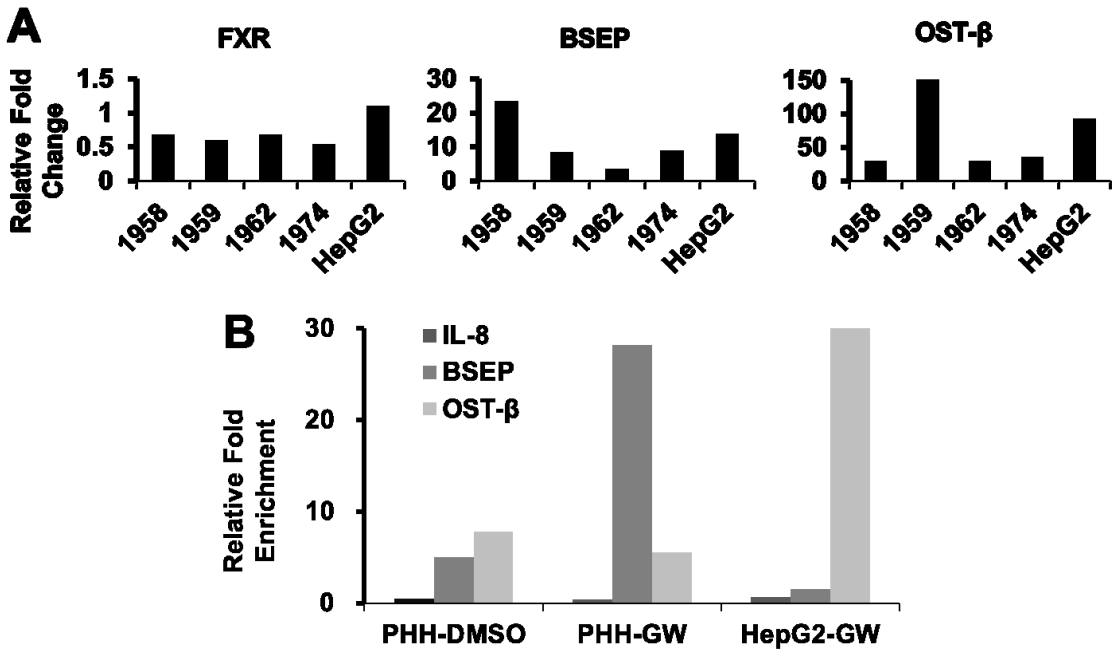

(A) RT-qPCR analysis of relative mRNA levels of FXR and FXR targets (BSEP, OST-β) in the selected 4 PHH donors (1958, 1959, 1962, and 1974) and HepG2 cells upon 24 hrs GW4064 treatments. For each PHH donors, we treated 3 wells of cells with GW4064, 3 with DMSO control. RNA from each well was collected and analyzed individually. Human 18S was used as the normalization control. Fold changes were normalized to DMSO control.

(B) ChIP-qPCR analysis of FXR antibody pull-down for the promoter regions of *BSEP*, *OST-β* and *IL-8* upon 1hr DMSO or GW4064 treatment for pooled chromatin from the selected 4 PHH donors and GW4064 treated HepG2 cells. Fold enrichment of FXR binding was normalized to rabbit immunoglobulin-G control antibody.

Figure 3.2 Genomic Distributions of FXR Binding Sites

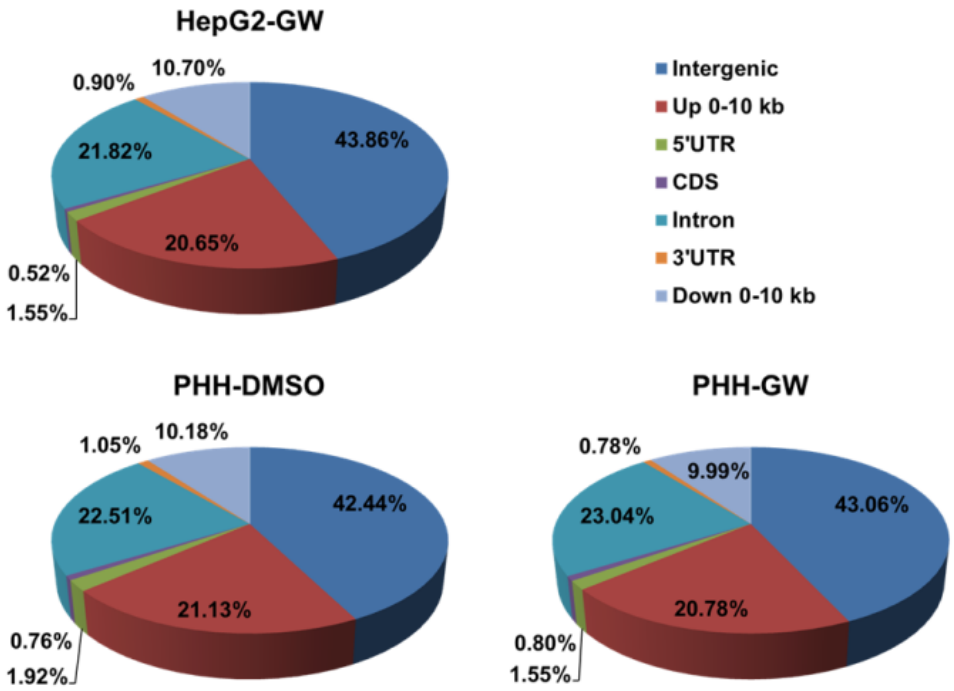

Percentage of FXR binding sites in the three datasets (HepG2-GW, PHH-DMSO, PHH-GW) that were distributed to >10 kb from genes (intergenic), 0-10 kb upstream of genes (Up 0-10 kb), 5'UTRs, coding sequence (CDS), introns, 3'UTRs, and 0-10 kb downstream of genes (Down 0-10 kb) were shown. The cut off score for the data analysis presented in **Figure 3.1, 3.2, 3.3** and **3.5** were 20 from ChIP-seq data analysis.

Figure 3.3 Distribution of Total FXR Binding Sites Relative to TSSs, and Intron Binding Profiles of FXR

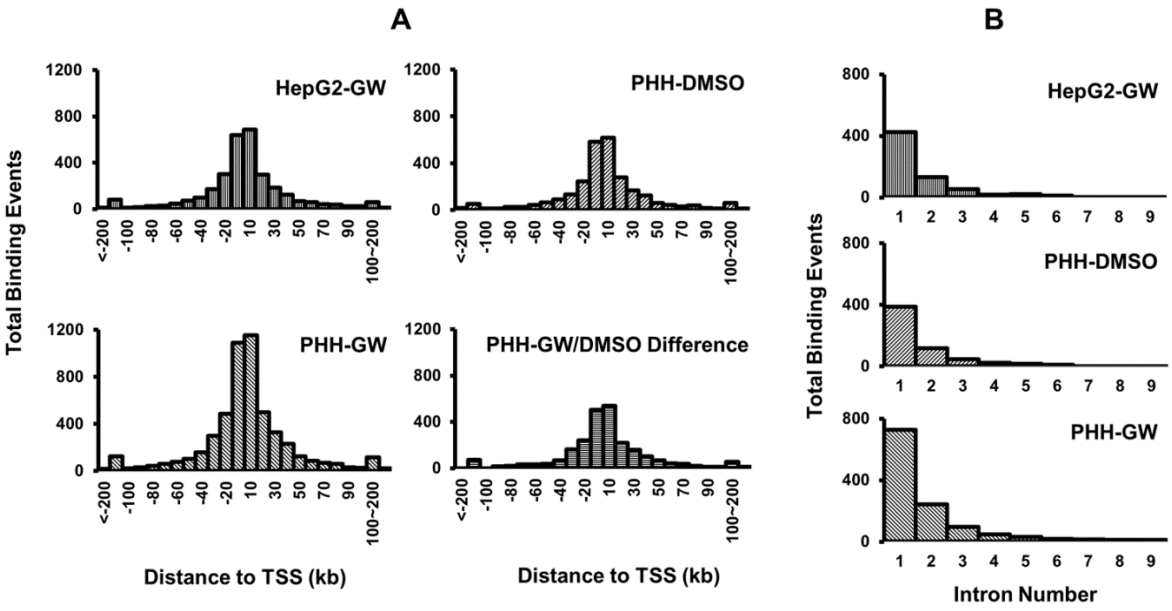

(A) The left panel shows the frequency distribution of FXR binding. The number of binding events (y-axis) was plotted against the distance from TSSs in 10 kb increments (x-axis) for the three datasets. The PHH-GW/DMSO difference was generated by plotting the frequency distribution against the subtracted total binding events from the PHH-GW to PHH-DMSO. It is interesting that this pattern was similar to the other three as well.

(B) The cumulative binding events of FXR distributed only to introns of RefSeq genes in the three datasets. The graph displays the total number of FXR binding peaks (y-axis) in PHH-DMSO and PHH-GW located within intron 1-9 of RefSeq genes (x-axis). Total of 62.8%, 62.4% and 60.2% of intron binding events were located in the first introns in HepG2-GW, PHH-DMSO, and PHH-GW, respectively.

Figure 3.4 Motif Analysis

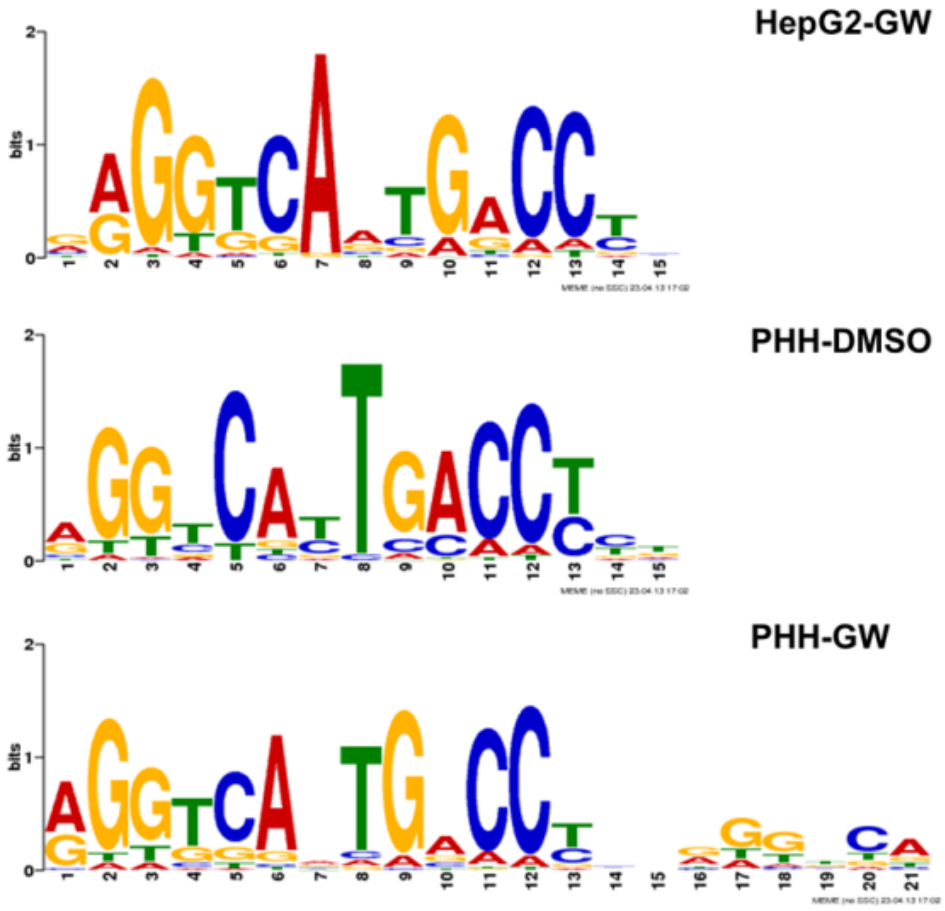

The most commonly identified sequence motifs from the top 500 FXR binding sites in the three datasets using MEME. These motifs were found in totally 246, 247, 240 sites from the top 500 peaks in HepG2-GW, PHH-DMSO, and PHH-GW, respectively. It is interesting that there is a putative nuclear half site next to the IR-1 site from PHH-GW, but not in HepG2-GW or PHH-DMSO.

Figure 3.5 Validation of ChIP-seq in PHHs

A

Genes	Peak location	PHH-DMSO	PHH-GW
ACTBP11	Up >10kb	119	213
AOC3	CDS	29	84
FABP3	Intron	32	168
HS6ST1	Intron	115	228
GFOD2	Up 0-10kb	89	274
PNMT	Up 0-10kb	55	68
UROC1	Up 0-10kb	N/F*	79

B

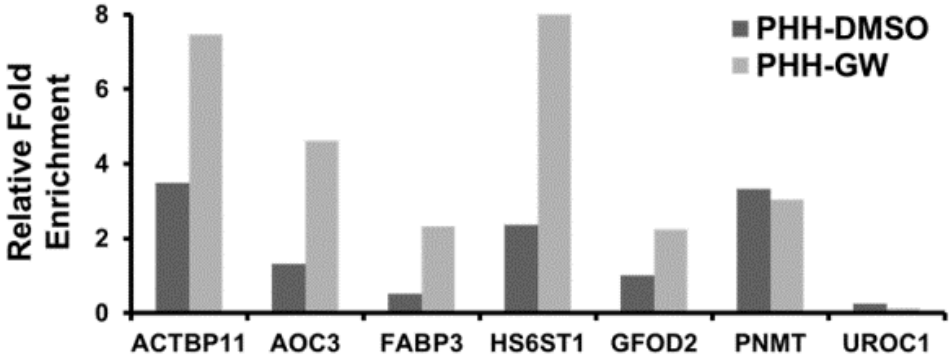

The location of FXR binding sites (second column on the left) and binding scores (the two columns on the right) for the selected novel FXR targets found in PHH-DMSO and PHH-GW were summarized in (A), and ChIP-qPCR results for these targets from pooled GW4064 or DMSO treated PHHs were presented in (B). FXR pull-down was normalized to rabbit immunoglobulin G control. Note that ACTBP11 is a pseudogene in humans. GW4064 treatment also induced the mRNA levels of AOC3, FABP3, PNMT and UROC1 in PHHs in RNA-seq (data not shown). *N/F stands for not found. Genes with their full names: *ACTBP11* (actin, beta pseudogene 11), *AOC3* (amine oxidase, copper containing 3), *FABP3* (fatty acid binding protein 3), *HS6ST1* (heparan sulfate 6-O-sulfotransferase 1), *GFOD2* (glucose-fructose oxidoreductase domain containing 2), *PNMT* (phenylethanolamine N-methyltransferase), and *UROC1* (urocanate hydratase 1).

Figure 3.6 Correlation of FXR Binding with Gene Expression Profiling

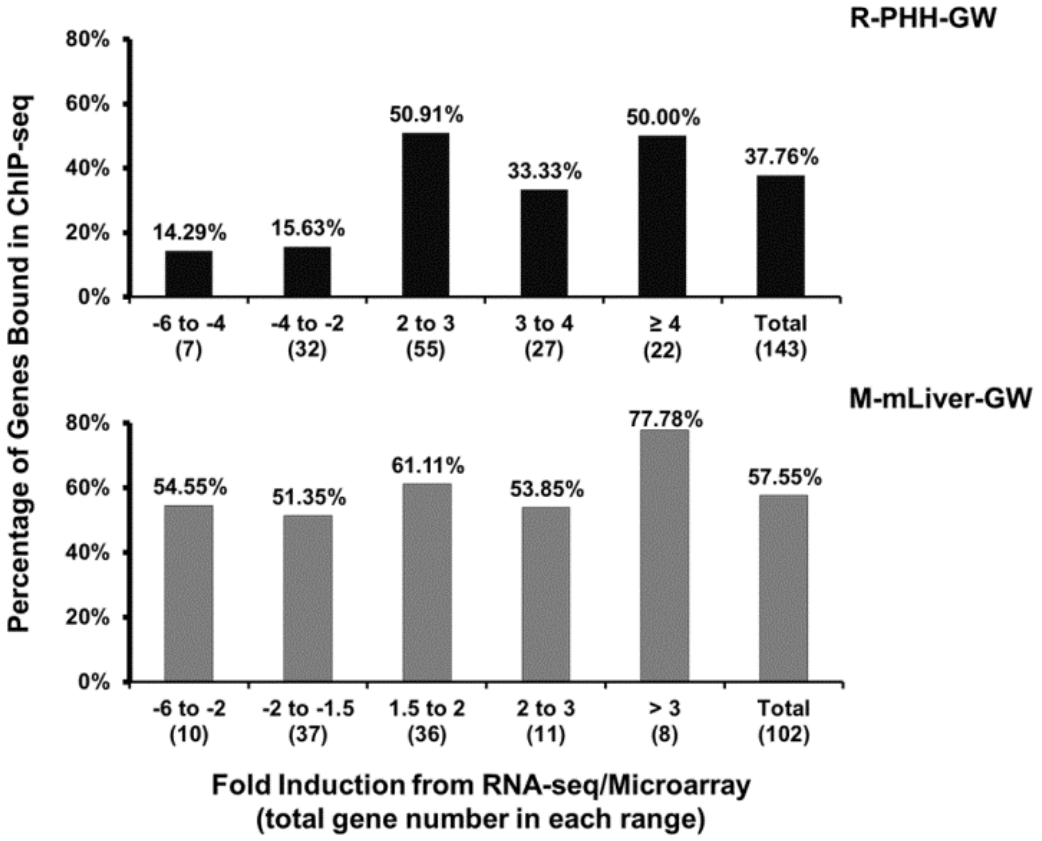

The binding of FXR to its target genes were correlated with genes that showed altered mRNA expression levels in RNA-seq for PHHs (R-PHH-GW) and microarray for mouse livers (M-mLiver-GW). The x axis displays the divided range of fold induction in R-PHH-GW or M-mLiver-GW. For RNA-seq, 143 altered genes with log2 fold change ≥2 (fold change ≥4, both up- and down- regulated), *p*-value <0.05 were used, whereas for microarray, 102 altered genes with fold change >1.5 (both up- and down- regulated), *p*-value <0.05 were used. The total number of genes from microarray or RNA-seq analysis in each fold range was listed in parenthesis. The y axis displays the percentage of genes found in M-mLiver-GW and R-PHH-GW, which were also bound by FXR in PHH-GW (top) and mLiver-GW (bottom). Note that for the y axis, the log2 fold change from RNA-seq data analysis was displayed for R-PHH-GW, while for M-mLiver-GW, the actual fold change generated from microarray data analysis was displayed.

Table 3.1 Summary of PHH Donors

Donor Serial #	Gender	Age	Diagnosis	RNA Induction	ChIP Enrichment
1st	Female	58	N/A	Good	N/A [§]
2nd	Female	85	Metastatic colon cancer and chemotherapy	Good	N/A [§]
1956	Male	Pediatric	Donor, fatty	Fair	N/A [§]
1958 *	Female	~ 60	5-10% steatosis	Good	Good
1959 *	Male	Mid age	Metastatic cancer, prior chemotherapy	Good	Good
1962 *	Female	~ 40	Adenocancer metastatic to liver	Good	Good
1974 *	Male	56	Organ donor	Good	Good
1983	Male	70	Organ donor	Good	Fair
MSUD	N/A	N/A	Maple syrup urine disease	Good	Good

* Selected PHH donors for ChIP-seq library preparation, which had enough chromatin yields to pool from both DMSO and GW4064 treatment. RNA samples from these four donors were also used and pooled for RNA-seq. Patient I.Ds, from 1956 to MSUD, was used by the tissue bank to record individual PHH. No personal identity information was obtained nor provided by the provider.

[§] N/A stands for not available. Due to limited quantity of cells, we didn't detect valid Ct values for the positive controls (promoter regions of FXR target genes) from the ChIP-qPCR assay for these PHH donors.

Table 3.2 Selected Known Human FXR Target Genes Identified in This Study *

	HepG2-GW		PHH-DMSO		PHH-GW	
Gene	**Distance To TSS**	**Binding Score**	**Distance To TSS**	**Binding Score**	**Distance To TSS**	**Binding Score**
ABCB11			-83	69	-103	319
FGF19	3655	153	3665	89	3695	251
ICAM1	58	65	58	91	88	111
MIR122	-36961	321	-36936	89	-36941	294
NR0B2	-128	116	-258	83	-178	112
	3262	189	3252	41	3212	69
OST-β	-53	160	-48	67	17	68
	10017	30	10087	67	10017	138
PPARα	-2819	161	-2839	126	-2789	203

* “Distance To TSS” is the distance of the peak of the binding site to the transcription start site (TSS) of the corresponding RefSeq gene. Note that the peak identified from ChIP-seq analysis may not overlap exactly with the IR-1 motif found from motif analysis. The binding score is the FXR antibody pull-down score normalized to rIgG control antibody generated by the sequencing analysis processes. Note that for most FXR targets listed, the binding scores retrieved from HepG2-GW and PHH-GW dataset are much larger than the scores from PHH-DMSO for the same peak. This is a general trend for most shared FXR targets among the three datasets. Genes with their full names: *MIR122* (microRNA 122), *PPARα* (peroxisome proliferator-activated receptor alpha).

Table 3.3 Comparison of DAVID Functional Annotation for PHH-GW versus mLiver-GW*

A. KEGG analysis						
	mLiver-GW (Total 970 genes)			PHH-GW (Total 343 genes)		
Term	Count	%	FDR	Count	%	FDR
Retinol metabolism				12	2.84	0.000336
Drug metabolism	23	1.82	0.000169	12	2.84	0.001458
Complement and coagulation cascades	21	1.66	0.003343	11	2.60	0.029460
Metabolism of xenobiotics by cytochrome P450	18	1.42	0.030918	10	2.36	0.057414
PPAR signaling pathway	26	2.06	0.000004	7	1.65	15.843098
B. GO-BP analysis						
	mLiver-GW (Total 970 genes)			PHH-GW (Total 343 genes)		
Term	Count	%	FDR	Count	%	FDR
organic ether metabolic process	11	0.87	3.117740	13	3.07	0.000010
triglyceride metabolic process	11	0.87	0.268143	12	2.84	0.000011
glycerolipid metabolic process	21	1.66	1.408123	19	4.49	0.000253
lipid transport	26	2.06	0.001436	18	4.26	0.000258
chemical homeostasis	45	3.56	0.750307	31	7.33	0.029556
monocarboxylic acid transport	8	0.63	0.387526	9	2.13	0.057257
response to wounding	53	4.19	0.000434	30	7.09	0.138013
oxidation reduction	86	6.80	0.000218	34	8.04	0.138493
cholesterol metabolic process	17	1.34	0.045242	11	2.60	0.187740
homeostatic process	70	5.53	0.036206	37	8.75	0.291825
steroid metabolic process	41	3.24	0.000000	16	3.78	0.337117
cellular amino acid derivative metabolic process	29	2.29	0.001080	12	2.84	5.666095

fatty acid metabolic process	41	3.24	0.000000	11	2.60	40.373990
regulation of cellular ketone metabolic process	8	0.63	1.457816	9	2.13	0.151048
acute-phase response	14	1.11	0.000078	9	2.13	0.010223
acute inflammatory response	26	2.06	0.000000	10	2.36	1.440881
coenzyme metabolic process	30	2.37	0.000427	9	2.13	51.626240
organic acid catabolic process	27	2.13	0.000000			
glucose metabolic process	32	2.53	0.000019			
cellular amino acid catabolic process	19	1.50	0.000029			
hexose metabolic process	35	2.77	0.000049			
monosaccharide metabolic process	36	2.85	0.000351			
L-phenylalanine catabolic process	6	0.47	0.018543			
pyruvate metabolic process	10	0.79	0.059427			

*Binding sites that were associated with 0-10 kb upstream of RefSeq genes were selected for DAVID functional annotation analyses. The cut off score for ChIP-seq datasets was 20. Totally 970 and 343 RefSeq genes were retrieved from mLiver-GW and PHH-GW, respectively. The categories were listed based on the FDR values from DAVID analyses for PHH-GW dataset.

Table 3.4 DAVID Functional Annotation for PHH RNA-seq*

A. KEGG analysis		
Term	**%**	**Genes**
Retinol metabolism	2.9508	*CYP1A1, CYP26B1, ADH1C, DHRS9, ADH1B, CYP26A1, CYP2A7, CYP1A2, UGT2B10, RDH16*
Cytokine-cytokine receptor interaction	4.918	*CXCL2, CX3CL1, EDAR, CCL15, CCL18, CXCL10, INHBB, CCL25, TNFRSF9, INHBA, TNFSF10, TNFRSF1B, CCL14, CCL20, CXCL13, IL1B*
PPAR signaling pathway	1.9672	*PPARD, HMGCS2, CYP7A1, FABP3, FABP6, ANGPTL4*
Steroid hormone biosynthesis	1.6393	*HSD3B2, CYP1A1, CYP7A1, UGT2B10, SULT1E1*
Tryptophan metabolism	1.3115	*KYNU, CYP1A1, IDO2, CYP1A2*
Drug metabolism	1.3115	*XDH, UPP1, CYP2A7, UGT2B10*
Tyrosine metabolism	1.3115	*PNMT, ADH1C, ADH1B, TAT, AOC3*
Calcium signaling pathway	2.623	*ADRB1, CYSLTR1, PHKA1, CACNA1H, BDKRB2, VDAC1P1, ITPKA, HTR2A*
Chemokine signaling pathway	2.623	*CCL25, CCL14, CCL20, CXCL13, CXCL2, CX3CL1, CCL15, CCL18, CXCL10*
B. GO-BP analysis		
Term	**%**	**Genes**
chemotaxis	4.2623	*CYSLTR1, CXCL2, CX3CL1, CCL15, CCL18, CXCL10, CCL25, CCL14, CCL20, CXCL13, IL1B, LECT2, DEFB1, FGF2*
oxidation reduction	7.8689	*HSD3B2, XDH, ALDH8A1, STEAP4, ADH1C, ADH1B, BBOX1, CYP7A1, CYP26B1, HSD17B6, LOXL4, ALDH6A1, CYP1A1, IDO2, DHRS9, CYP26A1, CYP1A2, CYP27C1, DIO3, ALOX15B, HAO2, CYP2A7, RDH16, DCXR, AOC3*
ion homeostasis	5.2459	*KNG1, MCHR1, PPARD, CYSLTR1, ATP1A2, BDKRB2, CCL15, S1PR3, CCL14, RHCG, CXCL13, MT2A, LGI4, IL1B, NPPB, NEDD4L, MT3*
immune response	5.9016	*ICAM1, KYNU, IGHG4, AQP9, CXCL2, CX3CL1, CCL15, CCL18, CXCL10, CCL25, TNFSF10, TNFRSF1B, CCL14, CCL20, CXCL13, SEMA7A, IL1B, DEFB1, CD14*
regulation of programmed cell death	6.5574	*KNG1, NUAK2, EEF1A2, BCL2A1, ACTN2, BDKRB2, SOX9, DAPK2, GDNF, INHBA, SERPINB9, TNFRSF9, TNFSF10, ALOX15B, TNFAIP8, IL1B, CFDP1, FGF2, PHLDA1, ANGPTL4*

*Functional genes with $\log_2$ fold enrichment ≥1 (fold change ≥2, both up- and down-regulated) and *p*-value <0.05 were selected for DAVID analysis, totally 291 RefSeq genes were retrieved from the PHH RNA-seq dataset (R-PHH-GW).

Table 3.5 Comparison of Genes from Selected Categories in DAVID Annotation for ChIP-seq*

A. KEGG Analysis		
Category	**mLiver-GW**	**PHH-GW**
Retinol metabolism		*CYP3A4, CYP2B6, CYP2C9, CYP2C18, CYP3A43, DGAT1, CYP2A6, CYP2A7, ADH1B, ADH1A, CYP3A7, CYP1A1,UGT2B10*
Drug metabolism	*CYP2D9, CYP3A25, CYP2A12, FMO5, GSTM3, UGT1A7C, ADH4, GSTK1, FMO3, GSTZ1, UGT1A@, GSTA2,GSTA4, CYP3A13, CYP3A11, GSTT1, GSTT2, CYP2E1, UGT1A1, UGT1A10, AOX1, CYP2D26, CYP2C38, CYP2C39, MGST1, GSTA3*	*CYP3A4, CYP2B6, CYP2C9, CYP2C18, ADH1B, CYP3A43, CYP2A6, CYP2A7, CYP3A7,CYP2D6, ADH1A,UGT2B10, GSTA3*
Complement and coagulation cascades	*KNG1, MBL1, KNG2, HC, C3, C4B, CFB, SERPINA1E, PLG, PROC, SERPINF2,CFH, C2, CFD, FGG, FGA, FGB, F2, SERPINE1, SERPINC1, CPB2*	*F11, MBL2, SERPINA1, BDKRB2, FGG, FGA, FGB, F2, SERPINE1, SERPINC1, CPB2*
Metabolism of xenobiotics by cytochrome P450	*GSTA2, GSTA3, GSTA4, CYP3A25, CYP3A13, CYP3A11, GSTT1, GSTT2, CYP2E1, UGT1A1, DHDH, UGT1A10, GSTM3, UGT1A7C, GSTK1, ADH4, GSTZ1, UGT1A@, CYP2C38, CYP2C39, MGST1*	*CYP3A43, CYP3A4, GSTA3, CYP3A7, CYP1A1, CYP2C18, CYP2C9, CYP2B6, ADH1B, ADH1A, UGT2B10*
PPAR signaling pathway	*ACOX2, PPARD,PPARA, APOA2, APOA5,APOC3,PCK1(HepG2), CPT1A, CPT1B, FABP5, APOA1, ACSL1, CYP7A1, ACAA1B, ACSL5, ANGPTL4, SCD1, ACADM, DBI, ADIPOQ, CYP27A1, UBC, CYP4A14, SLC27A2, SCP2, SLC27A4*	*PPARA, APOA2, APOA5,APOC3,CPT2, FABP1, ANGPTL4*
Steroid hormone biosynthesis	*CYP3A25, CYP3A13, HSD17B2, HSD17B1, CYP3A11, CYP21A1, UGT1A1, UGT1A10, CYP17A1, UGT1A7C, CYP7A1, SRD5A1, SULT1E1, UGT1A@*	*CYP3A43, CYP3A4, CYP3A7, HSD17B2, CYP1A1, UGT2B10*
Circadian rhythm	*NPAS2, CSNK1D, PER1, PER3, ARNTL, CRY1*	*NPAS2, BHLHE40, CRY1*
Linoleic acid metabolism	*CYP2J5, CYP3A25, CYP3A13, CYP3A11, PLA2G6, CYP2E1, CYP2C38, CYP2C39*	*CYP3A43, CYP3A4, CYP3A7, CYP2C18, CYP2C9, PLA2G6*

Glycerophospholipid metabolism	*CHPT1, GPD1, PEMT, PLA2G6, AGPAT2, AGPAT1, CRLS1, NAT6, PPAP2C, CHKB, LYPLA2, LCAT, PHOSPHO1,*	*CHPT1, GPD1, PEMT,PLA2G6, AGPAT2, AGPAT6*
B. GO-BP Analysis		
Category	**mLiver-GW**	**PHH-GW**
organic ether metabolic process	*MOGAT2, G6PC, APOA5, APOC1, LIPC, APOC3, SLC37A4, SLC22A4, LIPE, PCK1, INSIG2,*	*CYP1A1, IL6ST, APOC1, APOC2, AGPAT6, DGAT1, APOE, G6PC, APOC3, APOA2, APOA4, APOA5, LIPC*
monocarboxylic acid transport	*CPT1B, PPARD, SLC6A6, ABCC3, SLC27A2, CROT, SLC10A1, SLC27A4*	*MIP, SLC16A5, PPARA, CPT2, PLIN2, AQP8, FABP1, BDKRB2, SLC10A1*
regulation of cellular ketone metabolic process	*PPARA, HNF4A, INSIG2, AGT, MLXIPL, GNMT, ADIPOQ, BRCA1*	*APOA4, PPARA, AGT, APOA5, APOC3, APOC1, APOC2, CPT2, FABP1*
lipid transport	*RBP4, OSBP, PPARD, LDLR, APOC1, APOC2, APOA4, APOA2, APOA1, APOE, LCAT, APOC4, APOC3, APOA5, ATP8B1, LBP, OSBPL5, CPT1B, ABCG8, NPC1, ABCG5, LIPC, SLC27A2, SCP2, CROT, SLC27A4*	*PPARA, LDLR, APOC1, APOC2, APOA4, APOA2, P2RX7, APOE, APOC4, APOA5, APOC3, LBP, LIPC, BDKRB2, CPT2, FABP1, GLTPD2,PLIN2*
triglyceride metabolic process	*MOGAT2, G6PC, INSIG2, APOA5, APOC3, SLC37A4, APOC1, SLC22A4, LIPC, LIPE, PCK1*	*APOA4, APOA2, G6PC, AGPAT6, DGAT1, APOE, IL6ST, APOA5, APOC3, APOC1, APOC2, LIPC*
glycerolipid metabolic process	*MOGAT2, ALDH5A1, CHKB, SLC37A4, APOC1, PTEN, CHPT1, PCK1, G6PC, INSIG2, PIGG, APOC3, APOA5, PEMT, SLC22A4, ETNK2, LIPC, IPMK, ALG12, FABP5, LIPE*	*GPD1, ALDH5A1, IL6ST, APOC1, APOC2, CHPT1, APOA4, APOA2, AGPAT6, G6PC, DGAT1, APOE, APOA5, APOC3, PEMT, PLA2G6, LIPC, AGPAT2, IP6K3*

chemical homeostasis	*SLC9A8, PPARD, GCLC, FTL1, LDLR, ATOX1, SLC37A4, NR3C2, AQP4, TTC7, TRF, ASGR2, APOA2, GCKR, SLC24A3, APOE, GRIN2C, PXMP3, APOA5, MT2, LGI4, MT1, EIF2B4, SCO1, PRKCA, IBTK, SLC8A1, STIM2, MLXIPL, BAD, CSRP3, ADIPOQ, PARK7, USF2, QK, ATXN1, ABCG8, NPC1, G6PC, TSC1, LYST, VEGFA, LIPC, NR5A2, CLN6*	*FXYD1, GNA13, LDLR, IL6ST, ATP5B, OXT, APOC2, BDKRB2, TCF7L2, APOA4, GCKR, APOA2, NUBP1, SAA1, APOE, AGT, APOC4, APOA5, SERPINE1, APOC3, TGM2, QKI, PPP3CA, IBTK, P2RX7, G6PC, CCL14, F2, MT2A, CP, LIPC*
steroid metabolic process	*SC5D, OSBP, LDLR, MVD, HSD17B2, HSD17B1, SLC37A4, STAT5B, APOC1, RDH9, ACBD3, APOA2, APOA1, INSIG2, APOE, SAA1, SERPINA6, CYP7A1, LCAT, PXMP3, SULT1A1, APOC3, ATP8B1, SRD5A1, SULT1E1, DHCR24, OSBPL5, CYP21A1, AMACR, ESR1, RDH1, AFP, NPC1, G6PC, CYP17A1, PON1, LIPC, NR5A2, CLN8, LIPE, CLN6*	*CYP3A4, CYP1A1, HSD17B2, MVD, LDLR, APOC1, NR0B2, SREBF2, APOA4, APOA2, G6PC, APOE, SULT1A1, APOC3, INSIG1, LIPC*
fatty acid metabolic process	*PTGES3, ACOX2, PRKAG3, HACL1, PPARA, PPARD, SC5D, PRKAG2, STAT5B, ACOT5, ACOT4, ACOT3, PECR, APOA2, ACSL1, ELOVL5, FASN, ACOT12, ELOVL6, ACAA1B, ACSL5, SCD1, CPT1B, ACADM, ALDH5A1, EPHX2, ADIPOR2, LYPLA2, PHYH, ADIPOQ, CPT1A, BRCA1, QK, PTGDS, MAPK14, LIPC, AACS, SLC27A2, CROT, SLC27A4, DEGS1*	*PPARA, AGPAT6, CPT2, ECH1, ALDH5A1, ELOVL2, FASN, QKI, CYP4F3, LIPC, ACOT4*
oxidation reduction	*CYP2D9, ACOX2, CYP2J5, STEAP3, LDHA, SC5D, ALDH1L1, PRDX5, PDHB, GPX2, RDH9, PECR, CYP7A1, CPOX, SRD5A1, DHTKD1, DUS1L, SARDH, GFOD1, DHCR24, HPD, SQRDL, ACADM, CYP3A13, ALDH5A1, CYP3A11, CYCS, DECR2, QDPR, CYP26A1, RDH1, CYP2E1, GRHPR, CDO1, POR, DHDH, CYP27A1, H6PD, SLC37A2, CYP2D26, TXNRD2, DEGS1, CYP2U1, XDH, CYP3A25, NDUFB6, HSD17B2, HSD17B1, HSD17B13, AASS, MOSC2, EGLN2, KMO, PAH, ALDH3A2, PIPOX, CYP2A12, FMO5, ADH4, FMO3, HAAO, FASN, BDH1, BCKDHA, SCD1, CYP2G1, GPD1, CHDH, CYP21A1, HGD, PHYH, AKR1B7, CYP17A1, SLC25A13, LEPRE1, UOX, NDUFV1, CYP4F15, AOX1, PRODH2, CP,*	*STEAP3, CYP3A4, STEAP4, CYP3A7, HSD17B2, CYP2B6, CYP2C18, CYP2D7P1, CYP2D6, ADH1B, ADH1A, CYP3A43, PLOD2, PLOD3, FASN, LOXL4, SARDH, GFOD2, DUS3L, GPD1, PAOX, CYP1A1, CYP2C9, PYROXD2, ALDH5A1, CYB5A, IYD, SLC25A13, RRM2, CYP2A6, CYP4F3, CYP2A7, CP, KDM6B, AOC3*

	CYP2C38, CYP4A14, ACAD10, ALKBH2, CYP2C39	
response to wounding	*PPARA, JUB, PPARD, TRPV1, CRP, TLR3, SAA2, GRIN2C, SAA1, TICAM1, PROZ, CFH, LBP, CFD, KNG1, C4B, SAA3, SAA4, PROC, SERPINF2, LYST, F2, CTSB, LCP1, MBL1, RTN4RL1, C3, CXCL2, NINJ1, ABHD2, ITGB2, TRF, AHSG, FGG, IL17B, FGA, FGB, MAP3K1, SERPINC1, C2, PAPSS2, B4GALT1, LIPA, CFB, HC, SAAL1, EPHX2, PLG, ORM1, C1RL, HBEGF, ORM2, AI182371*	*GNA13, MBL2, PPARA, NMI, NDST1, TGFB3, ITGB3, BDKRB2, APOA2, FGG, FGA, FGB, SAA1, SERPINE1, APOA5, SERPINC1, SERPINA1, LBP, F11, CEBPB, CYP1A1, CCNB1, ORM1, P2RX7, SDC1, TSC2, F2, KDM6B, ORM2, AOC3*
cellular amino acid derivative metabolic process	*AHCY, GCLC, CHKB, STAT5B, AGMAT, AFMID, OAZ1, CSAD, GSTK1, SLC22A4, PEMT, ETNK2, GNMT, CHDH, P4HB, ACADM, ALDH5A1, NR4A2, GSTT1, GSTT2, GSTT3, CDO1, TPMT, CHPT1, GAMT, LIPC, PTMS, FABP5, MGST1*	*HAGH, APOA4, APOA2, AGPAT6, CKM, CYP1A1, PNMT, ALDH5A1, SULT1A1, PEMT, LIPC, CHPT1*
homeostatic process	*SLC9A8, PPARD, LDLR, ATOX1, TRPV1, STAT5B, PRDX5, AQP4, TENC1, GPX2, ASGR2, APOA2, DNAJC16, SLC24A3, APOE, GRIN2C, PXMP3, APOA5, MT2, MT1, LGI4, FAS, EIF2B4, PRKCA, IBTK, SLC12A7, MLXIPL, STIM2, QK, NPC1, G6PC, LYST, VEGFA, PDGFRB, TXNRD2, CLN6, XDH, GCLC, FTL1, STK11, CSF1, SLC37A4, NR3C2, EGLN2, SFXN1, TTC7, HSPA1A, TRF, ZC3H8, GCKR, FH1, EPO, SCO1, P4HB, SLC8A1, LIPA, SMG6, BAD, CSRP3, ADIPOQ, PLG, USF2, PARK7, ATXN1, ABCG8, TSC1, ID2, RHOT1, NR5A2, LIPC*	*FXYD1, GNA13, SIVA1, LDLR, IL6ST, ATP5B, OXT, APOC2, BDKRB2, TCF7L2, APOA4, ADRB3, GCKR, APOA2, NUBP1, APOE, SAA1, APOC4, AGT, APOA5, SERPINE1, APOC3, TGM2, QKI, PPP3CA, IBTK, SLC12A7, FOXP3, TXNDC11, P2RX7, G6PC, CCL14, F2, MT2A, CP, LIPC, CLCN6*
cholesterol metabolic process	*MVD, LDLR, APOC1, APOA2, APOA1, INSIG2, APOE, SAA1, LCAT, CYP7A1, APOC3, PON1, LIPC, CLN8, LIPE, CLN6, DHCR24*	*APOA4, APOA2, LDLR, MVD, APOE, APOC3, INSIG1, APOC1, NR0B2, LIPC, SREBF2*
acute-phase response	*TRPV1, SAAL1, CRP, SAA3, SAA4, TRF, AHSG, ORM1, SAA2, SERPINF2, SAA1, F2, LBP, ORM2*	*ORM1, MBL2, CEBPB, SAA1, F2, TSC2, SERPINA1, LBP, ORM2*

acute inflammatory response	*MBL1, C3, TRPV1, CRP, TRF, AHSG, SAA2, SAA1, CFH, C2, LBP, CFD, B4GALT1, HC, CFB, C4B, SAAL1, EPHX2, SAA3, SAA4, ORM1, SERPINF2, F2, C1RL, ORM2, AI182371*	*ORM1, MBL2, APOA2, CEBPB, SAA1, F2, TSC2, SERPINA1, LBP, ORM2*
coenzyme metabolic process	*ALDH1L1, GCLC, KMO, PDSS1, ACOT5, PIPOX, ACOT4, GCH1, ACOT3, GSTK1, ACOT12, HAAO, FH1, SUCLA2, NAPRT1, CES3, ALDH5A1, PDK4, GSTT1, GSTT2, ACLY, GSTT3, DLAT, HNF4A, PANK1, H6PD, FPGS, FLAD1, SCP2, MGST1*	*HAGH, GPD1, MTHFS, AGPAT6, PANK3, ALDH5A1, FTCD, ACLY, ACOT4*
organic acid catabolic process	*ACOX2, HACL1, BCKDK, PPARD, AHCY, AASS, PAH, FAH, AFMID, CSAD, GSTZ1, SARDH, HPD, BCKDHA, ACADM, HAL, FTCD, HGD, CDO1, TAT, ADIPOQ, PHYH, AMDHD1, PRODH2, UROC1, SLC27A2, SLC27A4*	
glucose metabolic process	*PTGES3, PRKAG3, RBP4, PPARA, LDHA, SLC37A4, CAR5A, PDHB, PPP1R3B, NISCH, GYS2, GNMT, DHTKD1, ENO1, GPD1, ALDH5A1, PDK4, BAD, DLAT, PPP1CC, ADIPOQ, CPT1A, PCK1, PGM2, PCX, G6PC, GBE1, H6PD, PYGL, SDS, MAPK14, FABP5*	
cellular amino acid catabolic process	*BCKDHA, BCKDK, AHCY, HAL, FTCD, HGD, AASS, PAH, CDO1, TAT, FAH, AFMID, AMDHD1, CSAD, PRODH2, GSTZ1, UROC1, SARDH, HPD*	
hexose metabolic process	*PTGES3, PRKAG3, RBP4, PPARA, LDHA, GNPDA1, SLC37A4, CAR5A, PDHB, PPP1R3B, NISCH, GYS2, GALE, GNMT, DHTKD1, ENO1, B4GALT1, GPD1, ALDH5A1, PDK4, BAD, DLAT, PPP1CC, ADIPOQ, CPT1A, PCK1, PGM2, PCX, G6PC, GBE1, H6PD, PYGL, SDS, MAPK14, FABP5*	
monosaccharide metabolic process	*PTGES3, PRKAG3, RBP4, PPARA, LDHA, GNPDA1, SLC37A4, CAR5A, PDHB, NISCH, PPP1R3B, UGT1A7C, GYS2, GALE, GNMT, UGT1A@, DHTKD1, ENO1, B4GALT1, GPD1, ALDH5A1, PDK4, BAD, DLAT, PPP1CC, ADIPOQ, UGT1A1, CPT1A, PCK1, PGM2, UGT1A10, PCX, G6PC, GBE1, H6PD, PYGL, SDS, MAPK14, FABP5*	
L-phenylalanine catabolic process	*HGD, GSTZ1, PAH, TAT, HPD, FAH*	
pyruvate metabolic process	*RBP4, GPD1, PCX, G6PC, SDS, PDK4, CAR5A, DLAT, AGXT, PCK1*	

* Detailed list of genes retrieved from DAVID analyses for **Table 3.3**. For GO-BP analysis, the same categories are listed here as in **Table 3.3**. For KEGG analysis, categories with FDR > 0.1 are also included. The orders of the categories listed here are the same as in **Table 3.3,** based on the FDR values from PHH-GW dataset. Please note that all mouse genes were kept in capitalized state as retrieved directly from DAVID analyses.

Chapter 4: Study the Roles of FXR and BAs in Mouse Models of PNALD

4.1 Introduction

Parenteral nutrition (PN), also known as intravenous feeding, is an effective method to obtain sufficient nutrition into the body through the veins. PN is mainly used for patients who cannot or should not obtain their nutrition through eating, and therefore is essential for them to maintain nutritional status and/or growth. To replace the enteral route of feeding, PN normally contains a combination of nutrients, including carbohydrates (dextrose), proteins (amino acids), lipids (fat emulsion), electrolytes, vitamins, and trace elements.

However, long-term PN feeding will lead to a spectrum of hepatobiliary diseases, including cholestasis, steatosis, fibrosis, and end stage liver complication, cirrhosis, summarized as parenteral nutrition associated liver diseases (PNALD) (Kumpf 2006). Among these, steatosis, cholestasis, and gallbladder sludge/stones are most common, while overlap can exist (Kumpf 2006). PN associated steatosis, or hepatic fat accumulation, is found predominantly in adults and is generally benign (Kumpf 2006). PNAC is a special type of cholestasis occurs predominantly in children but may also occur in adult patients after long-term PN therapy (Peyret et al. 2011). Prolonged gallbladder stasis after long-term PN therapy may progress to gallbladder sludge or gallstones, with subsequent development of cholecystitis (Kumpf 2006). In the clinic, the most effective treatment for PNALD is to increase enteral food intake (Ziegler and Leader 2006). Nevertheless, for patients with intestinal failure, clinical management is still challenging.

Currently, soybean oil based lipid emulsion (SOLE) is most commonly used in the world for the lipid components in PN solution (Waitzberg, Torrinhas and Jacintho 2006). And SOLE has been shown to be associated with the development of PNALD based on multiple reasons, including the presence of plant phytosterols and relatively large amount of pro-inflammatory ω-6 polyunsaturated fatty acids (PUFAs), as well as the lack of anti-inflammatory ω-3 PUFAs in SOLE (Vlaardingerbroek et al. 2014). In recent years, new generations of lipid emulsion, including fish oil based lipid emulsion (FOLE), which mainly contain ω-3 PUFAs, and SMOFlipid (a mixture of soybean oil, medium chain triglycerides (MCTs), olive oil, and fish oil), have been shown to be beneficial to improve or even reverse PNALD in both pediatric and adult patients (Waitzberg et al. 2006).

Most recent studies in animal models have made substantial progress in understanding the pathogenesis of PNALD, especially studies conducted in preterm piglets, which well-recapitulated the clinical symptoms found in preterm and neonatal patients (Vlaardingerbroek et al. 2014). To fully understand the underlying molecular mechanisms, mouse models are also valuable due to the well-established genetic-manipulation technologies in mice. Indeed, using toll like receptor 4 (TLR4) knockout mice, El Kasmi et al showed that TLR4 signaling mediated immune responses were critically involved in PN induced liver injury when PN mice were pretreated with dextran sulphate sodium (DSS) (El Kasmi et al. 2012), a toxic chemical agent, to induce intestinal damage to mimic human clinical conditions. In a later study, El Kasmi et al also showed that plant sterols contained in SOLE, particularly stigmasterols, were associated with the cholestatic liver injury observed in DSS pretreated mice (El Kasmi et

al. 2013). However, the findings from these mouse studies and those obtained from preterm piglets were inconsistent about the roles of plant sterols in the development of PNALD. While it was proposed that stigmasterols were FXR antagonists (El Kasmi et al. 2013), to dates, the roles of liver FXR and BA signaling pathways involved in the pathogenesis of PNALD are still poorly understood. In addition, recent studies have shown that intestinal FXR-FGF15 (fibroblast growth factor 15, FGF19 in humans) axis plays important roles in suppressing liver BA synthesis and protecting the liver from cholestatic liver injury, as well as inhibiting intestinal inflammation and maintaining intestinal barrier integrity (Modica et al. 2012, Gadaleta et al. 2011, Kong et al. 2012b). Nevertheless, the potential beneficial roles of the intestinal FXR-FGF15 pathway involved in the improvement and management of PNALD have not been explored.

In this study, we aim to establish a valid mouse PN model, and to characterize the detailed serum BA and liver gene expression profiles, to aid in future studies of the potential roles of FXR and BA signaling, as well as other contributing factors involved in the development and management of PNALD.

4.2 Results

Body Weight and Liver Weight for PN Mice

Upon flushing the catheters and connecting the mice to the infusion system, average body weight (B.W.) for both saline and PN mice were around 21.5 g (**Figure 4.1A)**. In a previous study, from which we obtained the setup of PN regimen (El Kasmi et al. 2012), the PN infusion rate was kept as 7 mL/d throughout the study, and the

calculated daily calorie intake was 8.4 kcal for the PN mice. We initially did administer the same PN solution to mice with similar initial body weight (B.W.) at the rate of 7 mL/d. However, after 8 days of PN infusion, these mice had an average of around 20% body weight (B.W.) loss. Therefore, we decided to increase the lipid content in the PN solution from 2 g per 100mL to 3 g per 100mL, as well as increase the infusion rate from 7 mL/d to 8 mL/d, for mice with an initial B.W. around 22 g. After receiving continuous intravenous infusion of the modified PN for 8 to 10 days (6 mL/d for day1, 8 mL/d afterwards), average B.W. change for PN mice was -2.10 g (range 0.06 to -3.44 g **Figure 4.1 A**), whereas average B.W. change for saline control mice was -0.06 g (range 1.28 to -2.02 g, **Figure 4.1 A**). PN mice had around 10% body weight loss (mean 10.0%, SEM 1.7%, **Figure 4.1 B**). This trend of B.W. change is similar to the trend reported previously (El Kasmi et al. 2012). In addition to body weight loss, liver weight decreased further in PN mice, as presented in **Figure 4.1 C,D**, with the ratio of liver weight (L.W.) to mouse B.W. further decreased in PN mice (mean 0.052, 0.038 and SEM 0.003, 0.004 for saline and PN mice, respectively, *p-value* < 0.05) (**Figure 4.1 D**). Upon animal sac, the gallbladders in PN mice were substantially smaller than those found in saline control mice (data not shown).

Liver Functional Tests

Serum levels of ALT were similar between the saline and PN mice (**Figure 4.2 A**). However, PN mice had significantly increased serum levels of AST (**Figure 4.2 B**, *p-value* < 0.005) and TSBA (**Figure 4.2 D**, *p-value* < 0.05), and significantly decreased

serum levels of ALP (**Figure 4.2 C**, *p-value* < 0.005), when compared to saline control mice. Decreased ALP levels and empty gallbladders observed in PN mice indicate that PN infusion was associated with diminished bile flow from the hepatocytes into the biliary tract. These data suggest that these PN mice may have increased risks of developing cholestatic liver dysfunction after long-term PN infusion, or when other risk factors are presented, such as intestinal damage caused by DSS pretreatment.

Liver Gene Expression

After 8 to 10 days infusion of PN at 8mL/d, liver mRNA levels of genes involved in BA homeostasis were quantified (**Figure 4.3**). Relative mRNA levels of *Cyp7a1* showed significant increase in the livers of PN mice compared to saline controls (around 3 fold, *p-value* < 0.05) (**Figure 4.3 A**). Relative mRNA levels of cytochrome P450, family 27, subfamily a, polypeptide 1 (*Cyp27a1*), *Fxr*, and bile salt export pump (*Bsep*) decreased 40% in PN mice (*p-value* < 0.05, 0.05, 0.005, respectively) (**Figure 4.3 A**). Relative mRNA levels of cytochrome P450, family 7, subfamily b, polypeptide 1 (*Cyp7b1*) and multidrug related protein 3 (*Mrp3*) decreased more than 70% (*p-value* < 0.005 for both), whereas relative mRNA levels of *Cyp8b1* decreased more than 90% (*p-value* < 0.005) (**Figure 4.3 A**). Expression of genes involved in cholesterol and lipid metabolism was also quantified. Relative mRNA levels of cluster of differentiation 36 (*Cd36*) decreased 50% with statistical significance (*p-value* < 0.05), whereas relative mRNA levels of fatty acid synthase (*Fas*), lipoprotein lipase (*Lpl*) and sterol regulatory element-binding protein-1c (*Srebp-1c*) increased significantly in the livers of PN mice

compared to saline control mice (*p-value* < 0.005, 0.05, 0.005, respectively) (**Figure 4.3 B**).

Microarray Profiling of Liver Gene Expression in PN Mice

Genes with fold change ≥ 4 (up-regulated) or ≤ -4 (down-regulated) obtained from the microarray analysis, with their full names and the corresponding fold changes, are presented in **Table 4.1**. The RT-qPCR was performed to validate the results obtained from the microarray analysis (**Figure 4.4**). Both up-regulated and down-regulated genes were tested. Among these, the relative mRNA levels of ATP-binding cassette, sub-family d (ALD), member 2 (*Abcd2*), *Nocturnin* and macrophage receptor with collagenous structure (*Marco*) increased significantly in PN mice compared to saline controls (2.2, 5, and 6.8 fold, *p-value* < 0.0005, 0.05, 0.05, for *Abcd2*, *Nocturnin*, and *Marco*, respectively). Relative mRNA level of cytochrome P450, family 2, subfamily b, polypeptide 10 (*Cyb2b10*) decreased more than 20 fold in PN mice (*p-value* < 0.005). However, for the other genes tested, the means of fold changes were less than 2, and without significance (**Figure 4.4**).

Kyoto Encyclopedia of Genes and Genomes (KEGG) Pathway analysis obtained from Database for Annotation, Visualization and Integrated Discovery (DAVID) also revealed additional alterations in the livers of PN mice (**Table 4.3**). Many genes, which are related to immune and inflammatory responses, were up-regulated, including genes involved in cytokine-cytokine receptor interaction (19 out of 28), Janus kinase-signal transducer and activator of transcription (JAK-STAT) signaling pathway (12 out of 15),

and natural killer cell mediated cytotoxicity (11 out of 15). And most genes in the category of fat digestion and absorption and biosynthesis of unsaturated fatty acids (FAs) were up-regulated (10 out of 11). On the contrary, majority of genes involved in metabolism of endobiotics and xenobiotics were down-regulated (13 out of 19 for drug metabolism - cytochrome P450, 10 out of 14 for retinol metabolism, 8 out of 12 for arachidonic acid metabolism, all the 8 for glutathione metabolism, and all the 6 for fatty acid metabolism).

Serum BA Profiling by UPLC-MS

Among all the 23 BAs, serum concentrations of GDCA, LCA, and GUDCA in both saline and PN samples were below the system detection limits. For the other 20 BAs, the analyzed concentrations for each BA in the serum of saline (n=4) and PN mice (n=5) were plotted in **Figure 4.5**, and the relative fold changes of each BA in PN samples compared to saline samples were plotted in **Figure 4.6.** For most BAs, levels of tauro-conjugates were much higher than the unconjugated BAs, whereas levels of glycol-conjugates were the lowest for most BAs (**Figure 4.5**). Total serum concentrations of the 20 BAs increased 5 fold in PN mice compared to saline controls (**Table 4.4**) (1601.2 ± 417.9 ng/mL (mean ± SEM) and 8112.4 ± 605 ng/mL (mean ± SEM), for saline control and PN mice, respectively, *p-value* < 0.05). Compared to saline controls, serum levels of TCDCA, β-MCA, T-β-MCA, T-α-MCA, ω-MCA, T-ω-MCA, TLCA, TUDCA increased significantly in PN mice (*p-value* < 0.05), whereas serum levels of GLCA in PN mice decreased dramatically below the detection limit (**Figure 4.5**). Among these, levels of

TCDCA, T-β-MCA, T-α-MCA, TLCA increased more than 10 fold in PN mice (**Figure 4.6**). Levels of CDCA increased 3 fold in PN mice, though without significance (*p-value*=0.09). Levels of TCA, GCA, α-MCA, and THDCA also increased dramatically in PN mice (**Figure 4.5**) and reaching significance (*p-value* < 0.07). The percentage of major BAs in the total serum BA pool was plotted in **Figure 4.7**. As shown, percentage of TCDCA, T-β-MCA, and T-α-MCA increased dramatically in PN mice. The total concentration and percentage of each BA species (unconjugated BA and its conjugates), total primary BAs and total secondary BAs, as well as the percentage of 12α-OH BAs (CA, DCA and their conjugates) and non-12α-OH BAs (CDCA, MCA, LCA, HDCA, UDCA and their conjugates) in the total BA pool were summarized in **Table 4.4**. As shown, the percentage of total primary and secondary BAs was similar in saline control mice (55.22% versus 44.78%), whereas in PN mice, the percentage of total primary BAs was 3.1 fold of that of the secondary BAs (75.75% versus 24.25%). In addition, the percentage of total 12α-OH BAs and non-12α-OH BAs was also similar in saline control mice (42.74% versus 57.26%), whereas the percentage of total non-12α-OH BAs was 2.67 fold of that of total 12α-OH in PN mice (72.95% versus 27.05%).

Liver Histology

H&E staining showed that overall liver histology between PN and saline control mice was similar (**Figure 4.8**). This phenotype is consistent with the results obtained from liver functional tests, suggesting that 8 days PN infusion in mice still does not affect liver functions or morphology despite altered gene expression and serum BA profiles.

4.3 Discussion

The PN regimen used in this study was modified based on a previous publication (El Kasmi et al. 2012), to maintain sufficient calorie intake for adult mice to prevent excessive body weight loss. From our unpublished data, when mice were infused with PN for 12 to 14 days, body weight loss was similar to that found in mice infused with PN for 8 days, average around 10%. So the daily calorie intake and infusion rate seem adequate to maintain steady energy requirement for the adult mice used in this study. One interesting change we observed in this model was that the liver weight decreased further in the PN mice. Future studies will be needed to uncover the underlying causes.

Similar to the previous study (El Kasmi et al. 2012), ALT levels were not increased in the PN mice, whereas AST levels increased significantly in our model, but were still in the normal range. We also saw significantly increased TSBA levels in the PN mice, similar to the study previously reported (El Kasmi et al. 2012). Interestingly, ALP levels decreased significantly in the PN mice. The trend of decreased ALP levels in PN mice is on the contrary to what is commonly observed in the neonatal incentive care unit (NICU), that the neonatal patients with PNAC normally had elevated levels of ALP. This difference between the adult mice and neonates may be due to species differences between mice and humans. In humans, FGF19 has been found to be expressed in human hepatocytes (Holt et al. 2003) and gallbladder epithelial cells (Zweers et al. 2012), whereas in adult WT mice, FGF15 is not expressed in the liver nor in the gallbladder (Inagaki et al. 2005). It has been shown that FGF15 is essential for gallbladder refill in mice (Inagaki et al. 2005). Therefore, the lack of enterohepatic circulation of BAs during PN infusion could lead to impaired FXR-FGF15 signaling,

causing diminished gallbladder refilling from the liver and subsequently less biliary exposure to BAs. In addition, recent studies also showed that elevated levels of ALP in patients with intestinal failure and PNALD could be caused by bone diseases, rather than liver diseases (Nandivada et al. 2014). From the KEGG pathway analysis, we did see that 10 out of 11 genes in the category of osteoclast differentiation were up-regulated in the Microarray-PN/Saline. Other than liver diseases, it has been shown that PN could also lead to metabolic bone disorders (MBD), for which, the underlying mechanisms are still poorly studied (Nandivada et al. 2014). Our findings from the microarray analysis could potentially provide insights into the association of PN induced liver dysfunction to the development of MBD.

The potential lack of enterohepatic FGF15 signaling could also be responsible for the up-regulation of *Cyp7a1* gene expression seen in the PN mice. It has been shown that WT mice with bile duct ligation also had a 3 fold increase of *Cyp7a1* expression, while expression of small heterodimer partner (*Shp*) was not changed (Inagaki et al. 2005). The increased expression of *Cyp7a*1 might also lead to the accumulation of cholesterol metabolites in the liver, which could in term, activate LXRα and induce the expression of LXRα target genes, including *Lpl*, *Srebp-1c, a*nd *Fas*, as shown in **Figure 4.5 B**. Long-term LXRα activation coupled with up-regulation of its target genes, could be responsible for PN induced liver steatosis, even though PN mice tend to lose body weight.

Similar to previous findings from PN piglets (Vlaardingerbroek et al. 2014), we also detected decreased gene expression of *Fxr*, *Bsep,* and *Mrp3* in the livers of PN mice. A previous report did show decreased expression of *Fxr* and *Bsep* in DSS

pretreated PN mice (PN/DSS), but the expression of these genes involved in BA homeostasis in PN-only mice were not reported (El Kasmi et al. 2012, El Kasmi et al. 2013). Nevertheless, the similar trends of the decreased expression of these genes in the adult mice and preterm piglets suggest common underlying mechanisms in different species, which are most likely PN dependent. Future studies will be needed to dissect out the mechanisms underlined, especially for the down-regulation of *Fxr* gene expression and FXR signaling. The increase of *Cyp7a1* and decrease of *Fxr*, *Bsep* and *Mrp3* gene expression, together could lead to BA levels buildup in the hepatocytes, leading to subsequent elevation of TSBA in PN mice. And the BA accumulation in PN mice could lead to cholestasis after long-term PN especially with the presence of additional risk factors, such as catheter related infections and intestinal tract inflammation, which could push the liver stress further into drastic liver damages in relatively short time, as those detected in PN/DSS mice (El Kasmi et al. 2012).

While expression of *Cyp7a1* increased around 3 fold, relative mRNA levels of *Cyp8b1* and *Cyp7b1* decreased dramatically in PN mouse livers (**Figure 4.3**). It has been shown that both *Cyp7b1* and *Cyp8b1* are directly regulated by retinoic acid-related orphan receptor alpha (RORα) (Wada et al. 2008, Pathak, Li and Chiang 2013). From detailed comparison of our microarray data (Microarray-PN/Saline) to previously published microarray data obtained from RORα) and retinoic acid-related orphan receptor gamma (RORγ) double knockout (DKO) mice (Microarray-DKO/WT) (Kang et al. 2007), we found similar trends of alterations for a big number of genes in the two datasets, while a few genes with different trends were also identified (**Table 4.2**). RORα and RORγ have been shown to play critical roles in regulating the expression of many

genes involved in phase I and phase II metabolism (Kang et al. 2007). The expression patterns of many genes involved in cellular metabolism in the liver are also regulated by the fast-feed circadian rhythm (Zhang, Guo and Klaassen 2011, Xu et al. 2012). And it has been shown that the expression of RORα and RORγ exhibited an oscillatory pattern consistent with the liver circadian rhythm (Kang et al. 2007)**.** Under continuous PN infusion, it is very likely that the normal fast-feed circadian rhythm, which is maintained in the saline control mice, is disrupted in the PN mice. It has also been shown that glucagon/protein kinase A (PKA) signaling could phosphorylate and stabilize RORα protein upon fasting, to induce CYP8B1 and diurnal rhythm (Pathak et al. 2013). The continuous supply of dextrose in the PN solution could potentially lead to down-regulation of PKA signaling, and therefore suppressing RORα target genes, such as *Cyp7b1* and *Cyp8a1*. Besides these direct targets of RORα and/or RORγ, many indirect target genes were also altered in the PN mice, possibly also due to the suppression of RORα and/or RORγ by the continuous PN infusion. It is also important to note that several genes listed in **Table 4.2** showed opposite direction of gene expression alterations. These changes could be mediated by additional transcriptional factors caused by PN infusion. For example, the expression of cytochrome P450, family 2, subfamily b, polypeptide 10 (*Cyp2b10*) has been shown to be directly regulated by both CAR and PXR. In this case, the potential alterations of CAR and/or PXR signaling could explain the dramatic decrease of *Cyp2b10* expression in PN mice. Future studies will be needed to validate the roles of RORα and/or RORγ, as well as other potential factors/mechanisms involved in the alteration of these genes in PN mice, and the potential contributions to the pathogenesis of PNALD. In the current clinical practice,

adult patients tend to receive cyclic PN, but still with continuous infusion. The continuous load of dextrose could still disrupt the normal fast-feed rhythm of many genes in these patients. Nevertheless, for preterm infants and neonates, continuous PN infusion is essential to promote their normal growth and development during the critical period. Therefore, it is critical to fully understand the underlying mechanism, in order to further optimize the PN strategy and prevent potential cause of liver damages.

Finally, preliminary data obtained from serum BA profiling by UPLC-MS were consistent with the gene expression results. In detail, consistent with a 3 fold increase of *Cyp7a1* gene expression, levels of the total 20 BAs increased dramatically in PN mice. CYP8B1 determines the ratio of 12α-OH BAs versus non-12α-OH BAs. As expected, the potential lack of intestinal FXR-FGF15 signaling and the decreased mRNA expression of *Cyp8b1* in PN mice together could be the cause of the dramatic increase of both the levels and the percentages of TCDCA, T-β-MCA, and T-α-MCA in PN mice (**Figure 4.6, 4.8**). Serum levels of CA, TCA, DCA, and TDCA also increased in PN mice, while the percentage of these BA species all decreased. As a result of these changes, the percentage of total non-12α-OH BAs was much higher in PN mice (**Table 4.3**). The dramatic decrease of the percentage of total secondary BAs in PN mice could also be caused by the decreased bile flow from the liver into the intestinal tract, leading to the proportional decrease of secondary BA formation in the gut. While the levels of unconjugated secondary BAs in saline and PN mice were similar (**Figure 4.5**), the levels of conjugated secondary BAs were much higher in PN mice, except for GLCA (undetectable). The increased levels of conjugated secondary BAs in PN mice could be caused by the decreased fecal loss of BAs in the gut, since fecal excretion mainly

counts for the direct loss of secondary BAs. Previous studies in germ-free mice suggest that T-β-MCA and T-α-MCA are FXR antagonists (Sayin et al. 2013). Therefore, the dramatic increase of serum levels of T-β-MCA and T-α-MCA in the PN mice is potentially associated with the increase of these BAs in the livers of PN mice, which could eventually lead to the down-regulation of FXR signaling in the PN mice.

In summary, we have established a valuable mouse PN model using C57BL/6J mice. Combining RNA microarray profiling and serum BA profiling, we characterized detailed the molecular and cellular alterations in the PN mice in great details. These findings will aid us in studying the underlying mechanisms of the pathogenesis of PNALD later on when PN infusion is combined with genetic, pharmacological, or toxicological manipulations in mice.

Figure 4.1 Body Weight and Liver Weight for Saline and PN Mice

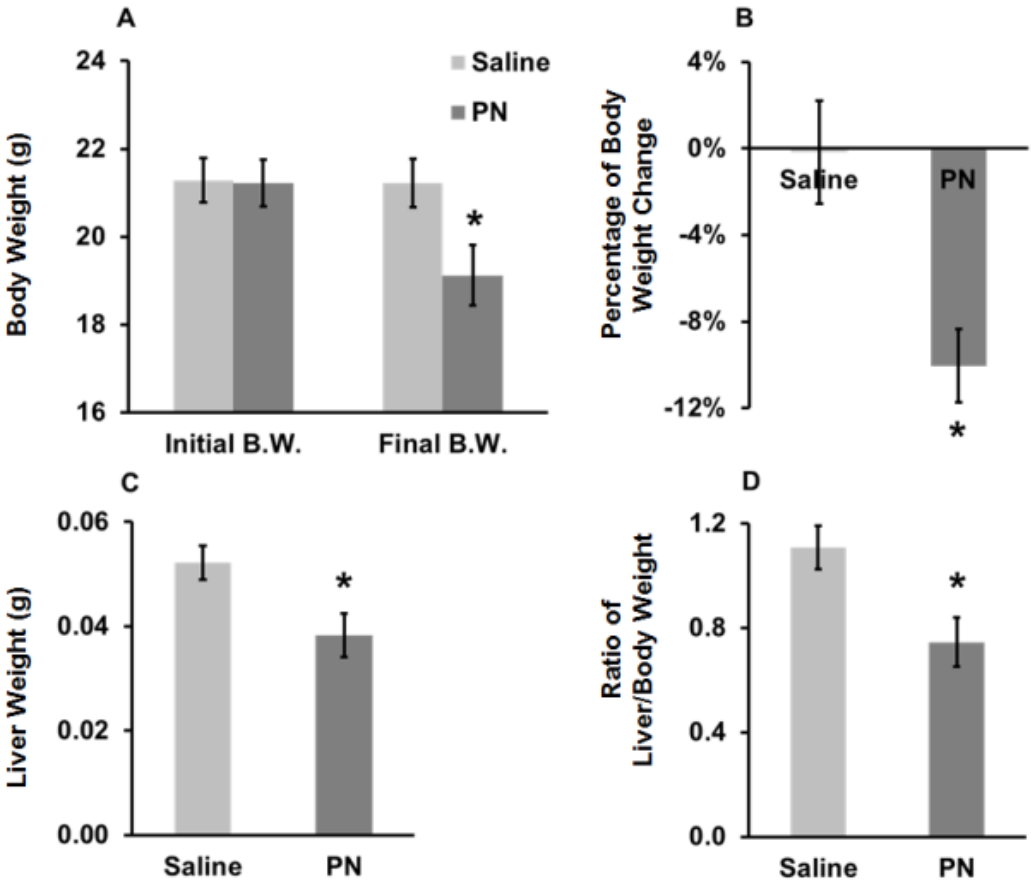

(A) initial B.W. (body weight) of saline (n=6) and PN (n=9) mice upon infusion setup and final B.W. upon animal sacrifice; (B) the percentage of body weight change relative to the initial body weight upon infusion setup; (C) liver weight upon animal sacrifice; (D) the ratio of liver weight to the final body weight upon animal sacrifice. PN mice received PN infusion for 8 days. Data were expressed as mean ± SEM (standard error of the mean). Compared with saline group, *p-*value* < 0.05, student's t-test.

Figure 4.2 Serum Biochemical Analyses for Saline and PN Mice

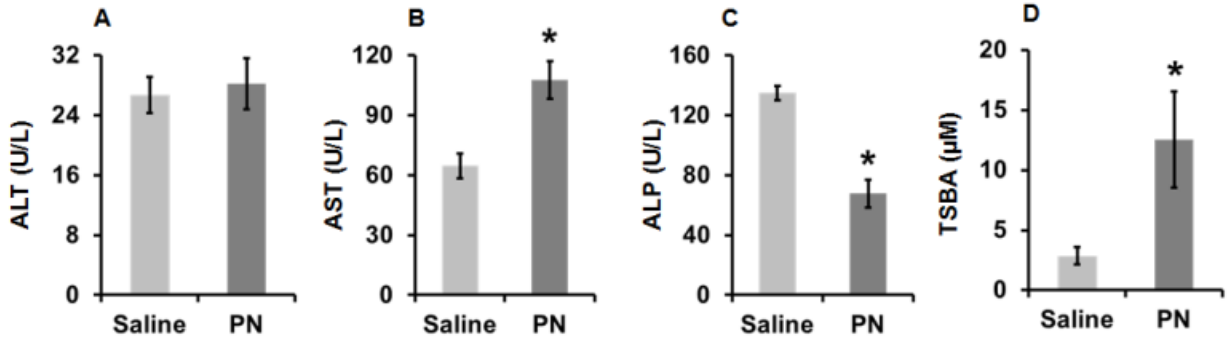

Serum levels of ALT (A), AST (B), ALP (C), and TSBA (D) in saline (n=6) and PN (n=9) mice. PN mice received PN infusion for 8 days. Compared with saline group, *p-$value$ < 0.05, student's t-test.

Figure 4.3 Liver Gene Expression in Saline and PN mice

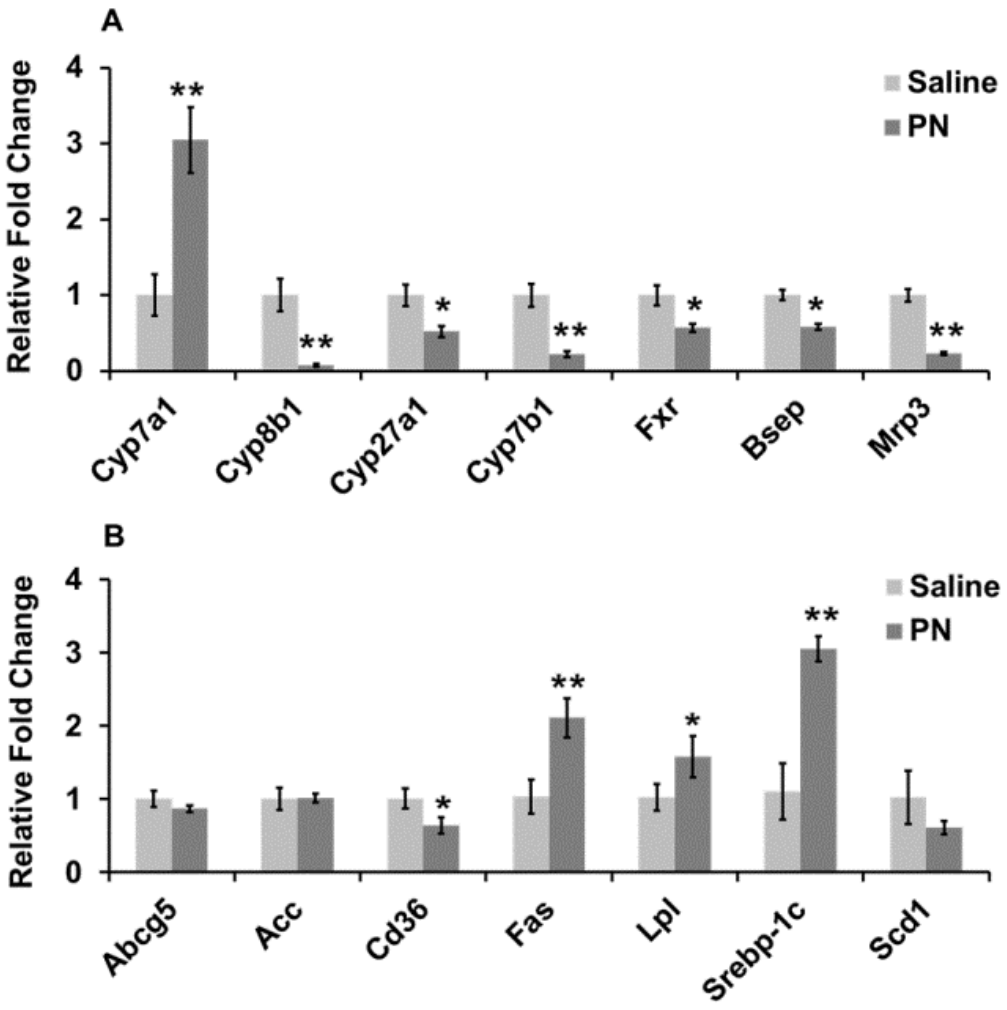

RT-qPCR analysis of relative mRNA expression of genes involved in (A) BA homeostasis and (B) cholesterol and lipid metabolism, in the liver of saline (n=6) and PN (n=8) mice. Gene expression data were expressed as mean ± SEM. PN mice received PN infusion for 8 days. Relative mRNA levels were first normalized to β-actin, and then relative fold changes were normalized to saline control group. Compared with saline control group, *p-$value$ < 0.05, **p-$value$ < 0.005, student's t-test.

Figure 4.4 Validation of Microarray Analysis (Microarray-PN/Saline)

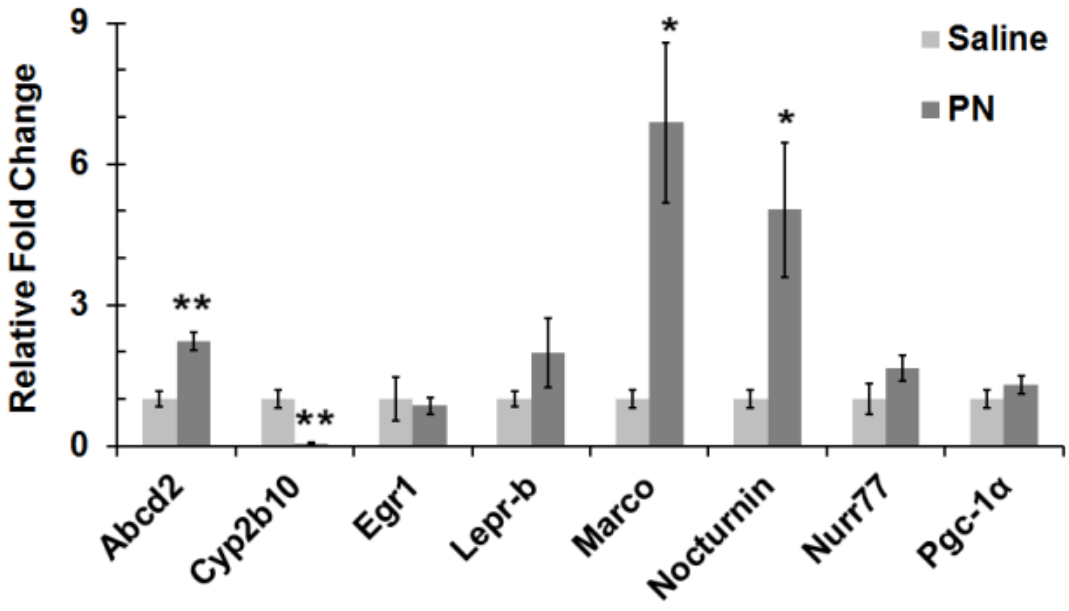

RT-qPCR validation of selected genes retrieved from Microarray-PN/Saline (genes with full name were shown in **Table 4.1**, *Nur77* is for *Nr4a1*). Gene expression data were expressed as mean ± SEM. PN mice (n=8) received PN infusion for 8 days. Relative mRNA levels were first normalized to β-actin, and then relative fold changes were normalized to saline control mice (n=6). Compared with saline control group, *p-value < 0.05, **p-value < 0.005, student's t-test.

Figure 4.5 Serum Levels of 20 BAs in Saline and PN Mice

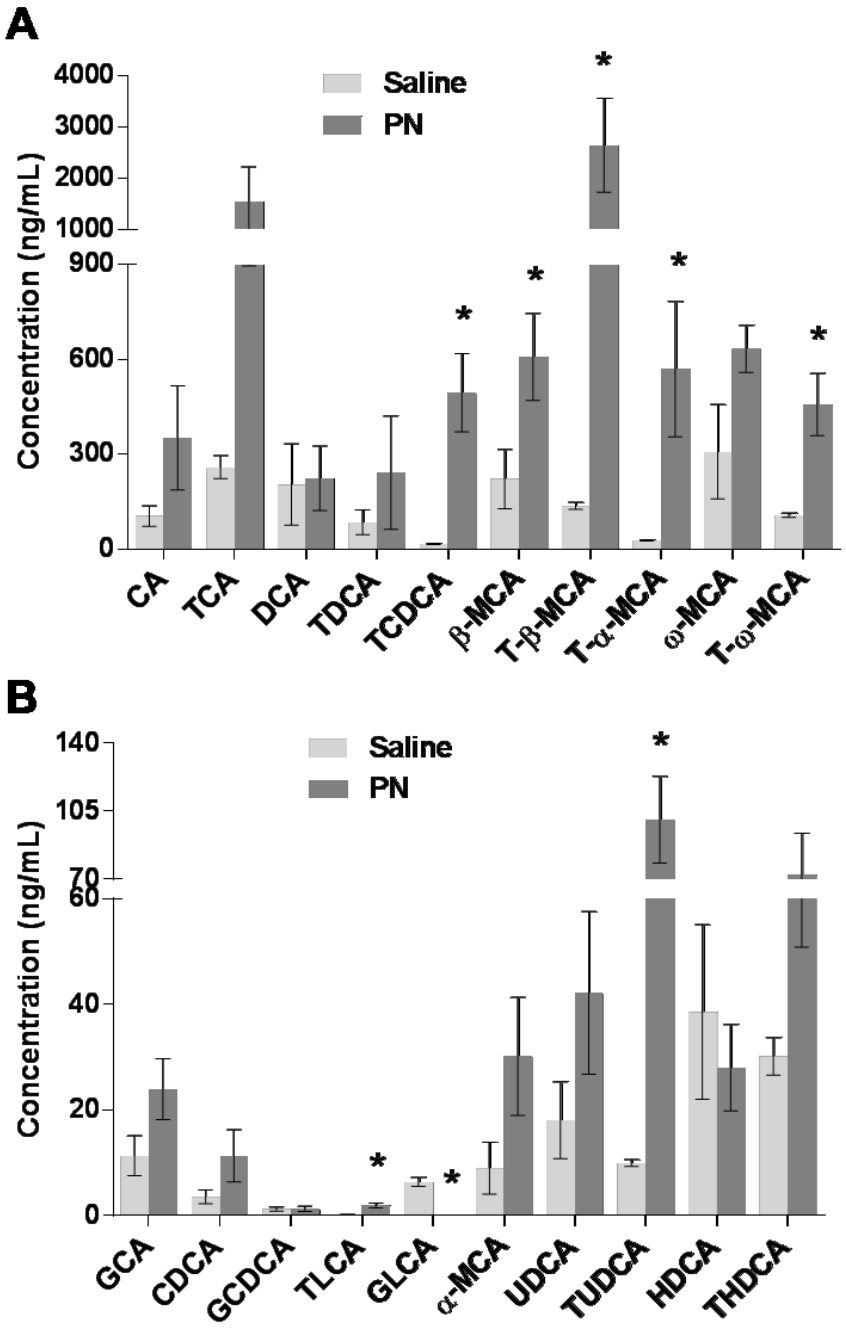

Quantified serum concentrations (ng/mL) of the 20 BAs in saline (n=4) and PN mice (n=5). Data were presented as mean ± SEM. Compared with saline control group, **p-value* < 0.05, student's *t*-test.

Figure 4.6 Relative Levels of Serum BAs in Saline and PN Mice

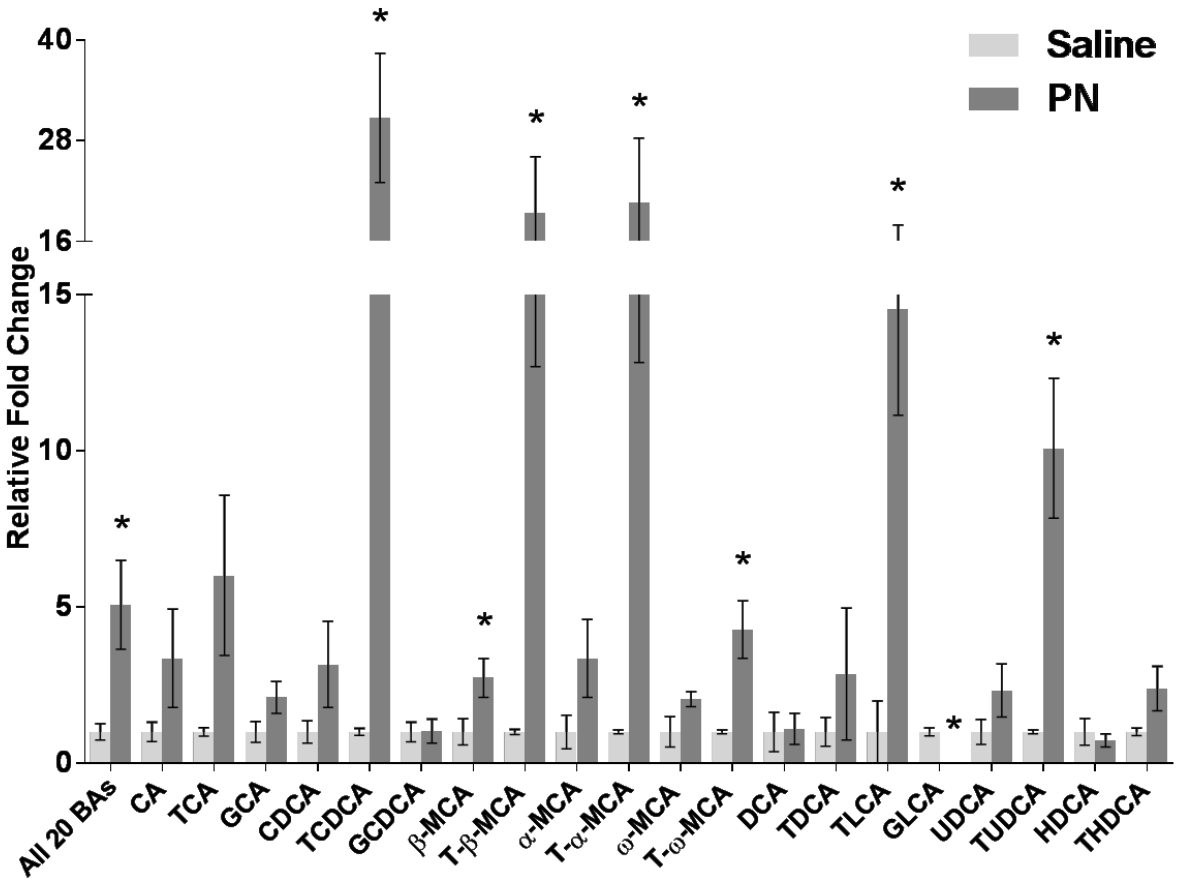

Relative levels of the 20 BAs in PN mice (n=5) was normalized to saline controls (n=4). For saline mice, the relative level of each BA was given arbitrarily as 1. Data were presented as mean ± SEM. Compared with saline control group, *p-$value$ < 0.05, student's t-test.

Figure 4.7 Compositions of Major BAs in Saline and PN Mice

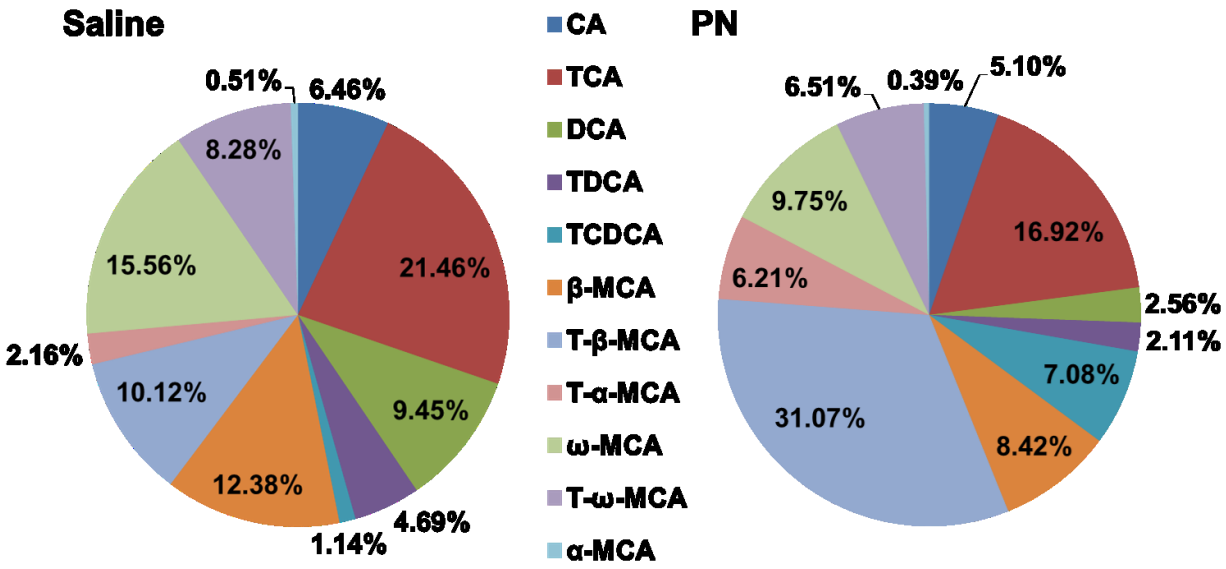

The mean percentages of the major BAs in the two groups are shown.

Figure 4.8 Liver Histology of Saline and PN Mice

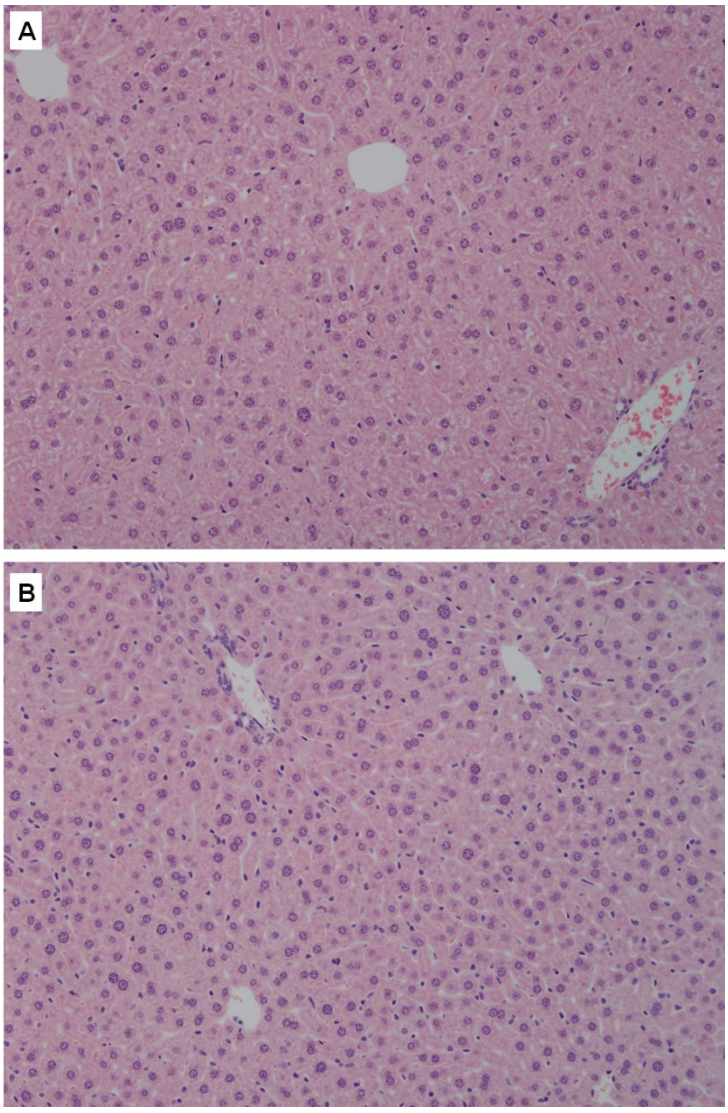

H&E staining of representative mouse livers from saline (A) and PN (B) mice at 20X magnification.

Table 4.1 Top Up- and Down-regulated Genes from Microarray Analysis Retrieved from Microarray-PN/Saline

Gene	Fold Change	Direction	Full Transcript Name
Sult1e1	17.17	Up	Sulfotransferase family 1E, member 1, mRNA
Fmo3	7.68	Up	Flavin containing monooxygenase 3 (Fmo3), mRNA
Lepr	7.05	Up	Leptin receptor (Lepr), transcript variant 2, mRNA
Abcd2	5.97	Up	ATP-binding cassette, sub-family D (ALD), member 2, mRNA
Cyp17a1	5.28	Up	Cytochrome P450, family 17, subfamily a, polypeptide 1 (Cyp17a1), mRNA
Nr4a1	5.16	Up	Nuclear receptor subfamily 4, group A, member 1, mRNA
Marco	5.15	Up	Macrophage receptor with collagenous structure (Marco), mRNA
Egr1	5.1	Up	Early growth response 1 (Egr1), mRNA
Ccrn4l	5.02	Up	NOCTURNIN (Nocturnin)
Btg2	4.64	Up	B-cell translocation gene 2, anti-proliferative (Btg2), mRNA
Cyp4a12a	9.17	Down	Cytochrome P450, family 4, subfamily a, polypeptide 12a, mRNA
Ces2	8.37	Down	Carboxylesterase 2 (Ces2), mRNA
Cyp2b10	6.72	Down	Cyp2b10-like pseudogene, mRNA sequence
Orm3	6.61	Down	Orosomucoid 3, mRNA
Hist1h2bg	6.28	Down	Histone cluster 1, H2bg, mRNA
Clec2h	6.12	Down	C-type lectin domain family 2, member h (Clec2h), mRNA
Orm2	6.07	Down	Orosomucoid 2 (Orm2), mRNA
Cyp4a12b	4.87	Down	highly similar to CYTOCHROME P450 4A8
Cml5	4.85	Down	Camello-like 5 (Cml5), mRNA
Selenbp2	4.49	Down	Selenium binding protein 2, mRNA
Cyp2c55	4.28	Down	Cytochrome P450, family 2, subfamily c, polypeptide 55, mRNA

Table 4.2 Comparison of Microarray Analysis

		Microarray-PN/Saline		Microarray-DKO/WT	
Functional Category	Gene	Fold Change	Direction	Fold Change	Direction
Cytochrome P450	Cyp2b9	9.4	Up	8.9	Up
	Cyp8b1	3.56	Down	4.6	Down
	Cyp7b1	2.22	Down	7.4	Down
	Cyp2b10	**6.72**	**Down**	**3.1**	**Up**
	Cyp4a10	**2.74**	**Down**	**2.5**	**Up**
Steroid	Hmgcr	2.61	Up	2.5	Up
	Hsd17b7	1.68	Up	3	Up
	Hsd3b4	2.45	Down	5.4	Down
	Hsd3b5	2.39	Down	15.8	Down
Lipid and fatty acid	Scd2	2.11	Up	2.6	Up
	Elovl6	1.66	Up	3.9	Up
	Elovl3	3.01	Down	7.7	Down
Cell signaling	Igfbp1	2.88	Up	5.7	Up
Transport	Abcd2	5.97	Up	2.4	Up
	Apoa4	3.87	Up	2.1	Up
Carbohydrate	Ppp1r3c	3.55	Down	2.2	Down
Circadian rhythm	Rora	1.6	Down	3	Down
	Rorc	1.61	Down	2.3	Down
	Ccrn4l	5.02	Up	3.5	Up
Miscellaneous	Keg1	2.22	Down	2	Down
	Lpin2	2.57	Up	1.8	Up
	Selenbp2	4.49	Down	5.1	Down
	Ccnb1	**2.22**	**Up**	**2.2**	**Down**

Selected genes with the corresponding fold changes and directions of change were retrieved from Microarray-PN/Saline and Microarray-DKO/WT. The functional categories of these genes were obtained from the previous microarray study (Kang et al. 2007).

The genes with different directions of changes in the two microarray datasets were highlighted in bold.

Table 4.3 KEGG Pathway Analysis for Microarray-PN/Saline

KEGG Pathway	List	Up	Down	Gene Set
Cytokine-cytokine receptor interaction	28	19	9	243
Neuroactive ligand-receptor interaction	16	11	5	309
Jak-STAT signaling pathway	15	12	3	146
Natural killer cell mediated cytotoxicity	15	11	4	132
Osteoclast differentiation	11	10	1	107
Staphylococcus aureus infection	11	9	2	48
Glycolysis / Gluconeogenesis	9	6	3	58
p53 signaling pathway	9	7	2	65
Inositol phosphate metabolism	7	7	0	55
Fat digestion and absorption	6	6	0	41
Biosynthesis of unsaturated fatty acids	5	4	1	24
Steroid biosynthesis	4	4	0	18
Drug metabolism - cytochrome P450	19	6	13	74
Retinol metabolism	14	4	10	64
Steroid hormone biosynthesis	13	5	8	46
Arachidonic acid metabolism	12	4	8	82
Complement and coagulation cascades	11	4	7	70
Glutathione metabolism	8	0	8	53
Pentose and glucuronate interconversions	7	1	6	22
Fatty acid metabolism	6	0	6	45
Circadian rhythm - mammal	4	1	3	21
Bile secretion	16	9	7	65
PPAR signaling pathway	15	8	7	74

Total number of genes retrieved from Microarray-PN/Saline for each KEGG category was listed in the “List” column. Total number of genes for each category in DAVID was listed in “Gene set” column.

Table 4.4 Summary of Serum BAs in PN and Saline Mice

	Concentration (ng/mL)			Percentage	
Total BAs	Saline	PN	Fold*	Saline	PN
Total CA	376.1	1938.3	5.2	28.6%	22.4%
Total CDCA	21.0	507.8	24.2	1.5%	7.3%
Total α/β-MCA	396.0	3863.2	9.8	25.2%	46.1%
Total DCA	289.1	466.2	1.6	14.1%	4.7%
Total LCA	6.5	1.9	0.3	0.5%	0.0%
Total ω-MCA	415.6	1091.6	2.6	23.8%	16.3%
Total HDCA	28.1	142.9	5.1	1.8%	2.0%
Total UDCA	68.8	100.3	1.5	4.5%	1.3%
Total primary BAs	793.1	6309.4	8.0	55.2%	75.8%
Total secondary BAs	808.1	1803.0	2.2	44.8%	24.2%
Total 12α-OH BA	665.1	2404.6	3.6	42.7%	27.1%
Total non-12α-OH BA	936.0	5707.8	6.1	57.3%	72.9%
Total BAs	1601.2	8112.4	5.1		

* “Fold” is calculated by dividing the corresponding serum BA concentration in PN mice by the BA concentration in saline mice.

Chapter 5: Summary and Future Directions

For the first aim of this dissertation (Chapter 3), using genome-wide analysis tools, we obtained a global picture of FXR binding in HepG2 cells and PHHs, as well as the transcriptome profiles of PHHs upon GW4064 activation of FXR. Our comparison analysis showed overall similar profiles of FXR binding in cultured HepG2 cells and PHHs compared to that in mice in a genome-wide scale. These results will provide critical insights in future translational studies, especially when studies in mice need to be extrapolated into human conditions. In terms of species similarities, the pathway of complement and coagulation cascade is of particular interest. Both mouse and human FXR was found to bind to the promoter regions of many genes in this pathway (**Table 3.5**), including the three genes encoding the three protein components of fibrinogen, fibrinogen alpha chain (*FGA*), fibrinogen beta chain (*FGB*), and fibrinogen gamma chain (*FGG*), and the gene encoding the important anti-coagulant protein antithrombin (*SERPINC1*) (**Table 3.5**). In addition, FXR has been shown to have physical interaction with HNF-4α and the two NRs co-regulate many genes in this pathway (Thomas et al. 2013). Preliminary PN studies have also been performed in mice, but we encountered infusion problems for those mice. Preliminary dissections of mice died from the PN infusion suggest that these mice may have problems associated with their coagulation system. Nevertheless, biochemical analyses for serum samples obtained from non-surgical FXR-hepKO mice didn't show obvious alterations in these mice (data not shown). Therefore, we speculate that the FXR-hepKO mice are prone to have coagulation problems, likely stronger coagulation responses than control mice, and certain components in the PN solution pushed the coagulation system in these mice

further to pathological levels and caused the problems we have consistently seen in these mice. Future studies will be needed to dissect out the molecular mechanisms underlined, and the implications to the study of human FXR functions. In terms of species differences, the pathway of retinol metabolism may be worth future analysis. This pathway was enriched in the pathway analyses for both ChIP-seq and RNA-seq for the PHHs, but not enriched in the ChIP-seq analysis for the mouse livers (**Table 3.4, 3.5**).

For the second aim of this dissertation (Chapter 4), using microarray profiling and serum BA profiling, we identified novel molecular signatures of the PN mice, especially those involved in BAs synthesis and metabolism. The results obtained from this study will provide valuable insights in guiding future studies of PNALD in our laboratory. First of all, liver and intestinal BA profiles will be characterized, not only to uncover the comprehensive profiles of the enterohepatic circulation of BAs in the PN mice, but also to provide in-depth mechanistic insights about the potential roles of FXR and BA signaling and BA cytotoxicity in the pathogenesis of PNALD.

As mentioned, we are also conducting PN studies in FXR-hepKO mice. Preliminary results obtained so far are still ambiguous, probably due to the coagulation problems mentioned previously. We are in the process of investigating and modifying different components in the PN solution, in order to avoid the potential coagulation problems and more importantly, to obtain valuable results from the FXR-hepKO-PN mice. These results will provide indispensable mechanistic insights associated with the roles of FXR and BA signaling involved in the pathogenesis and/or future management of PNALD.

We also plan to study the potential roles of FXR and BA signaling in PN/DSS mice once the PN/DSS mouse model is well established. In terms of new generations of lipid emulsions for PN study, we plan to start from FOLE. Eventually, different lipid emulsions, different pharmacological and/or toxicological treatment for mice, and mice with different genetic manipulations will be tested in various combinations to study the molecular and cellular mechanisms underlying the development, progression, and potentially reversal of PNALD.

Bibliography

Ananthanarayanan, M., N. Balasubramanian, M. Makishima, D. J. Mangelsdorf & F. J. Suchy (2001) Human bile salt export pump promoter is transactivated by the farnesoid X receptor/bile acid receptor. *J Biol Chem,* 276**,** 28857-65.

Ananthanarayanan, M., S. Li, N. Balasubramaniyan, F. J. Suchy & M. J. Walsh (2004) Ligand-dependent activation of the farnesoid X-receptor directs arginine methylation of histone H3 by CARM1. *J Biol Chem,* 279**,** 54348-57.

Anisfeld, A. M., H. R. Kast-Woelbern, M. E. Meyer, S. A. Jones, Y. Zhang, K. J. Williams, T. Willson & P. A. Edwards (2003) Syndecan-1 expression is regulated in an isoform-specific manner by the farnesoid-X receptor. *J Biol Chem,* 278**,** 20420-8.

Bailey, T. L., M. Boden, F. A. Buske, M. Frith, C. E. Grant, L. Clementi, J. Ren, W. W. Li & W. S. Noble (2009) MEME SUITE: tools for motif discovery and searching. *Nucleic Acids Res,* 37**,** W202-8.

Ballatori, N., W. V. Christian, J. Y. Lee, P. A. Dawson, C. J. Soroka, J. L. Boyer, M. S. Madejczyk & N. Li (2005) OSTalpha-OSTbeta: a major basolateral bile acid and steroid transporter in human intestinal, renal, and biliary epithelia. *Hepatology,* 42**,** 1270-9.

Bauer, U. M., S. Daujat, S. J. Nielsen, K. Nightingale & T. Kouzarides (2002) Methylation at arginine 17 of histone H3 is linked to gene activation. *EMBO Rep,* 3**,** 39-44.

Beale, E. F., R. M. Nelson, R. L. Bucciarelli, W. H. Donnelly & D. V. Eitzman (1979) Intrahepatic cholestasis associated with parenteral nutrition in premature infants. *Pediatrics,* 64**,** 342-7.

Berg, D. J., J. Zhang, J. V. Weinstock, H. F. Ismail, K. A. Earle, H. Alila, R. Pamukcu, S. Moore & R. G. Lynch (2002) Rapid development of colitis in NSAID-treated IL-10-deficient mice. *Gastroenterology,* 123**,** 1527-42.

Berrabah, W., P. Aumercier, C. Gheeraert, H. Dehondt, E. Bouchaert, J. Alexandre, M. Ploton, C. Mazuy, S. Caron, A. Tailleux, J. Eeckhoute, T. Lefebvre, B. Staels & P. Lefebvre (2014) Glucose sensing O-GlcNAcylation pathway regulates the nuclear bile acid receptor farnesoid X receptor (FXR). *Hepatology,* 59**,** 2022-33.

Borude, P., G. Edwards, C. Walesky, F. Li, X. Ma, B. Kong, G. L. Guo & U. Apte (2012) Hepatocyte-specific deletion of farnesoid X receptor delays but does not inhibit liver regeneration after partial hepatectomy in mice. *Hepatology,* 56**,** 2344-52.

Borum, P. R. (1993) Use of the colostrum-deprived piglet to evaluate parenteral feeding formulas. *J Nutr,* 123**,** 391-4.

Botham, K. M. & G. S. Boyd (1983) The metabolism of chenodeoxycholic acid to beta-muricholic acid in rat liver. *Eur J Biochem,* 134**,** 191-6.

Brown, M. S. & J. L. Goldstein (2009) Cholesterol feedback: from Schoenheimer's bottle to Scap's MELADL. *J Lipid Res,* 50 Suppl**,** S15-27.

Calder, P. C. (2007) Immunomodulation by omega-3 fatty acids. *Prostaglandins Leukot Essent Fatty Acids,* 77**,** 327-35.

Cariou, B., K. van Harmelen, D. Duran-Sandoval, T. H. van Dijk, A. Grefhorst, M. Abdelkarim, S. Caron, G. Torpier, J. C. Fruchart, F. J. Gonzalez, F. Kuipers & B. Staels (2006) The farnesoid X receptor modulates adiposity and peripheral insulin sensitivity in mice. *J Biol Chem,* 281**,** 11039-49.

Carter, B. A., O. A. Taylor, D. R. Prendergast, T. L. Zimmerman, R. Von Furstenberg, D. D. Moore & S. J. Karpen (2007) Stigmasterol, a soy lipid-derived phytosterol, is an antagonist of the bile acid nuclear receptor FXR. *Pediatr Res,* 62**,** 301-6.

Cavicchi, M., P. Beau, P. Crenn, C. Degott & B. Messing (2000) Prevalence of liver disease and contributing factors in patients receiving home parenteral nutrition for permanent intestinal failure. *Ann Intern Med,* 132**,** 525-32.

Chao, F., W. Gong, Y. Zheng, Y. Li, G. Huang, M. Gao, J. Li, R. Kuruba, X. Gao, S. Li & F. He (2010) Upregulation of scavenger receptor class B type I expression by activation of FXR in hepatocyte. *Atherosclerosis,* 213**,** 443-8.

Chawla, A., J. J. Repa, R. M. Evans & D. J. Mangelsdorf (2001) Nuclear receptors and lipid physiology: opening the X-files. *Science,* 294**,** 1866-70.

Chawla, R. K., C. J. Berry, M. H. Kutner & D. Rudman (1985) Plasma concentrations of transsulfuration pathway products during nasoenteral and intravenous hyperalimentation of malnourished patients. *Am J Clin Nutr,* 42**,** 577-84.

Chong, H. K., J. Biesinger, Y. K. Seo, X. Xie & T. F. Osborne (2012) Genome-wide analysis of hepatic LRH-1 reveals a promoter binding preference and suggests a role in regulating genes of lipid metabolism in concert with FXR. *BMC Genomics,* 13**,** 51.

Chong, H. K., A. M. Infante, Y. K. Seo, T. I. Jeon, Y. Zhang, P. A. Edwards, X. Xie & T. F. Osborne (2010) Genome-wide interrogation of hepatic FXR reveals an asymmetric IR-1 motif and synergy with LRH-1. *Nucleic Acids Res,* 38**,** 6007-17.

Christensen, R. D., E. Henry, S. E. Wiedmeier, J. Burnett & D. K. Lambert (2007) Identifying patients, on the first day of life, at high-risk of developing parenteral nutrition-associated liver disease. *J Perinatol,* 27**,** 284-90.

Claudel, T., Y. Inoue, O. Barbier, D. Duran-Sandoval, V. Kosykh, J. Fruchart, J. C. Fruchart, F. J. Gonzalez & B. Staels (2003) Farnesoid X receptor agonists suppress hepatic apolipoprotein CIII expression. *Gastroenterology,* 125**,** 544-55.

Claudel, T., E. Sturm, H. Duez, I. P. Torra, A. Sirvent, V. Kosykh, J. C. Fruchart, J. Dallongeville, D. W. Hum, F. Kuipers & B. Staels (2002) Bile acid-activated nuclear receptor FXR suppresses apolipoprotein A-I transcription via a negative FXR response element. *J Clin Invest,* 109**,** 961-71.

Clayton, P. T., A. Bowron, K. A. Mills, A. Massoud, M. Casteels & P. J. Milla (1993) Phytosterolemia in children with parenteral nutrition-associated cholestatic liver disease. *Gastroenterology,* 105**,** 1806-13.

Cowan, E., P. Nandivada & M. Puder (2013) Fish oil-based lipid emulsion in the treatment of parenteral nutrition-associated liver disease. *Curr Opin Pediatr,* 25**,** 193-200.

Craddock, A. L., M. W. Love, R. W. Daniel, L. C. Kirby, H. C. Walters, M. H. Wong & P. A. Dawson (1998) Expression and transport properties of the human ileal and renal sodium-dependent bile acid transporter. *Am J Physiol,* 274**,** G157-69.

Craig, R. M., T. Neumann, K. N. Jeejeebhoy & H. Yokoo (1980) Severe hepatocellular reaction resembling alcoholic hepatitis with cirrhosis after massive small bowel resection and prolonged total parenteral nutrition. *Gastroenterology,* 79**,** 131-7.

Cui, J., T. S. Heard, J. Yu, J. L. Lo, L. Huang, Y. Li, J. M. Schaeffer & S. D. Wright (2002) The amino acid residues asparagine 354 and isoleucine 372 of human farnesoid X receptor confer the receptor with high sensitivity to chenodeoxycholate. *J Biol Chem,* 277**,** 25963-9.

de Meijer, V. E., K. M. Gura, J. A. Meisel, H. D. Le & M. Puder (2009) Parenteral fish oil as monotherapy for patients with parenteral nutrition-associated liver disease. *Pediatr Surg Int,* 25**,** 123-4.

de Meijer, V. E., H. D. Le, J. A. Meisel, K. M. Gura & M. Puder (2010) Parenteral fish oil as monotherapy prevents essential fatty acid deficiency in parenteral nutrition-dependent patients. *J Pediatr Gastroenterol Nutr,* 50**,** 212-8.

Degirolamo, C., S. Modica, M. Vacca, G. Di Tullio, A. Morgano, A. D'Orazio, K. Kannisto, P. Parini & A. Moschetta (2014) Prevention of spontaneous hepatocarcinogenesis in FXR null mice by intestinal specific FXR re-activation. *Hepatology*.

Deng, Y., H. Wang, Y. Lu, S. Liu, Q. Zhang, J. Huang, R. Zhu, J. Yang, R. Zhang, D. Zhang, W. Shen, G. Ning & Y. Yang (2013) Identification of Chemerin as a Novel FXR Target Gene Down-Regulated in the Progression of Nonalcoholic Steatohepatitis. *Endocrinology,* 154**,** 1794-801.

Denson, L. A., E. Sturm, W. Echevarria, T. L. Zimmerman, M. Makishima, D. J. Mangelsdorf & S. J. Karpen (2001) The orphan nuclear receptor, shp, mediates bile acid-induced inhibition of the rat bile acid transporter, ntcp. *Gastroenterology,* 121**,** 140-7.

Desnoyers, L. R., R. Pai, R. E. Ferrando, K. Hotzel, T. Le, J. Ross, R. Carano, A. D'Souza, J. Qing, I. Mohtashemi, A. Ashkenazi & D. M. French (2008) Targeting FGF19 inhibits tumor growth in colon cancer xenograft and FGF19 transgenic hepatocellular carcinoma models. *Oncogene,* 27**,** 85-97.

Dorney, S. F., M. E. Ament, W. E. Berquist, J. H. Vargas & E. Hassall (1985) Improved survival in very short small bowel of infancy with use of long-term parenteral nutrition. *J Pediatr,* 107**,** 521-5.

Downes, M., M. A. Verdecia, A. J. Roecker, R. Hughes, J. B. Hogenesch, H. R. Kast-Woelbern, M. E. Bowman, J. L. Ferrer, A. M. Anisfeld, P. A. Edwards, J. M. Rosenfeld, J. G. Alvarez, J. P. Noel, K. C. Nicolaou & R. M. Evans (2003) A chemical, genetic, and structural analysis of the nuclear bile acid receptor FXR. *Mol Cell,* 11**,** 1079-92.

Dudley, M. A., L. J. Wykes, A. W. Dudley, Jr., D. G. Burrin, B. L. Nichols, J. Rosenberger, F. Jahoor, W. C. Heird & P. J. Reeds (1998) Parenteral nutrition selectively decreases protein synthesis in the small intestine. *Am J Physiol,* 274**,** G131-7.

Dudrick, S. J., D. W. Wilmore, H. M. Vars & J. E. Rhoads (1968) Long-term total parenteral nutrition with growth, development, and positive nitrogen balance. *Surgery,* 64**,** 134-42.

Duerksen, D. R., J. E. Van Aerde, G. Chan, A. B. Thomson, L. J. Jewell & M. T. Clandinin (1996) Total parenteral nutrition impairs bile flow and alters bile composition in newborn piglet. *Dig Dis Sci,* 41**,** 1864-70.

Dufer, M., K. Horth, R. Wagner, B. Schittenhelm, S. Prowald, T. F. Wagner, J. Oberwinkler, R. Lukowski, F. J. Gonzalez, P. Krippeit-Drews & G. Drews (2012) Bile acids acutely stimulate insulin secretion of mouse beta-cells via farnesoid X receptor activation and K(ATP) channel inhibition. *Diabetes,* 61**,** 1479-89.

Edgar, R., M. Domrachev & A. E. Lash (2002) Gene Expression Omnibus: NCBI gene expression and hybridization array data repository. *Nucleic Acids Res,* 30**,** 207-10.

El Kasmi, K. C., A. L. Anderson, M. W. Devereaux, S. A. Fillon, J. K. Harris, M. A. Lovell, M. J. Finegold & R. J. Sokol (2012) Toll-like receptor 4-dependent Kupffer cell activation and liver injury in a novel mouse model of parenteral nutrition and intestinal injury. *Hepatology,* 55**,** 1518-28.

El Kasmi, K. C., A. L. Anderson, M. W. Devereaux, P. M. Vue, W. Zhang, K. D. Setchell, S. J. Karpen & R. J. Sokol (2013) Phytosterols promote liver injury and Kupffer cell activation in parenteral nutrition-associated liver disease. *Sci Transl Med,* 5**,** 206ra137.

Ellegard, L., A. Sunesson & I. Bosaeus (2005) High serum phytosterol levels in short bowel patients on parenteral nutrition support. *Clin Nutr,* 24**,** 415-20.

Feng, Y., J. E. McDunn & D. H. Teitelbaum (2010) Decreased phospho-Akt signaling in a mouse model of total parenteral nutrition: a potential mechanism for the development of intestinal mucosal atrophy. *Am J Physiol Gastrointest Liver Physiol,* 298**,** G833-41.

Feng, Y. & D. H. Teitelbaum (2013) Tumour necrosis factor--induced loss of intestinal barrier function requires TNFR1 and TNFR2 signalling in a mouse model of total parenteral nutrition. *J Physiol,* 591**,** 3709-23.

Fitzgibbons, S. C., B. A. Jones, M. A. Hull, D. Zurakowski, D. Duro, C. Duggan, D. Boctor, D. L. Sigalet & T. Jaksic (2010) Relationship between biopsy-proven parenteralnutrition-associated liver fibrosis and biochemical cholestasis in children with short bowel syndrome. *J Pediatr Surg,* 45**,** 95-9; discussion 99.

Forman, B. M., E. Goode, J. Chen, A. E. Oro, D. J. Bradley, T. Perlmann, D. J. Noonan, L. T. Burka, T. McMorris, W. W. Lamph, R. M. Evans & C. Weinberger (1995) Identification of a nuclear receptor that is activated by farnesol metabolites. *Cell,* 81**,** 687-93.

Friday, K. E. & E. W. Lipkin (1990) Long-term parenteral nutrition in unrestrained nonhuman primates: an experimental model. *Am J Clin Nutr,* 51**,** 470-6.

Gadaleta, R. M., K. J. van Erpecum, B. Oldenburg, E. C. Willemsen, W. Renooij, S. Murzilli, L. W. Klomp, P. D. Siersema, M. E. Schipper, S. Danese, G. Penna, G. Laverny, L. Adorini, A. Moschetta & S. W. van Mil (2011) Farnesoid X receptor activation inhibits inflammation and preserves the intestinal barrier in inflammatory bowel disease. *Gut,* 60**,** 463-72.

Gao, H., S. Falt, A. Sandelin, J. A. Gustafsson & K. Dahlman-Wright (2008) Genome-wide identification of estrogen receptor alpha-binding sites in mouse liver. *Mol Endocrinol,* 22**,** 10-22.

Gardes, C., E. Chaput, A. Staempfli, D. Blum, H. Richter & G. M. Benson (2013) Differential regulation of bile acid and cholesterol metabolism by the farnesoid X receptor in Ldlr -/- mice versus hamsters. *J Lipid Res,* 54**,** 1283-99.

Garruti, G., H. H. Wang, L. Bonfrate, O. de Bari, D. Q. Wang & P. Portincasa (2012) A pleiotropic role for the orphan nuclear receptor small heterodimer partner in lipid homeostasis and metabolic pathways. *J Lipids,* 2012**,** 304292.

Geggel, H. S., M. E. Ament, J. R. Heckenlively, D. A. Martin & J. D. Kopple (1985) Nutritional requirement for taurine in patients receiving long-term parenteral nutrition. *N Engl J Med,* 312**,** 142-6.

Gleghorn, E. E., R. J. Merritt, D. H. Henton, H. M. Neustein, B. Landing & F. R. Sinatra (1989) A subacute rabbit model for hepatobiliary dysfunction during total parenteral nutrition. *J Pediatr Gastroenterol Nutr,* 9**,** 246-55.

Goldstein, R. M., T. Hebiguchi, G. D. Luk, F. Taqi, T. R. Guilarte, F. A. Franklin, Jr., P. W. Niemiec & D. L. Dudgeon (1985) The effects of total parenteral nutrition on gastrointestinal growth and development. *J Pediatr Surg,* 20**,** 785-91.

Gong, Y., Z. B. Huang, E. Christensen & C. Gluud (2008) Ursodeoxycholic acid for primary biliary cirrhosis. *Cochrane Database Syst Rev***,** CD000551.

Gong, Y. Z., E. T. Everett, D. A. Schwartz, J. S. Norris & F. A. Wilson (1994) Molecular cloning, tissue distribution, and expression of a 14-kDa bile acid-binding protein from rat ileal cytosol. *Proc Natl Acad Sci U S A,* 91**,** 4741-5.

Goodwin, B., S. A. Jones, R. R. Price, M. A. Watson, D. D. McKee, L. B. Moore, C. Galardi, J. G. Wilson, M. C. Lewis, M. E. Roth, P. R. Maloney, T. M. Willson & S.

A. Kliewer (2000) A regulatory cascade of the nuclear receptors FXR, SHP-1, and LRH-1 represses bile acid biosynthesis. *Mol Cell,* 6**,** 517-26.

Grober, J., I. Zaghini, H. Fujii, S. A. Jones, S. A. Kliewer, T. M. Willson, T. Ono & P. Besnard (1999) Identification of a bile acid-responsive element in the human ileal bile acid-binding protein gene. Involvement of the farnesoid X receptor/9-cis-retinoic acid receptor heterodimer. *J Biol Chem,* 274**,** 29749-54.

Groen, A., M. R. Romero, C. Kunne, S. J. Hoosdally, P. H. Dixon, C. Wooding, C. Williamson, J. Seppen, K. Van den Oever, K. S. Mok, C. C. Paulusma, K. J. Linton & R. P. Oude Elferink (2011) Complementary functions of the flippase ATP8B1 and the floppase ABCB4 in maintaining canalicular membrane integrity. *Gastroenterology,* 141**,** 1927-37 e1-4.

Guo, G. L., S. Santamarina-Fojo, T. E. Akiyama, M. J. Amar, B. J. Paigen, B. Brewer, Jr. & F. J. Gonzalez (2006) Effects of FXR in foam-cell formation and atherosclerosis development. *Biochim Biophys Acta,* 1761**,** 1401-9.

Gura, K. M., S. Lee, C. Valim, J. Zhou, S. Kim, B. P. Modi, D. A. Arsenault, R. A. Strijbosch, S. Lopes, C. Duggan & M. Puder (2008) Safety and efficacy of a fish-oil-based fat emulsion in the treatment of parenteral nutrition-associated liver disease. *Pediatrics,* 121**,** e678-86.

Hall, R. I., J. P. Grant, L. H. Ross, R. A. Coleman, M. G. Bozovic & S. H. Quarfordt (1984) Pathogenesis of hepatic steatosis in the parenterally fed rat. *J Clin Invest,* 74**,** 1658-68.

Han, Y. Y., S. L. Lai, W. J. Ko, C. H. Chou & H. S. Lai (2012) Effects of fish oil on inflammatory modulation in surgical intensive care unit patients. *Nutr Clin Pract,* 27**,** 91-8.

Hart, S. N., Y. Li, K. Nakamoto, E. A. Subileau, D. Steen & X. B. Zhong (2010) A comparison of whole genome gene expression profiles of HepaRG cells and HepG2 cells to primary human hepatocytes and human liver tissues. *Drug Metab Dispos,* 38**,** 988-94.

Hata, S., S. Kamata, R. Nezu, Y. Takagi & A. Okada (1989) A newborn rabbit model for total parenteral nutrition: effects of nutritional components on cholestasis. *JPEN J Parenter Enteral Nutr,* 13**,** 265-71.

Higgins, G. M. & R. M. Anderson (1931) Experimental pathology of the liver. I. Restoration of the liver of the white rat following partial surgical removal. *Arch Pathol* 12**,** 186–202.

Hirokane, H., M. Nakahara, S. Tachibana, M. Shimizu & R. Sato (2004) Bile acid reduces the secretion of very low density lipoprotein by repressing microsomal triglyceride transfer protein gene expression mediated by hepatocyte nuclear factor-4. *J Biol Chem,* 279**,** 45685-92.

Holt, J. A., G. Luo, A. N. Billin, J. Bisi, Y. Y. McNeill, K. F. Kozarsky, M. Donahee, D. Y. Wang, T. A. Mansfield, S. A. Kliewer, B. Goodwin & S. A. Jones (2003) Definition of a novel growth factor-dependent signal cascade for the suppression of bile acid biosynthesis. *Genes Dev,* 17**,** 1581-91.

Huang, L., A. Zhao, J. L. Lew, T. Zhang, Y. Hrywna, J. R. Thompson, N. de Pedro, I. Royo, R. A. Blevins, F. Pelaez, S. D. Wright & J. Cui (2003) Farnesoid X receptor

activates transcription of the phospholipid pump MDR3. *J Biol Chem,* 278**,** 51085-90.

Huang, W., K. Ma, J. Zhang, M. Qatanani, J. Cuvillier, J. Liu, B. Dong, X. Huang & D. D. Moore (2006) Nuclear receptor-dependent bile acid signaling is required for normal liver regeneration. *Science,* 312**,** 233-6.

Huber, R. M., K. Murphy, B. Miao, J. R. Link, M. R. Cunningham, M. J. Rupar, P. L. Gunyuzlu, T. F. Haws, A. Kassam, F. Powell, G. F. Hollis, P. R. Young, R. Mukherjee & T. C. Burn (2002) Generation of multiple farnesoid-X-receptor isoforms through the use of alternative promoters. *Gene,* 290**,** 35-43.

Inagaki, T., M. Choi, A. Moschetta, L. Peng, C. L. Cummins, J. G. McDonald, G. Luo, S. A. Jones, B. Goodwin, J. A. Richardson, R. D. Gerard, J. J. Repa, D. J. Mangelsdorf & S. A. Kliewer (2005) Fibroblast growth factor 15 functions as an enterohepatic signal to regulate bile acid homeostasis. *Cell Metab,* 2**,** 217-25.

Jain, A. K., B. Stoll, D. G. Burrin, J. J. Holst & D. D. Moore (2012) Enteral bile acid treatment improves parenteral nutrition-related liver disease and intestinal mucosal atrophy in neonatal pigs. *Am J Physiol Gastrointest Liver Physiol,* 302**,** G218-24.

James, B. E., P. G. Hendry & R. A. MacMahon (1979) Total parenteral nutrition of premature infants. 2. Requirement for micronutrient elements. *Aust Paediatr J,* 15**,** 67-71.

Jia, L., B. P. Berman, U. Jariwala, X. Yan, J. P. Cogan, A. Walters, T. Chen, G. Buchanan, B. Frenkel & G. A. Coetzee (2008) Genomic androgen receptor-

occupied regions with different functions, defined by histone acetylation, coregulators and transcriptional capacity. *PLoS One,* 3**,** e3645.

John, S., P. J. Sabo, T. A. Johnson, M. H. Sung, S. C. Biddie, S. L. Lightman, T. C. Voss, S. R. Davis, P. S. Meltzer, J. A. Stamatoyannopoulos & G. L. Hager (2008) Interaction of the glucocorticoid receptor with the chromatin landscape. *Mol Cell,* 29**,** 611-24.

Kang, H. S., M. Angers, J. Y. Beak, X. Wu, J. M. Gimble, T. Wada, W. Xie, J. B. Collins, S. F. Grissom & A. M. Jetten (2007) Gene expression profiling reveals a regulatory role for ROR alpha and ROR gamma in phase I and phase II metabolism. *Physiol Genomics,* 31**,** 281-94.

Kansagra, K., B. Stoll, C. Rognerud, H. Niinikoski, C. N. Ou, R. Harvey & D. Burrin (2003) Total parenteral nutrition adversely affects gut barrier function in neonatal piglets. *Am J Physiol Gastrointest Liver Physiol,* 285**,** G1162-70.

Kast, H. R., B. Goodwin, P. T. Tarr, S. A. Jones, A. M. Anisfeld, C. M. Stoltz, P. Tontonoz, S. Kliewer, T. M. Willson & P. A. Edwards (2002) Regulation of multidrug resistance-associated protein 2 (ABCC2) by the nuclear receptors pregnane X receptor, farnesoid X-activated receptor, and constitutive androstane receptor. *J Biol Chem,* 277**,** 2908-15.

Kast, H. R., C. M. Nguyen, C. J. Sinal, S. A. Jones, B. A. Laffitte, K. Reue, F. J. Gonzalez, T. M. Willson & P. A. Edwards (2001) Farnesoid X-activated receptor induces apolipoprotein C-II transcription: a molecular mechanism linking plasma triglyceride levels to bile acids. *Mol Endocrinol,* 15**,** 1720-8.

Kemper, J. K., Z. Xiao, B. Ponugoti, J. Miao, S. Fang, D. Kanamaluru, S. Tsang, S. Y. Wu, C. M. Chiang & T. D. Veenstra (2009) FXR acetylation is normally dynamically regulated by p300 and SIRT1 but constitutively elevated in metabolic disease states. *Cell Metab,* 10**,** 392-404.

Kim, I., K. Morimura, Y. Shah, Q. Yang, J. M. Ward & F. J. Gonzalez (2007) Spontaneous hepatocarcinogenesis in farnesoid X receptor-null mice. *Carcinogenesis,* 28**,** 940-6.

Kir, S., S. A. Beddow, V. T. Samuel, P. Miller, S. F. Previs, K. Suino-Powell, H. E. Xu, G. I. Shulman, S. A. Kliewer & D. J. Mangelsdorf (2011) FGF19 as a postprandial, insulin-independent activator of hepatic protein and glycogen synthesis. *Science,* 331**,** 1621-4.

Kiristioglu, I., P. Antony, Y. Fan, B. Forbush, R. L. Mosley, H. Yang & D. H. Teitelbaum (2002) Total parenteral nutrition-associated changes in mouse intestinal intraepithelial lymphocytes. *Dig Dis Sci,* 47**,** 1147-57.

Kiristioglu, I. & D. H. Teitelbaum (1998) Alteration of the intestinal intraepithelial lymphocytes during total parenteral nutrition. *J Surg Res,* 79**,** 91-6.

Klein, G. L., W. E. Berquist, M. E. Ament, J. W. Coburn, N. L. Miller & A. C. Alfrey (1984) Hepatic aluminum accumulation in children on total parenteral nutrition. *J Pediatr Gastroenterol Nutr,* 3**,** 740-3.

Kong, B., I. L. Csanaky, L. M. Aleksunes, M. Patni, Q. Chen, X. Ma, H. Jaeschke, S. Weir, M. Broward, C. D. Klaassen & G. L. Guo (2012a) Gender-specific reduction of hepatic Mrp2 expression by high-fat diet protects female mice from ANIT toxicity. *Toxicol Appl Pharmacol,* 261**,** 189-95.

Kong, B., J. Huang, Y. Zhu, G. Li, J. Williams, S. Shen, L. M. Aleksunes, J. R. Richardson, U. Apte, D. A. Rudnick & G. L. Guo (2014) Fibroblast growth factor 15 deficiency impairs liver regeneration in mice. *Am J Physiol Gastrointest Liver Physiol,* 306**,** G893-902.

Kong, B., L. Wang, J. Y. Chiang, Y. Zhang, C. D. Klaassen & G. L. Guo (2012b) Mechanism of tissue-specific farnesoid X receptor in suppressing the expression of genes in bile-acid synthesis in mice. *Hepatology,* 56**,** 1034-43.

Kostrubsky, V. E., V. Ramachandran, R. Venkataramanan, K. Dorko, J. E. Esplen, S. Zhang, J. F. Sinclair, S. A. Wrighton & S. C. Strom (1999) The use of human hepatocyte cultures to study the induction of cytochrome P-450. *Drug Metab Dispos,* 27**,** 887-94.

Kumpf, V. J. (2006) Parenteral nutrition-associated liver disease in adult and pediatric patients. *Nutr Clin Pract,* 21**,** 279-90.

Lambert, G., M. J. Amar, G. Guo, H. B. Brewer, Jr., F. J. Gonzalez & C. J. Sinal (2003) The farnesoid X-receptor is an essential regulator of cholesterol homeostasis. *J Biol Chem,* 278**,** 2563-70.

Langmead, B., C. Trapnell, M. Pop & S. L. Salzberg (2009) Ultrafast and memory-efficient alignment of short DNA sequences to the human genome. *Genome Biol,* 10**,** R25.

Laroui, H., S. A. Ingersoll, H. C. Liu, M. T. Baker, S. Ayyadurai, M. A. Charania, F. Laroui, Y. Yan, S. V. Sitaraman & D. Merlin (2012) Dextran sodium sulfate (DSS) induces colitis in mice by forming nano-lipocomplexes with medium-chain-length fatty acids in the colon. *PLoS One,* 7**,** e32084.

Le, H. D., V. E. de Meijer, E. M. Robinson, D. Zurakowski, A. K. Potemkin, D. A. Arsenault, E. M. Fallon, A. Malkan, B. R. Bistrian, K. M. Gura & M. Puder (2011) Parenteral fish-oil-based lipid emulsion improves fatty acid profiles and lipids in parenteral nutrition-dependent children. *Am J Clin Nutr,* 94**,** 749-58.

Lee, H., Y. Zhang, F. Y. Lee, S. F. Nelson, F. J. Gonzalez & P. A. Edwards (2006) FXR regulates organic solute transporters alpha and beta in the adrenal gland, kidney, and intestine. *J Lipid Res,* 47**,** 201-14.

Lee, J., S. Seok, P. Yu, K. Kim, Z. Smith, M. Rivas-Astroza, S. Zhong & J. K. Kemper (2012) Genomic analysis of hepatic farnesoid X receptor binding sites reveals altered binding in obesity and direct gene repression by farnesoid X receptor in mice. *Hepatology,* 56**,** 108-17.

Leveille-Webster, C. R. & I. M. Arias (1994) Mdr 2 knockout mice link biliary phospholipid deficiency with small bile duct destruction. *Hepatology,* 19**,** 1528-31.

Lew, J. L., A. Zhao, J. Yu, L. Huang, N. De Pedro, F. Pelaez, S. D. Wright & J. Cui (2004) The farnesoid X receptor controls gene expression in a ligand- and promoter-selective fashion. *J Biol Chem,* 279**,** 8856-61.

Li, D., R. Gaedigk, S. N. Hart, J. S. Leeder & X. B. Zhong (2012a) The role of CYP3A4 mRNA transcript with shortened 3'-untranslated region in hepatocyte differentiation, liver development, and response to drug induction. *Mol Pharmacol,* 81**,** 86-96.

Li, G., A. M. Thomas, S. N. Hart, X. Zhong, D. Wu & G. L. Guo (2010) Farnesoid X receptor activation mediates head-to-tail chromatin looping in the Nr0b2 gene encoding small heterodimer partner. *Mol Endocrinol,* 24**,** 1404-12.

Li, G., A. M. Thomas, J. A. Williams, B. Kong, J. Liu, Y. Inaba, W. Xie & G. L. Guo (2012b) Farnesoid X receptor induces murine scavenger receptor Class B type I via intron binding. *PLoS One,* 7**,** e35895.

Li, M. K. & J. M. Crawford (2004) The pathology of cholestasis. *Semin Liver Dis,* 24**,** 21-42.

Li, T. & J. Y. Chiang (2014) Bile Acid Signaling in Metabolic Disease and Drug Therapy. *Pharmacol Rev,* 66**,** 948-983.

Li, T., M. Matozel, S. Boehme, B. Kong, L. M. Nilsson, G. Guo, E. Ellis & J. Y. Chiang (2011) Overexpression of cholesterol 7alpha-hydroxylase promotes hepatic bile acid synthesis and secretion and maintains cholesterol homeostasis. *Hepatology,* 53**,** 996-1006.

Lilja, H. E., Y. Finkel, M. Paulsson & S. Lucas (2011) Prevention and reversal of intestinal failure-associated liver disease in premature infants with short bowel syndrome using intravenous fish oil in combination with omega-6/9 lipid emulsions. *J Pediatr Surg,* 46**,** 1361-7.

Ling, P. R., M. Sheikh, P. Boyce, M. Keane-Ellison, A. Thibault, P. Burke, S. Freedman & B. R. Bistrian (2001) Cholecystokinin (CCK) secretion in patients with severe short bowel syndrome (SSBS). *Dig Dis Sci,* 46**,** 859-64.

Liu, Y., J. Binz, M. J. Numerick, S. Dennis, G. Luo, B. Desai, K. I. MacKenzie, T. A. Mansfield, S. A. Kliewer, B. Goodwin & S. A. Jones (2003) Hepatoprotection by the farnesoid X receptor agonist GW4064 in rat models of intra- and extrahepatic cholestasis. *J Clin Invest,* 112**,** 1678-87.

Lupien, M., J. Eeckhoute, C. A. Meyer, Q. Wang, Y. Zhang, W. Li, J. S. Carroll, X. S. Liu & M. Brown (2008) FoxA1 translates epigenetic signatures into enhancer-driven lineage-specific transcription. *Cell,* 132**,** 958-70.

Ma, K., P. K. Saha, L. Chan & D. D. Moore (2006) Farnesoid X receptor is essential for normal glucose homeostasis. *J Clin Invest,* 116**,** 1102-9.

Madara, J. L. & J. Stafford (1989) Interferon-gamma directly affects barrier function of cultured intestinal epithelial monolayers. *J Clin Invest,* 83**,** 724-7.

Maglich, J. M., J. A. Caravella, M. H. Lambert, T. M. Willson, J. T. Moore & L. Ramamurthy (2003) The first completed genome sequence from a teleost fish (Fugu rubripes) adds significant diversity to the nuclear receptor superfamily. *Nucleic Acids Res,* 31**,** 4051-8.

Makishima, M. (1999) Identification of a Nuclear Receptor for Bile Acids. *Science,* 284**,** 1362-1365.

Makishima, M., A. Y. Okamoto, J. J. Repa, H. Tu, R. M. Learned, A. Luk, M. V. Hull, K. D. Lustig, D. J. Mangelsdorf & B. Shan (1999) Identification of a nuclear receptor for bile acids. *Science,* 284**,** 1362-5.

Mangelsdorf, D. J., C. Thummel, M. Beato, P. Herrlich, G. Schutz, K. Umesono, B. Blumberg, P. Kastner, M. Mark, P. Chambon & R. M. Evans (1995) The nuclear receptor superfamily: the second decade. *Cell,* 83**,** 835-9.

McMahan, R. H., X. X. Wang, L. L. Cheng, T. Krisko, M. Smith, K. El Kasmi, M. Pruzanski, L. Adorini, L. Golden-Mason, M. Levi & H. R. Rosen (2013) Bile Acid receptor activation modulates hepatic monocyte activity and improves nonalcoholic Fatty liver disease. *J Biol Chem,* 288**,** 11761-70.

Modica, S., R. M. Gadaleta & A. Moschetta (2010) Deciphering the nuclear bile acid receptor FXR paradigm. *Nucl Recept Signal,* 8**,** e005.

Modica, S., M. Petruzzelli, E. Bellafante, S. Murzilli, L. Salvatore, N. Celli, G. Di Tullio, G. Palasciano, T. Moustafa, E. Halilbasic, M. Trauner & A. Moschetta (2012) Selective activation of nuclear bile acid receptor FXR in the intestine protects mice against cholestasis. *Gastroenterology,* 142**,** 355-65 e1-4.

Nandivada, P., A. K. Potemkin, S. J. Carlson, M. I. Chang, E. Cowan, A. A. O'Loughlin, K. M. Gura & M. Puder (2014) Elevated Alkaline Phosphatase in Infants With Parenteral Nutrition-Associated Liver Disease Reflects Bone Rather Than Liver Disease. *JPEN J Parenter Enteral Nutr*.

Neimark, E., F. Chen, X. Li & B. L. Shneider (2004) Bile acid-induced negative feedback regulation of the human ileal bile acid transporter. *Hepatology,* 40**,** 149-56.

Omata, J., J. F. Pierre, A. F. Heneghan, F. H. Tsao, Y. Sano, M. A. Jonker & K. A. Kudsk (2013) Parenteral nutrition suppresses the bactericidal response of the small intestine. *Surgery,* 153**,** 17-24.

Othman, R. A., S. B. Myrie & P. J. Jones (2013) Non-cholesterol sterols and cholesterol metabolism in sitosterolemia. *Atherosclerosis,* 231**,** 291-9.

Otte, K., H. Kranz, I. Kober, P. Thompson, M. Hoefer, B. Haubold, B. Remmel, H. Voss, C. Kaiser, M. Albers, Z. Cheruvallath, D. Jackson, G. Casari, M. Koegl, S. Paabo, J. Mous, C. Kremoser & U. Deuschle (2003) Identification of farnesoid X receptor beta as a novel mammalian nuclear receptor sensing lanosterol. *Mol Cell Biol,* 23**,** 864-72.

Parks, D. J., S. G. Blanchard, R. K. Bledsoe, G. Chandra, T. G. Consler, S. A. Kliewer, J. B. Stimmel, T. M. Willson, A. M. Zavacki, D. D. Moore & J. M. Lehmann (1999) Bile acids: natural ligands for an orphan nuclear receptor. *Science,* 284**,** 1365-8.

Pathak, P., T. Li & J. Y. Chiang (2013) Retinoic acid-related orphan receptor alpha regulates diurnal rhythm and fasting induction of sterol 12alpha-hydroxylase in bile acid synthesis. *J Biol Chem,* 288**,** 37154-65.

Pawlik, D., R. Lauterbach & J. Hurkala (2011) The efficacy of fish-oil based fat emulsion administered from the first day of life in very low birth weight newborns. *Med Wieku Rozwoj,* 15**,** 306-11.

Peyret, B., S. Collardeau, S. Touzet, I. Loras-Duclaux, H. Yantren, M. C. Michalski, J. Chaix, L. Restier-Miron, R. Bouvier, A. Lachaux & N. Peretti (2011) Prevalence of liver complications in children receiving long-term parenteral nutrition. *Eur J Clin Nutr,* 65**,** 743-9.

Pineda Torra, I., L. P. Freedman & M. J. Garabedian (2004) Identification of DRIP205 as a coactivator for the Farnesoid X receptor. *J Biol Chem,* 279**,** 36184-91.

Pircher, P. C., J. L. Kitto, M. L. Petrowski, R. K. Tangirala, E. D. Bischoff, I. G. Schulman & S. K. Westin (2003) Farnesoid X receptor regulates bile acid-amino acid conjugation. *J Biol Chem,* 278**,** 27703-11.

Popescu, I. R., A. Helleboid-Chapman, A. Lucas, B. Vandewalle, J. Dumont, E. Bouchaert, B. Derudas, J. Kerr-Conte, S. Caron, F. Pattou & B. Staels (2010) The nuclear receptor FXR is expressed in pancreatic beta-cells and protects human islets from lipotoxicity. *FEBS Lett,* 584**,** 2845-51.

Puiman, P. & B. Stoll (2008) Animal models to study neonatal nutrition in humans. *Curr Opin Clin Nutr Metab Care,* 11**,** 601-6.

Qin, P., L. A. Borges-Marcucci, M. J. Evans & D. C. Harnish (2005) Bile acid signaling through FXR induces intracellular adhesion molecule-1 expression in mouse liver and human hepatocytes. *Am J Physiol Gastrointest Liver Physiol,* 289**,** G267-73.

Rayyan, M., H. Devlieger, F. Jochum & K. Allegaert (2012) Short-term use of parenteral nutrition with a lipid emulsion containing a mixture of soybean oil, olive oil, medium-chain triglycerides, and fish oil: a randomized double-blind study in preterm infants. *JPEN J Parenter Enteral Nutr,* 36**,** 81S-94S.

Renga, B., A. Mencarelli, P. Vavassori, V. Brancaleone & S. Fiorucci (2010) The bile acid sensor FXR regulates insulin transcription and secretion. *Biochim Biophys Acta,* 1802**,** 363-72.

Ridlon, J. M., D. J. Kang & P. B. Hylemon (2006) Bile salt biotransformations by human intestinal bacteria. *J Lipid Res,* 47**,** 241-59.

Rizzo, G., B. Renga, E. Antonelli, D. Passeri, R. Pellicciari & S. Fiorucci (2005) The methyl transferase PRMT1 functions as co-activator of farnesoid X receptor (FXR)/9-cis retinoid X receptor and regulates transcription of FXR responsive genes. *Mol Pharmacol,* 68**,** 551-8.

Rodriguez-Garay, E. A. (2003) Cholestasis: human disease and experimental animal models. *Ann Hepatol,* 2**,** 150-8.

Russell, D. W. (2003) The enzymes, regulation, and genetics of bile acid synthesis. *Annu Rev Biochem,* 72**,** 137-74.

Ryan, K. K., V. Tremaroli, C. Clemmensen, P. Kovatcheva-Datchary, A. Myronovych, R. Karns, H. E. Wilson-Perez, D. A. Sandoval, R. Kohli, F. Backhed & R. J. Seeley (2014) FXR is a molecular target for the effects of vertical sleeve gastrectomy. *Nature*.

Sangild, P. T., Y. M. Petersen, M. Schmidt, J. Elnif, T. K. Petersen, R. K. Buddington, G. Greisen, K. F. Michaelsen & D. G. Burrin (2002) Preterm birth affects the intestinal response to parenteral and enteral nutrition in newborn pigs. *J Nutr,* 132**,** 3786-94.

Savkur, R. S., J. S. Thomas, K. S. Bramlett, Y. Gao, L. F. Michael & T. P. Burris (2005) Ligand-dependent coactivation of the human bile acid receptor FXR by the peroxisome proliferator-activated receptor gamma coactivator-1alpha. *J Pharmacol Exp Ther,* 312**,** 170-8.

Sayin, S. I., A. Wahlstrom, J. Felin, S. Jantti, H. U. Marschall, K. Bamberg, B. Angelin, T. Hyotylainen, M. Oresic & F. Backhed (2013) Gut microbiota regulates bile acid metabolism by reducing the levels of tauro-beta-muricholic acid, a naturally occurring FXR antagonist. *Cell Metab,* 17**,** 225-35.

Schreuder, T. C., H. A. Marsman, M. Lenicek, J. R. van Werven, A. J. Nederveen, P. L. Jansen & F. G. Schaap (2010) The hepatic response to FGF19 is impaired in patients with nonalcoholic fatty liver disease and insulin resistance. *Am J Physiol Gastrointest Liver Physiol,* 298**,** G440-5.

Seol, W., H. S. Choi & D. D. Moore (1995) Isolation of proteins that interact specifically with the retinoid X receptor: two novel orphan receptors. *Mol Endocrinol,* 9**,** 72-85.

Serhan, C. N., S. Hong, K. Gronert, S. P. Colgan, P. R. Devchand, G. Mirick & R. L. Moussignac (2002) Resolvins: a family of bioactive products of omega-3 fatty acid transformation circuits initiated by aspirin treatment that counter proinflammation signals. *J Exp Med,* 196**,** 1025-37.

Shah, S., U. R. Sanford, J. C. Vargas, H. Xu, A. Groen, C. C. Paulusma, J. P. Grenert, L. Pawlikowska, S. Sen, R. P. Elferink & L. N. Bull (2010) Strain background modifies phenotypes in the ATP8B1-deficient mouse. *PLoS One,* 5**,** e8984.

Shneider, B. L., P. A. Dawson, D. M. Christie, W. Hardikar, M. H. Wong & F. J. Suchy (1995) Cloning and molecular characterization of the ontogeny of a rat ileal sodium-dependent bile acid transporter. *J Clin Invest,* 95**,** 745-54.

Sinal, C. J., M. Tohkin, M. Miyata, J. M. Ward, G. Lambert & F. J. Gonzalez (2000) Targeted disruption of the nuclear receptor FXR/BAR impairs bile acid and lipid homeostasis. *Cell,* 102**,** 731-44.

Sinha, J., F. Chen, T. Miloh, R. C. Burns, Z. Yu & B. L. Shneider (2008) beta-Klotho and FGF-15/19 inhibit the apical sodium-dependent bile acid transporter in enterocytes and cholangiocytes. *Am J Physiol Gastrointest Liver Physiol,* 295**,** G996-G1003.

Sitzmann, J. V., H. A. Pitt, P. A. Steinborn, Z. R. Pasha & R. C. Sanders (1990) Cholecystokinin prevents parenteral nutrition induced biliary sludge in humans. *Surg Gynecol Obstet,* 170**,** 25-31.

Song, X., A. Vasilenko, Y. Chen, L. Valanejad, R. Verma, B. Yan & R. Deng (2014) Transcriptional dynamics of bile salt export pump during pregnancy: Mechanisms and implications in intrahepatic cholestasis of pregnancy. *Hepatology*.

Spector, A. A., X. Fang, G. D. Snyder & N. L. Weintraub (2004) Epoxyeicosatrienoic acids (EETs): metabolism and biochemical function. *Prog Lipid Res,* 43**,** 55-90.

Spencer, A. U., S. Yu, T. F. Tracy, M. M. Aouthmany, A. Llanos, M. B. Brown, M. Brown, R. J. Shulman, R. B. Hirschl, P. A. Derusso, J. Cox, J. Dahlgren, P. J. Strouse, J. I. Groner & D. H. Teitelbaum (2005) Parenteral nutrition-associated cholestasis in neonates: multivariate analysis of the potential protective effect of taurine. *JPEN J Parenter Enteral Nutr,* 29**,** 337-43; discussion 343-4.

St-Pierre, M. V., G. A. Kullak-Ublick, B. Hagenbuch & P. J. Meier (2001) Transport of bile acids in hepatic and non-hepatic tissues. *J Exp Biol,* 204**,** 1673-86.

Steinberg, D. & J. L. Witztum (2009) Inhibition of PCSK9: a powerful weapon for achieving ideal LDL cholesterol levels. *Proc Natl Acad Sci U S A,* 106**,** 9546-7.

Stoll, B., D. A. Horst, L. Cui, X. Chang, K. J. Ellis, D. L. Hadsell, A. Suryawan, A. Kurundkar, A. Maheshwari, T. A. Davis & D. G. Burrin (2010) Chronic parenteral nutrition induces hepatic inflammation, steatosis, and insulin resistance in neonatal pigs. *J Nutr,* 140**,** 2193-200.

Sun, X., H. Yang, K. Nose, S. Nose, E. Q. Haxhija, H. Koga, Y. Feng & D. H. Teitelbaum (2008) Decline in intestinal mucosal IL-10 expression and decreased intestinal barrier function in a mouse model of total parenteral nutrition. *Am J Physiol Gastrointest Liver Physiol,* 294**,** G139-47.

Sungurtekin, H., S. Degirmenci, U. Sungurtekin, B. E. Oguz, N. Sabir & B. Kaptanoglu (2011) Comparison of the effects of different intravenous fat emulsions in patients with systemic inflammatory response syndrome and sepsis. *Nutr Clin Pract,* 26**,** 665-71.

Tan, J. T., E. Dudl, E. LeRoy, R. Murray, J. Sprent, K. I. Weinberg & C. D. Surh (2001) IL-7 is critical for homeostatic proliferation and survival of naive T cells. *Proc Natl Acad Sci U S A,* 98**,** 8732-7.

Thomas, A. M., S. N. Hart, B. Kong, J. Fang, X. B. Zhong & G. L. Guo (2010) Genome-wide tissue-specific farnesoid X receptor binding in mouse liver and intestine. *Hepatology,* 51**,** 1410-9.

Thomas, A. M., S. N. Hart, G. Li, H. Lu, Y. Fang, J. Fang, X. B. Zhong & G. L. Guo (2013) Hepatocyte Nuclear Factor 4 Alpha and Farnesoid X Receptor Co-regulates Gene Transcription in Mouse Livers on a Genome-Wide Scale. *Pharm Res,* 30**,** 2188-98.

Trapnell, C., A. Roberts, L. Goff, G. Pertea, D. Kim, D. R. Kelley, H. Pimentel, S. L. Salzberg, J. L. Rinn & L. Pachter (2012) Differential gene and transcript expression analysis of RNA-seq experiments with TopHat and Cufflinks. *Nat Protoc,* 7**,** 562-78.

Trauner, M., P. J. Meier & J. L. Boyer (1998) Molecular pathogenesis of cholestasis. *N Engl J Med,* 339**,** 1217-27.

Truskett, P. G., E. C. Shi, M. Rose, P. A. Sharp & J. M. Ham (1987) Model of TPN-associated hepatobiliary dysfunction in the young pig. *Br J Surg,* 74**,** 639-42.

Tsai, S., P. J. Strouse, R. A. Drongowski, S. Islam & D. H. Teitelbaum (2005) Failure of cholecystokinin-octapeptide to prevent TPN-associated gallstone disease. *J Pediatr Surg,* 40**,** 263-7.

Uriarte, I., M. G. Fernandez-Barrena, M. J. Monte, M. U. Latasa, H. C. Chang, S. Carotti, U. Vespasiani-Gentilucci, S. Morini, E. Vicente, A. R. Concepcion, J. F. Medina, J.

J. Marin, C. Berasain, J. Prieto & M. A. Avila (2013) Identification of fibroblast growth factor 15 as a novel mediator of liver regeneration and its application in the prevention of post-resection liver failure in mice. *Gut,* 62**,** 899-910.

Urizar, N. L., A. B. Liverman, D. T. Dodds, F. V. Silva, P. Ordentlich, Y. Yan, F. J. Gonzalez, R. A. Heyman, D. J. Mangelsdorf & D. D. Moore (2002) A natural product that lowers cholesterol as an antagonist ligand for FXR. *Science,* 296**,** 1703-6.

van Aerde, J. E., M. Keelan, M. T. Clandinin & A. B. Thomson (1997) Lipids in total parenteral nutrition solutions differentially modify lipids in piglet intestinal brush border and microsomal membranes. *JPEN J Parenter Enteral Nutr,* 21**,** 63-71.

Vlaardingerbroek, H., K. Ng, B. Stoll, N. Benight, S. Chacko, L. A. Kluijtmans, W. Kulik, E. J. Squires, O. Olutoye, D. Schady, M. L. Finegold, J. B. van Goudoever & D. G. Burrin (2014) New generation lipid emulsions prevent PNALD in chronic parenterally fed preterm pigs. *J Lipid Res,* 55**,** 466-77.

Wada, T., H. S. Kang, M. Angers, H. Gong, S. Bhatia, S. Khadem, S. Ren, E. Ellis, S. C. Strom, A. M. Jetten & W. Xie (2008) Identification of oxysterol 7alpha-hydroxylase (Cyp7b1) as a novel retinoid-related orphan receptor alpha (RORalpha) (NR1F1) target gene and a functional cross-talk between RORalpha and liver X receptor (NR1H3). *Mol Pharmacol,* 73**,** 891-9.

Waitzberg, D. L., R. S. Torrinhas & T. M. Jacintho (2006) New parenteral lipid emulsions for clinical use. *JPEN J Parenter Enteral Nutr,* 30**,** 351-67.

Wang, H., J. Chen, K. Hollister, L. C. Sowers & B. M. Forman (1999) Endogenous bile acids are ligands for the nuclear receptor FXR/BAR. *Mol Cell,* 3**,** 543-53.

Wang, H., V. I. Khaoustov, B. Krishnan, W. Cai, B. Stoll, D. G. Burrin & B. Yoffe (2006) Total parenteral nutrition induces liver steatosis and apoptosis in neonatal piglets. *J Nutr,* 136**,** 2547-52.

Wang, Y. D., W. D. Chen, M. Wang, D. Yu, B. M. Forman & W. Huang (2008) Farnesoid X receptor antagonizes nuclear factor kappaB in hepatic inflammatory response. *Hepatology,* 48**,** 1632-43.

Watanabe, M., S. M. Houten, L. Wang, A. Moschetta, D. J. Mangelsdorf, R. A. Heyman, D. D. Moore & J. Auwerx (2004) Bile acids lower triglyceride levels via a pathway involving FXR, SHP, and SREBP-1c. *Journal of Clinical Investigation,* 113**,** 1408-1418.

Watanabe, M., Y. Ueno, T. Yajima, Y. Iwao, M. Tsuchiya, H. Ishikawa, S. Aiso, T. Hibi & H. Ishii (1995) Interleukin 7 is produced by human intestinal epithelial cells and regulates the proliferation of intestinal mucosal lymphocytes. *J Clin Invest,* 95**,** 2945-53.

Watanabe, M., M. Yamazaki, R. Okamoto, S. Ohoka, A. Araki, T. Nakamura & T. Kanai (2003) Therapeutic approaches to chronic intestinal inflammation by specific targeting of mucosal IL-7/IL-7R signal pathway. *Curr Drug Targets Inflamm Allergy,* 2**,** 119-23.

Wetterau, J. R., M. C. Lin & H. Jamil (1997) Microsomal triglyceride transfer protein. *Biochim Biophys Acta,* 1345**,** 136-50.

Williams, J. A., A. M. Thomas, G. Li, B. Kong, L. Zhan, Y. Inaba, W. Xie, W. X. Ding & G. L. Guo (2012) Tissue specific induction of p62/Sqstm1 by farnesoid X receptor. *PLoS One,* 7**,** e43961.

Wojcik, M., D. Janus, K. Dolezal-Oltarzewska, A. Kalicka-Kasperczyk, K. Poplawska, D. Drozdz, K. Sztefko & J. B. Starzyk (2012) A decrease in fasting FGF19 levels is associated with the development of non-alcoholic fatty liver disease in obese adolescents. *J Pediatr Endocrinol Metab,* 25**,** 1089-93.

Xu, Y. Q., D. Zhang, T. Jin, D. J. Cai, Q. Wu, Y. Lu, J. Liu & C. D. Klaassen (2012) Diurnal variation of hepatic antioxidant gene expression in mice. *PLoS One,* 7**,** e44237.

Yamazaki, M., T. Yajima, M. Tanabe, K. Fukui, E. Okada, R. Okamoto, S. Oshima, T. Nakamura, T. Kanai, M. Uehira, T. Takeuchi, H. Ishikawa, T. Hibi & M. Watanabe (2003) Mucosal T cells expressing high levels of IL-7 receptor are potential targets for treatment of chronic colitis. *J Immunol,* 171**,** 1556-63.

Yang, H., R. Finaly & D. H. Teitelbaum (2003) Alteration in epithelial permeability and ion transport in a mouse model of total parenteral nutrition. *Crit Care Med,* 31**,** 1118-25.

Yang, H., D. L. Gumucio & D. H. Teitelbaum (2008) Intestinal specific overexpression of interleukin-7 attenuates the alternation of intestinal intraepithelial lymphocytes after total parenteral nutrition administration. *Ann Surg,* 248**,** 849-56.

Yang, H., X. Sun, E. Q. Haxhija & D. H. Teitelbaum (2007) Intestinal epithelial cell-derived interleukin-7: A mechanism for the alteration of intraepithelial lymphocytes in a mouse model of total parenteral nutrition. *Am J Physiol Gastrointest Liver Physiol,* 292**,** G84-91.

Zhan, L., H. X. Liu, Y. Fang, B. Kong, Y. He, X. B. Zhong, J. Fang, Y. J. Wan & G. L. Guo (2014) Genome-wide binding and transcriptome analysis of human farnesoid X receptor in primary human hepatocytes. *PLoS One,* 9**,** e105930.

Zhang, L., Y. D. Wang, W. D. Chen, X. Wang, G. Lou, N. Liu, M. Lin, B. M. Forman & W. Huang (2012a) Promotion of liver regeneration/repair by farnesoid X receptor in both liver and intestine in mice. *Hepatology,* 56**,** 2336-43.

Zhang, Y., L. W. Castellani, C. J. Sinal, F. J. Gonzalez & P. A. Edwards (2004) Peroxisome proliferator-activated receptor-gamma coactivator 1alpha (PGC-1alpha) regulates triglyceride metabolism by activation of the nuclear receptor FXR. *Genes Dev,* 18**,** 157-69.

Zhang, Y., H. R. Kast-Woelbern & P. A. Edwards (2003) Natural structural variants of the nuclear receptor farnesoid X receptor affect transcriptional activation. *J Biol Chem,* 278**,** 104-10.

Zhang, Y., F. Y. Lee, G. Barrera, H. Lee, C. Vales, F. J. Gonzalez, T. M. Willson & P. A. Edwards (2006a) Activation of the nuclear receptor FXR improves hyperglycemia and hyperlipidemia in diabetic mice. *Proc Natl Acad Sci U S A,* 103**,** 1006-11.

Zhang, Y., F. Li, A. D. Patterson, Y. Wang, K. W. Krausz, G. Neale, S. Thomas, D. Nachagari, P. Vogel, M. Vore, F. J. Gonzalez & J. D. Schuetz (2012b) Abcb11 deficiency induces cholestasis coupled to impaired beta-fatty acid oxidation in mice. *J Biol Chem,* 287**,** 24784-94.

Zhang, Y., T. Liu, C. A. Meyer, J. Eeckhoute, D. S. Johnson, B. E. Bernstein, C. Nusbaum, R. M. Myers, M. Brown, W. Li & X. S. Liu (2008) Model-based analysis of ChIP-Seq (MACS). *Genome Biol,* 9**,** R137.

Zhang, Y., X. Wang, C. Vales, F. Y. Lee, H. Lee, A. J. Lusis & P. A. Edwards (2006b) FXR deficiency causes reduced atherosclerosis in Ldlr-/- mice. *Arterioscler Thromb Vasc Biol,* 26**,** 2316-21.

Zhang, Y., L. Yin, J. Anderson, H. Ma, F. J. Gonzalez, T. M. Willson & P. A. Edwards (2010) Identification of novel pathways that control farnesoid X receptor-mediated hypocholesterolemia. *J Biol Chem,* 285**,** 3035-43.

Zhang, Y. K., G. L. Guo & C. D. Klaassen (2011) Diurnal variations of mouse plasma and hepatic bile acid concentrations as well as expression of biosynthetic enzymes and transporters. *PLoS One,* 6**,** e16683.

Ziegler, T. R. & L. M. Leader (2006) Parenteral nutrition: transient or permanent therapy in intestinal failure? *Gastroenterology,* 130**,** S37-42.

Zweers, S. J., K. A. Booij, M. Komuta, T. Roskams, D. J. Gouma, P. L. Jansen & F. G. Schaap (2012) The human gallbladder secretes fibroblast growth factor 19 into bile: towards defining the role of fibroblast growth factor 19 in the enterobiliary tract. *Hepatology,* 55**,** 575-83.